Dissertation

submitted to the

Combined Faculties for the Natural Sciences and for Mathematics

of the Ruperto-Carola University of Heidelberg, Germany

for the degree of

Doctor of Natural Sciences

Presented by

B.Sc. Yuri Frosi

born in Rome, Italy

Oral examination: 19th December 2014

Analysis of the interplay between condensin and chromatin

Referees: Dr. Jan Ellenberg
Prof. Dr. Oliver Gruss

This work was carried out at the European Molecular Biology Laboratory (EMBL) from January 2011 to May 2014 under the supervision of Dr. Christian Häring.

Zusammenfassung

Der fünf Untereinheiten umfassende Condensinkomplex spielt eine essentielle Rolle in der strukturellen Organisation des eukaryotischen Genoms. Er wird vor allem für die Aufrechterhaltung der Struktur kondensierter Chromosomen während der Zellteilung benötigt. Trotz dieser Schlüsselfunktion sind die molekularen Mechanismen der Condensin-gesteuerten Prozesse nur unvollständig verstanden. Um über die molekulare Funktionsweise des Condensinkomplexes mehr Aufschluss zu erhalten, habe ich die Art der Wechselwirkung zwischen Condensin und seinem Substrat, der chromosomalen DNA, analysiert.

Die "Structural Maintenance of Chromosomes" (SMC) Untereinheiten bilden mit der Kleisin Untereinheit (von griechisch kleisimo - verschliessen) des Condensinkomplexes eine dreiteilige Ringstruktur. Es ist vorgeschlagen worden, dass dieser Ring Chromatinstränge umschliesst und dadurch intrachromosomale Verknüpfungen formt. Um dieses Ringmodell zu testen habe ich mittels spezifischer chemischer Reaktion die Kontaktstellen zwischen den SMC2-, SMC4- und Brn1- (Kleisin) Untereinheiten des Condensinkomplexes aus Bäckerhefe kovalent geschlossen. Anschließend habe ich die Wechselwirkung der verbundenen Condensin Untereinheiten mit kleinen zirkulären Minichromosomen in Hefe getestet. Chemische Zirkulation des Condensinkomplexes erzeugte ein Condensin-DNA Hybrid, das sogar nach Proteindenaturierung stabil blieb. Die im ersten Teil der Arbeit beschriebenen Experimente beweisen demnach, dass Condensinringe Chromatinstränge topologisch umschliessen.

Aus der Erkenntnis, dass Condensin Chromosomen als Ring umschliesst ergibt sich, dass für das Laden und Entladen des Rings auf Chromosomen mindestens eine der drei Schnittstellen zwischen den Ringuntereinheiten temporär geöffnet sein muss. Im zweiten Teil dieser Arbeit liefere ich Hinweise darauf, dass in Hefe die SMC2-Brn1 Kontaktregion als mögliches Tor für die DNA-Passage dient. Zudem beschreibe ich Experimente, die die Bedingungen zum Öffnen oder Schließen dieses Tors untersuchen, die für das Laden oder Entladen Condensins auf Chromosomen in menschlichen Zellen eine Rolle spielen.

Wie könnte das Öffnen und Schliessen der Condensinringe reguliert werden? Im dritten Teil der Arbeit habe ich untersucht, ob der Scc2-Scc4-Komplex, der für den Zusammenhalt von Schwesterchromatiden im Condensin verwandten Cohesinkomplex benötigt wird, auch bei Condensinringen eine ähnlich wichtige Rolle für das topologische Umschließen von Chromosomen spielt. Meine Experimente zeigen, dass das Entfernen des

Scc2-Scc4-Komplexes aus dem Zellkern keine nennenswerten Auswirkungen auf die Bindung Condensins an Chromosomen hat, während es die Bindung Cohesins an Chromosomen effektiv unterbindet. Dies legt nahe, dass sich die ersten Reaktionsschritte in den Lademechanismen der beiden verwandten Komplexe unterscheiden.

Summary

The multi-subunit condensin protein complex plays essential roles in the structural organization of eukaryotic genomes. Its function is particularly important for the maintenance of mitotic chromosome structure during their segregation into daughter cells. Despite its key roles, the molecular mechanisms of condensin action have remained poorly understood. To shed light into the function of condensin complexes, I have analysed the nature of the interaction of condensin with its chromosomal substrate.

The Structural Maintenance of Chromosomes (SMC) and kleisin subunits of condensin form a tripartite ring structure, which has been proposed to encircle chromatin fibres and thereby form intra-chromosomal linkages. To test this 'ring model', I generated covalently closed condensin rings by site specific cross-linking the interfaces between the Smc2, Smc4 and Brn1 kleisin subunits of budding yeast condensin complexes and then tested their interaction with small circular yeast minichromosomes. Chemical circularization of condensin complexes produced condensin-DNA species that remained even after protein denaturation. The experiments described in the first part of this thesis hence proof that condensin rings topologically encircle chromatin fibres.

The finding that condensin encircles chromosomes implies that entry and exit of chromosomes into and out of condensin rings requires the temporary disengagement of at least one of the three ring subunit interfaces. In the second part of this thesis, I provide evidence that, in yeast, the Smc2-Brn1 interface forms a possible gate for DNA passage. I furthermore describe experiments that aim to test the requirement of this gate to open for either condensin loading or unloading from chromosomes in human cells.

How might opening and closing of condensin rings be regulated? In the third part of this thesis, I tested whether the Scc2-Scc4 complex, which is required for the entrapment of sister chromatids in the condensin-related cohesin ring complex, plays a similar role for the topological loading onto chromosomes of condensin rings. My experiments demonstrate that depletion of Scc2-Scc4 from the nucleus, while inhibiting cohesin binding to chromosomes, has no notable effect on condensin's chromosomal association. This suggests that the first step in loading mechanisms differs between the related complexes.

Table of contents

I Introduction

1. Chromosome dynamics during cell divisions

All living cells arise from pre-existing cells. The process whereby new cells are formed is called cell division or mitosis, which classically involves the division of the cell's nucleus (karyokinesis) and cytoplasm (cytokinesis). In unicellular organisms, cell division is contributing to asexual reproduction. It leads to an increase in the total number of individuals. In multicellular organisms, cell division has a more sophisticated role. For example, trillions of cell divisions occur in a controlled manner to produce a human body from the fertilized egg (the zygote). Once an organism is fully developed, cell reproduction is still necessary to repair or regenerate tissues. For example, new blood and skin cells are constantly being produced. All multicellular organisms therefore use cell division for growth and the maintenance and repair of cells and tissues.

Each mitotic event produces two new cells, which like the mother cell have a ‘memory’ of how to run all the fundamental cellular programs. This cellular ‘memory’ is transferred from one cell to the other from generation to generation. In the beginning of the last century, it became clear that this memory or genetic information is encoded in the nuclear material called chromatin, which is formed by long DNA filaments and various proteins, and that DNA itself is the hereditary vehicle (Morgan et al., 1915).

Chromatin is organized into distinct entities, the chromosomes. To produce genetically identical offspring, the cell needs to first duplicate and then equally segregate the duplicated chromosomes. DNA replication generates two identical sister chromatids, which are tightly associated (cohesed) and are not distinguishable using conventional light microscopy. At the onset of mitosis (prophase), sister chromatids undergo a progressive compaction process that results in ‘thread’-like structures, which can now be clearly distinguished in the light microscope as mitotic chromosomes. These chromosomes have the length and mechanical resistance needed for their segregation in the later stages of mitosis. Mitotic chromosome assembly therefore represents one of the most critical steps of mitosis.

Upon Nuclear Envelope Breakdown (NEB) during prometaphase, sister chromatids become connected to the microtubules of the mitotic spindle, which emanate from each of the two centrosomes. At metaphase, all sister chromatid pairs have become bi-oriented at the equator of the cell. Correct alignment and spindle-attachment of the sister chromatids is monitored by the Spindle Assembly Checkpoint (SAC). Only when the SAC is satisfied, sister chromatids split almost synchronously and are pulled by microtubules towards opposite poles during anaphase. When segregation is complete, a new nuclear envelope forms around the segregated chromatids, chromosomes de-condense and the mitotic spindle disassembles during telophase. Finally, cell division is completed when an actin–myosin ring severs the cell into two genetically identical daughter cells during cytokinesis (Fig 1).

Failures in mitotic chromosome assembly lead to chromosome mis-segregation and chromosome arm breakage during cytokinesis, frequently with catastrophic outcomes for the daughter cells (Uemura et al., 1984, Saka et al., 1994, Strunnikov et al., 1995).

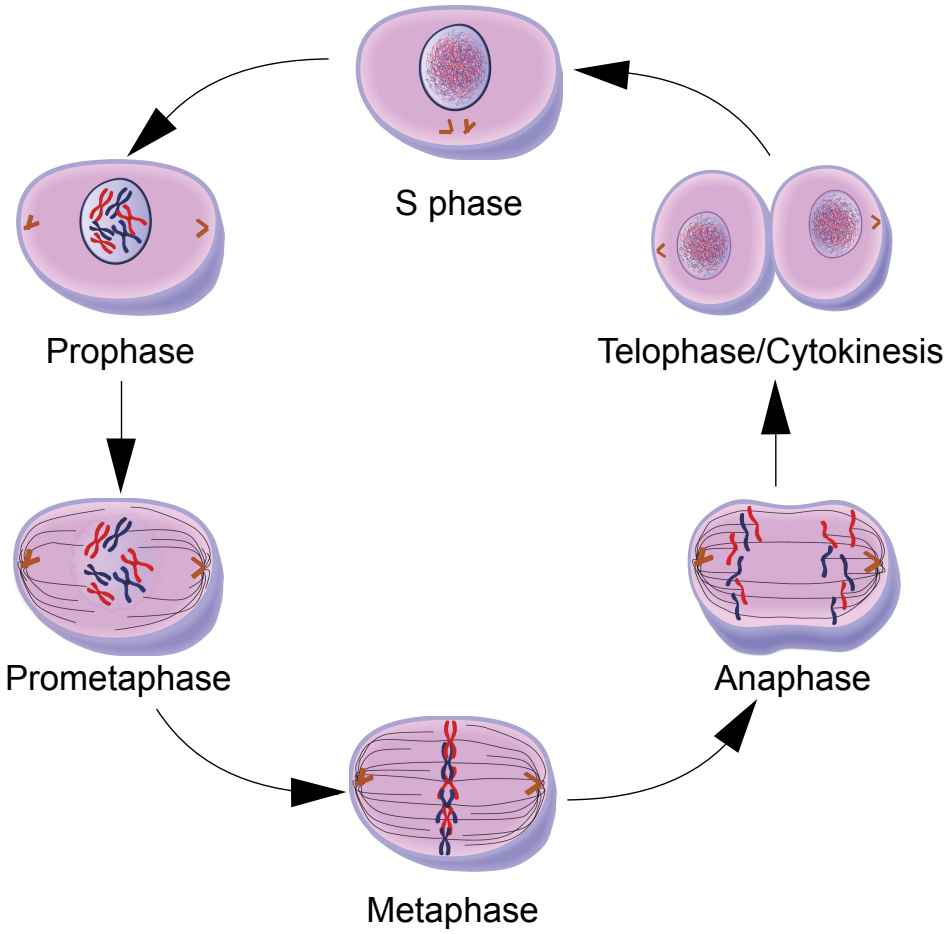

Figure 1. Chromatin re-arrangements during cell divisions. In order to ensure equal partitioning of chromosomes during mitosis, immediately after replication (S phase) chromatin fibers are starting to compact (prophase). Mitotic chromosomes maintain their highly organized structures from prophase until late anaphase to allow individual sister chromatids to be segregated properly by spindle microtubules during anaphase. Finally, cytokinesis produces two genetically identical daughter cells. Centrosomes are indicated as orange V-shaped structures, microtubules are inducated as black lines, chromosomes are indicated in red and blue.

2. Mitotic chromosome condensation

In preparation for cell division, chromosomes undergo extensive spatial reorganization and, in many species, shut down transcription of most genes (Taylor et al., 1960). This process culminates in a highly condensed and morphologically reproducible metaphase chromosome state and is termed chromosome condensation. The primary function of mitotic chromosome condensation is thought to be the reduction of chromosome arm length, which ensures that chromosome arms clear the plane of cytokinesis during anaphase and thereby avoid being severed during cell division.

A second function of chromosome condensation is to facilitate the proper resolution of sister chromatids during anaphase (Belmont 2006). Sister chromatids are connected by DNA intertwinings (catenanes), which arise as a result of DNA replication (Sundin and Varshavsky, 1981), and proteinaceous links by the cohesin complex (Michealis et al., 1997). Both linkages need to be cleared before chromosome segregation to prevent sister chromatid breakages when chromatids are pulled apart during anaphase. As condensation proceeds, proteinaceous (see Chapter 3.1) and topological links between sister chromatids are removed in a process known as chromosome resolution. The latter is achieved by the action of topoisomerase II (topo II), the enzyme that promotes the decatenation of intertwined sister DNAs by cleaving both strands of a DNA double helix and allowing the passage of another DNA strand through the break (Berger et al., 1996).

In coordination with chromosome resolution, the volume occupied by chromatin is considerably reduced to facilitate the transition from loosly structured interphase chromosomes into highly structured mitotic chromosomes. A cell's DNA is about hundred thousand times longer than the length of the cell itself (Hirano, 2000). If chromosomes were not properly condensed at anaphase onset, they were unlikely to segregate properly and risk to become severed during cytokinesis by the abscission machinery (Vagnarelli, 2012). Another major problem is that during anaphase, individualized sister chromatids have to withstand the pulling force of the spindle microtubules to avoid missegregation. Therefore mitotic condensation has to increase the mechanical rigidity of chromosomes and in particular of specialized chromosome regions like the centromere.

The understanding of the organization of mitotic chromosomes has remained one of the most challenging tasks in cell biology. A milestone in unrevealing chromosome structure came with the identification of nucleosomes as the first level of nuclear chromatin organization, where 145-147 base pairs (bp) of DNA are wrapped around an octamer of positively charged histone proteins (Kornberg, 1974; Richmond et al., 1984; Luger et al., 1997; Davey et al., 2002). This so-called 10 nm chromatin fiber, in which nucleosomes are connected via short DNA linkers (Oudet et la, 1975), shortens the length of the linear DNA about 7-fold (beads-on-a-string model). This level of organization is, however, not

sufficient to explain the high degree of compaction observed during mitotic chromosome formation.

Based on several biochemical and structural studies, different models for the arrangement of the chromatin fibers into mitotic chromosomes were suggested. These models can be subdivided into three groups: (1) the hierarchical model, (2) the loops-on-a-scaffold model and (3) the network model.

2.1. The hierarchical model

The hierarchical folding model is based on several levels of DNA packaging based on regular nucleosome-nucleosome contacts. The first of these folding levels was suggested to be the transformation of 10 nm into 30 nm fibers, which could be observed by increasing salt concentrations in *in vitro* experiments (Hansen et al. 1989). Further folding levels might explain the formation of mitotic chromosomes (Fig. 2A).

This model is, however, under intense debate. To date there exists little to no *in vivo* evidence for the presence of regular 30 nm fibers in mitotic chromosomes (Maeshima et al., 2010). Moreover, early ultrastructural investigations (Ris et al., 1970) and more recent light microscopy studies of mitotic chromosomes suggested that nucleosomes are arranged irregularly within mitotic chromosomes (Strukov and Belmont, 2009).

2.2. The loops-on-a-scaffold model

A different hypothesis arose from the discovery that chromosome structure remnants can be observed even in absence of histones. Selective removal of histones from isolated mitotic chromosomes showed that long loops of DNA seemed to emanate from residual non-histone proteins, which were arranged in a structure of the original chromosome size and shape. This led to a simple model in which mitotic chromosomes are rather static structures composed by a central protein "scaffold" that anchors the bases of DNA loops (Stubblefield and Wray, 1971; Paulson and Laemmli, 1977; Fig. 2B).

Although this model suggested for the first time that non-histone proteins might organize the higher-order structure of mitotic chromosomes, it cannot account for the observed dynamic property of chromosomes and their own scaffold components. By using fluorescence recovery after photobleaching (FRAP) techniques, several studies have in fact shown that only very few components of the nucleus are immobile, i.e. chromatin itself, chromatin-bound core histones (Phair and Misteli, 2000) and structural components of the nuclear lamina (Moir et al., 2000), whereas most other nuclear proteins move rapidly throughout the nucleus. For example, further FRAP experiments revealed that chromosome-bound topo II, which was identified as one of the major component of the

protein ‘scaffold’ (Earnshaw et al., 1985), is rapidly exchanged with the cytoplasmic pool, indicating that topo II belong to the class of the mobile protein instead (Christensen et al., 2002).

2.3. The network model

A different approach to gain insights into mitotic chromosome organization is to measure their micromechanical properties (Poirier et al., 2000). Mitotic chromosomes were shown to be very elastic, since they can be stretched to many times their normal length and then they can still relax back to their original length. Interestingly, the elastic properties were lost upon partial DNA digestion with micrococcal nuclease or restriction endonucleases that recognize 4-bp sequences (Poirier and Marko, 2002), whereas exposure to proteinase K caused only a small effect on elasticity (Pope et al., 2006). This suggests that the mechanical integrity of mitotic chromosomes is largely dependent on DNA and not a protein scaffold. These findings led to the proposal of a chromatin ‘network’ model, which predicts that mitotic chromosomes are formed by a (complex) network of distant DNA fibers cross-linked by, for example, individual proteins (Nicklas, 1983; Houchmandzadeh and Dimitrov, 1999; Poirier et al., 2002; Alipour and Marko, 2012; see Fig. 2C) whose identities are still under intense debate.

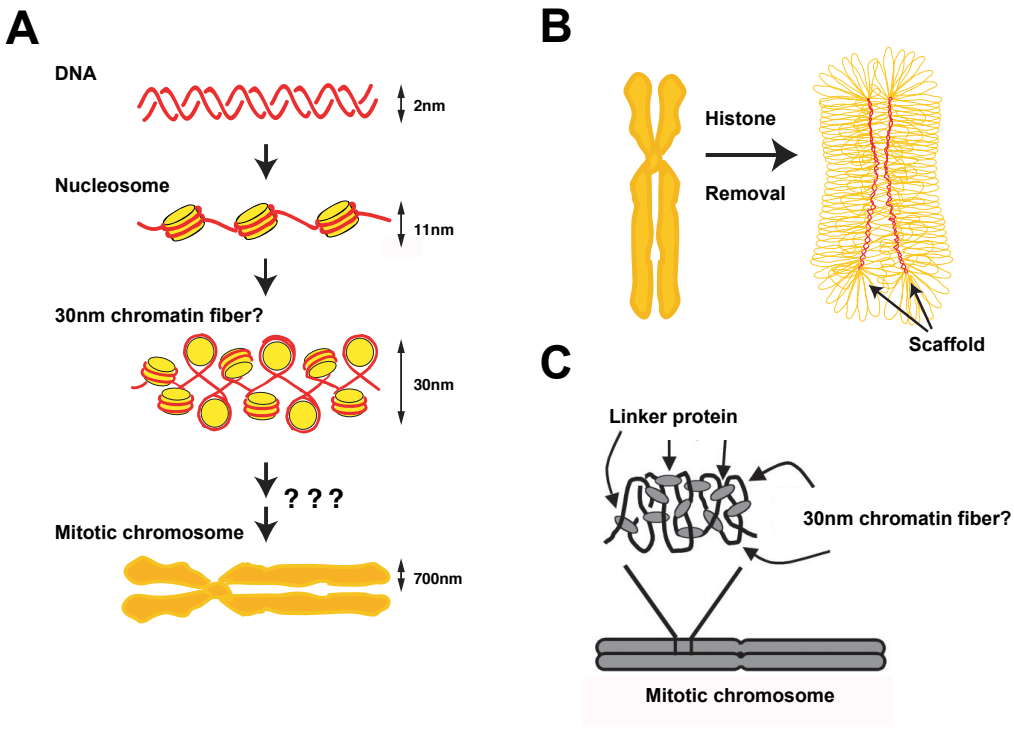

Figure 2. Models of mitotic chromosome architecture. **A** According to the 'hierarchical model', the DNA molecule is progressively compacted by nucleosome-nucleosome interactions into the final mitotic chromosome. It is still unclear whether the 30 nm chromatin fiber does exist *in vivo* and how it would be further compacted into the chromatids (700 nm). **B** Schematic representation of a histone-depleted mitotic chromosome. Histones were gently extracted from the isolated mitotic chromosome with an excess of the polyanions dextran sulfate and heparin. After removing histones, DNA remained highly organized by the 'chromosome scaffold' (drawn in red), keeping the size and shape of the original chromosomes (adapted from Maeshima and Eltsov, 2007). **C** In the 'network model', chromatin fibers (in black) are cross-linked by protein (grey ovals) to form a network-type structure. In this model, protein linkers are the only structural elements that maintain the higher chromosomal organization (adapted from Poirier and Marko, 2002).

3. SMC proteins: master regulators of chromosome dynamics

Structural Maintenance of Chromosome (SMC) proteins were identified as major protein constituents of mitotic chromosomes, together with histones and topo II (Hirano and Mitchson, 1994; Hirano et al., 1997). Protein complexes build on SMC proteins are now

recognized as one of the most fundamental classes of proteins that regulate the structural and functional organization of chromosomes from bacteria to humans (Losada et al., 2002; Nasmyth and Haering, 2005). Their fundamental contribution to chromosome dynamics hence started even before the acquisition of histones during evolution (Hirano, 2006).

SMC proteins are characterized by a long stretch of flexible anti-parallel coiled coil, with an ATP Binding Cassette (ABC) ATPase ('head') at one end and a dimerization ('hinge') domain at the other end. Two SMC proteins interact via their hinge domains to form V-shaped molecules. ATP binding by the head domains induces their engagement (Lammens et al., 2004), resulting in O-shaped molecules. It has been hypotized that ATP binding and hydrolysis by the head domains might produce large-scale structural rearrangements that could be fundamental for the engagement of SMC protein complexes with DNA (see below).

Three different SMC complexes exist in eukaryotes, named cohesin, condensin and Smc5-Smc6 complex (Nasmyth and Haering, 2005). They cover a vast repertoire of chromosome functions. Genetic and cell biology studies have demonstrated their central contributions for sister chromatid cohesion, chromosome segregation during mitosis and meiosis, chromosome-wide gene expression and recombinatorial DNA damage repair (Hirano, 2006).

3.1 Cohesin complexes

3.1.1 Composition and architecture

Cohesin is the best-characterized of the three eukaryotic SMC protein complexes. The core complex contains four subunits, two SMC subunits (Smc1 and Smc3) and two non-SMC subunits (Scc1 and Scc3). All four subunits had been originally identified in genetic screens for yeast mutants that lose cohesion before anaphase onset (Michaelis et al., 1997; Guacci et al., 1997). Cohesin's major function is hence to physically link sister chromatids from the time of their generation by DNA replication during S phase until their segregation upon anaphase onset, when sister chromatid cohesion is lost.

Cohesin's Smc1 and Smc3 subunits heterodimerize via their hinge domains to produce the typical V-shaped SMC dimer. The kleisin subunit Scc1 connects via its N-terminal helical motif and its C-terminal winged-helix domain (WHD) the heads of Smc3 and Smc1, respectively (Haering et al., 2002), and its cleavage by the site-specific protease separase triggers loss of cohesion at the metaphase-to-anaphase transition. The three subunits hence form a ring-like architecture with a diameter of about 40 nm (Fig. 3A). The ring

architecture is well supported by electron micrographs of purified cohesin complexes (Anderson et al., 2002; Fig. 3B). The fourth subunit, Scc3, is recruited to the complex mainly by its interaction with the Scc1 kleisin subunit (Haering et al., 2002). The core cohesin complex interacts with several other proteins, including Wapl/Rad61, Pds5, Eco1 and Sororin, which are thought to have roles in the regulation of cohesin binding to chromosomes, as well as the establishment and maintenance of cohesion (Losada et al., 2005; Gandhi et al., 2006; Kueng et al., 2006; Chan et al., 2012; Panizza et al., 2000).

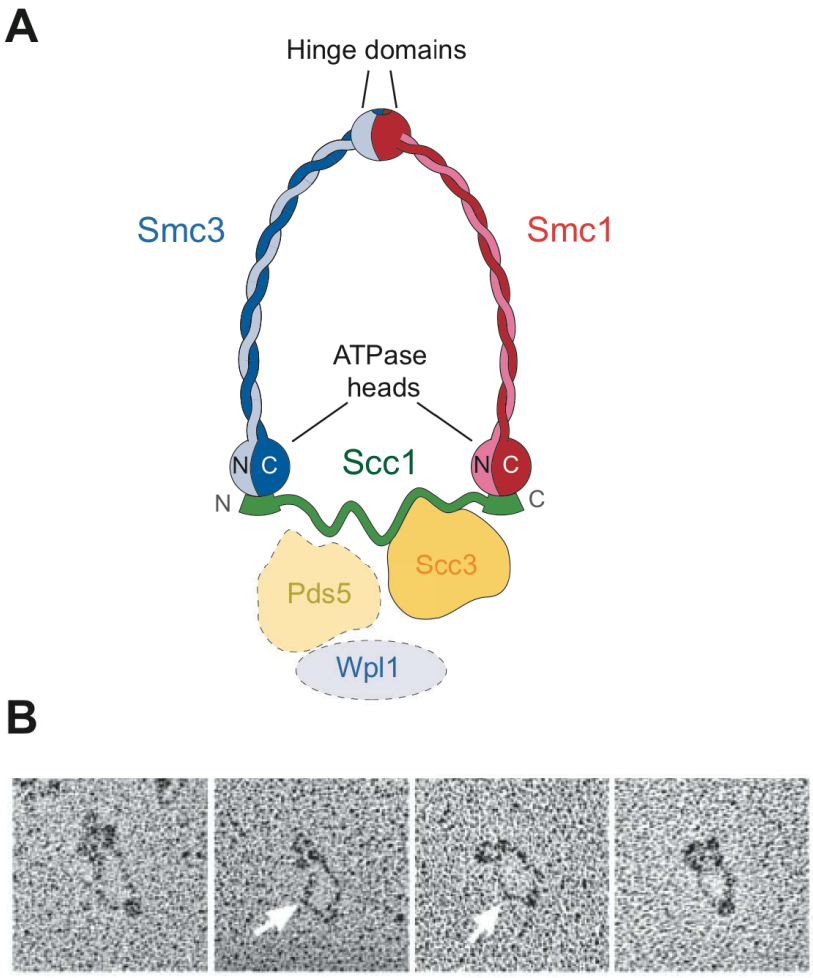

Figure 3. Architecture of the cohesin holocomplex. **A** The budding yeast cohesin holocomplex and its general organization. The complex core subunits are represented by Smc1, Smc3, Scc1 and Scc3. The less stably associated Pds5 and Wpl1 proteins are drawn with dashed borders. **B** Electron micrographs of rotary shadowed cohesin purified from human cells. Cohesin complex display a clear ring conformation. Some of the images show a kink (white arrows) in the coiled coil domain (images reproduced from Anderson et al., 2002).

3.1.2 Biological role

Cohesin was originally identified and named for its role in mediating sister chromatid cohesion, which is essential for chromosome segregation and DNA damage repair. By holding replicated sister chromatids together until anaphase, cohesin generates a counteracting force to the pulling by the microtubule spindle, which allows proper chromosome alignment and segregation. Yeast cells harboring mutant cohesin complexes that fail to associate with chromosomes cannot establish cohesion (Arumugam et al. 2003; Weitzer et al., 2003; Gruber et al., 2006). Without cohesion, sister chromatids could not be segregated equally between the forming daughter cells, resulting in aneuploidy. For the same reason, cohesin plays a crucial role during meiosis I and II. The increase of cohesion defects with increasing maternal age in humans is thought to contributes to the increased incidence of aneuploidy (reviewed in Peters and Nishiyama, 2012).

In addition, sister chromatid cohesion facilitates the 'error-free' repair of DNA double-strand (DSB) breaks of replicated chromosomes by allowing the use of the undamaged sister chromatid as a template for homologous recombination (HR) (reviewed in Watrin et al., 2006a). This is examplified by the finding that mutation of the cohesin subunit Scc1 in *S. pombe* (Rad21) rendered cells hypersensitive to DNA breaks (Phipps et al., 1985; Birkenbihl et al., 1992). Cohesin's role in DNA damage repair is further supported by the specific localization of cohesin to the sites of double-strand breaks (DSBs), which was shown by both immunofluorescence (IF) and chromatin immunoprecipitation (ChIP) experiments (Kim et al., 2002; Strom et al., 2004). Several lines of evidence indicate that cohesin is involved in many other cellular processes (e.g. transcriptional regulation, chromosome condensation and morphogenesis) in addition to its major function in sister chromatids cohesion (reviewed in Mannini et al., 2010).

In several model organism, cohesin loading onto chromosome is achieved through its interaction with Scc2/Scc4 complex (Toth et al., 1999; Ciosk et al., 2000; Seitan et al., 2006; Waitrin et al., 2006b), although other factors might also be required for efficient cohesin recruitment at specific chromosomal sites (Gillespie and Hirano, 2004; Dubey and Gartenberg, 2007). Establishment of sister chromatid cohesion requires that cohesin is loaded onto chromosomes before DNA replication onset and that Smc3 is acetylated by the Eco1 family of acetyltransferase during replication (Ivanov et al., 2002; Zhang et al., 2008; Rowland et al., 2009). It has been proposed that loaded cohesin becomes 'cohesive' by topologically embracing both sister chromatids inside its ring (see below). The mechanism by which cohesin is converted to the 'cohesive' state during DNA replication is not completely understood. In vertebrates, Smc3 acetylation enables the binding of sororin to Pds5, which counteracts Wapl's ability to remove cohesin from chromatin (Schmitz et al.,

2007; Nishiyama al., 2010). Because sororin homologs have not been found in yeast, it remains to be determined how acetylation makes cohesin refractory to Wap1's anti-establishment activity in yeast.

To ensure the timely dissolution of sister chromatid cohesion and thereby ensure proper chromosome segregation during mitosis, yeast cohesin is cleaved by the protease separase at the metaphase-anaphase transition. In humans, most cohesin on chromatid arms is already removed during prophase by Wapl (prophase pathway), and this process is facilitated by Polo-like kinase 1-dependent phosphorylation of the Scc3 subunits SA1 and SA2 (Gandhi et al., 2006; Kueng et al., 2006; Hauf et al., 2005). Only a small amount of cohesin remains associated with centromeres and is protected from the prophase pathway by the shugoshin-PP2A complex (Kitajima et al., 2006; Riedel et al., 2006; Tang et al., 2006). This centromeric pool of cohesin is cleaved by separase at the metaphase-anaphase transition to allow sister-chromatid separation (Waizenegger et al., 2000). Finally, through the Hos1 mediated de-acetylation of Smc3, cohesin complexes are recycled for the establishment of cohesion in the next cell cycle (Beckouet et al., 2010; Borges et al., 2010).

3.1.3 Cohesin's interaction with chromosomes

How does cohesin hold sister chromatids together? The large ring-shaped architecture suggested that cohesin could trapp DNA molecules inside the ring created by Scc1, Smc1 and Smc3 (Haering et al., 2002). The cohesin ring would, in principle, be large enough to encircle two 10 nm chromatin fibers, thus explaining how sister chromatids are held together and also how separase could abruptly destroy cohesion at the metaphase-anaphase transition by opening the ring (see Fig. 4A).

After many years of intense debate, several lines of evidence now strongly support the 'ring model'. The strongest experimental demonstration of the entrapment of sister DNAs within cohesin rings comes from biochemical studies that probe the interaction between cohesin and small circular minichromosomes isolated from budding yeast. As predicted by the ring entrapment model, cohesin's association with minichromosomes is relased upon linearization of the minichromosome DNA by restriction enzyme cleavage, thus suggesting that cohesin rings can slide along the DNA fiber (Ivanov and Nasmyth, 2005). Consistent with the idea that cohesin concatenates sister chromatids by encircling both sisters inside the tripartite ring, covalent closure of cohesin rings produces DNA–cohesin structures that are resistant to protein denaturation (Fig. 4B–D; Haering et al., 2008). Finally, topological loading of cohesin onto naked DNA could recently be reproduced with purified fission yeast cohesin (Murayama and Uhlmann, 2014).

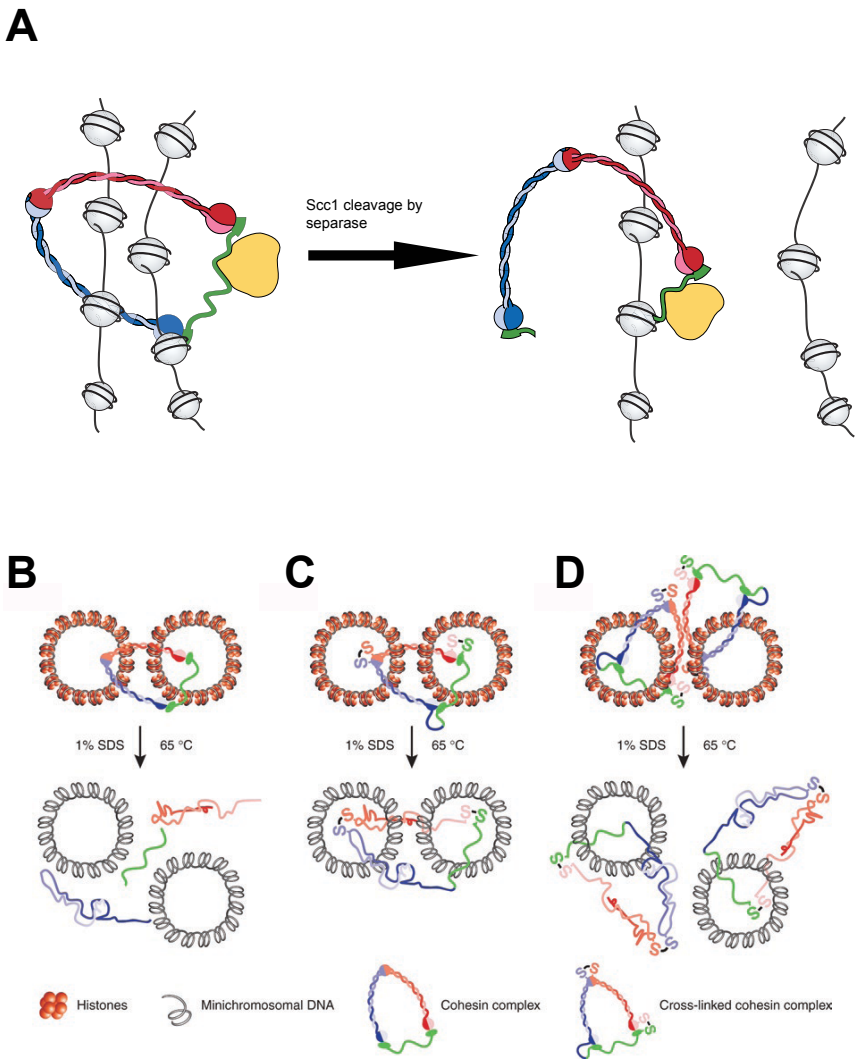

Figure 4. Sister chromatids are held toghether by individual cohesin rings. **A** The ring entrapment model predicts that cohesin connects sister chromatid (represented here as two 10 nm-fiber molecules) by trapping them inside its ring. At anaphase onset, the cleavage of Scc1 by separase opens the cohesin ring, releasing the connection between sisters. **B and C** Ring model representation in which a single cohesin topologically encircles two sister circular minichromosomes. Cohesin complexes (B) are chemically circularized by fusion of the C terminus of Smc3 with the N terminus of Scc1 and crosslinking of engineered cysteine residues at the Smc1–Smc3 and Smc1–Scc1 interfaces (C). **D** Oligomerization model representation in which cohesion between two sister minichromosomes is generated by association of two chromatin-bound modified cohesin complexes. Models in B-D were challenged by using cross-linking to create covalently closed cohesin rings. If the ring model were correct, only covalently closed cohesin rings should hold sister chromatids together even after protein denaturation (C). The direct binding or oligomerization models instead predict that protein denaturation would destroy sister chromatid cohesion (B and D) (adapted from Cipack et al., 2008)

3.2. Condensin

3.2.1 Composition and architecture

Eukaryotic condensin is a pentameric complex (Hirano et al., 1997) with a molecular mass of about 650 kilo Dalton. In yeast, the condensin complex consists of the two SMC subunits, Smc2 and Smc4, the kleisin subunit Brn1, and the two HEAT-repeat (Huntingtin, Elongation factor 3, the A subunit of protein phosphatase 2A, TOR lipid kinase) subunits Ycg1 and Ycs4. In vertebrates, two different condensin complexes exist, which are named condensin I and II. Both complexes contain the same two SMC subunits, SMC2 and SMC4, but differ in the composition of their three non-SMC components (CAP-D2, CAP-G and CAP-H for condensin I; CAP-D3, CAP-G2 and CAP-H2 for condensin II) (see Table 1; Ono et al., 2003; Yeong et al., 2003; Savvidou et al., 2005). Condensin I is more homologous by sequence similarity to the single condensin complex present in unicellular organisms (Thadani et al., 2012).

	SMC		kleisin	HEAT-repeat		
S. cerevisiae	Smc2	Smc4	Brn1	Ycs4	Ycg1	
S. pombe	Cut14	Cut3	Cnd2	Cnd1	Cnd3	
D. melanogaster	Smc2	Smc4 (Gluon)	Barren (Cap-H)	Cap-D2	Cap-G	Condensin I
			Cap-H2	Cap-D3	?	Condensin II
C. elegans	MIX-1	SMC-4*	DPY-26	DPY-28	CAPG-1	Condensin I
			KLE-2	HCP-6	CAPG-2	Condensin II
vertebrates	SMC2 (CAP-E)	SMC4 (CAP-C)	CAP-H	CAP-D2	CAP-G	Condensin I
			CAP-H2	CAP-D3	CAP-G2	Condensin II

Table 1. Subunits of eukaryotic condensin complexes (modified from Piazza et al., 2013)

While cohesin displays V-shaped and ring-shaped conformations (Figure 3B), condensin's structure appears more closed with the coiled-coil arms emanating from the hinge in close contact over most of their lengths (Fig. 5B). EM images of condensin purified from human cells or *Xenopus* oocytes condensin show mostly 65 nm-long rod-shaped molecules,

corresponding to the SMCs coiled coils that separate a large globular domain, possibly formed by the Smc2-Smc4 ATPase heads plus the three non-SMC subunits on one end, and a small globular domain, presumably formed by Smc2-Smc4 hinges on the other end (Anderson et al., 2002). A similar 'head-to-tail' structure was observed also in atomic force microscopy images using purified condensin complexes from fission yeast (Yoshimura et al., 2002). It has been hypothesized that the differences in open and closed structures could contribute to the different roles of condensin and cohesin *in vivo* (Hirano, 2005a).

Biochemical experiments using recombinant human condensin complexes demonstrated that their subunit geometry is similar to that of cohesin complexes (Onn et al., 2007). The kleisin subunits of condensin I and II contact the head domain of SMC2 and SMC4 via their N-terminal helical and C-terminal WHD domains, respectively. In addition, the kleisin subunits function as scaffolds for the binding of the HEAT repeat subunits (Figure 5A). All kleisins might therefore connect the head domains of their associated SMC subunits to form ring structures comparable to cohesin. However, the interactions between the kleisin and SMC subunits might be regulated differently between different SMC complexes. While the assembly of the Scc1 kleisin subunit with the Smc1–Smc3 dimer depends on ATP binding by the Smc1 head domain (Arumugan et al., 2003; Weitzer et al., 2003), condensin's SMC-kleisin interactions can apparently be formed even when the ATPase head domains of Smc2 and Smc4 are not bound to ATP (Onn et al., 2007).

Strikingly, the asymmetric architecture of kleisin's interaction with the SMC head domains is even conserved in prokaryotes. Crystal structures of N- and C-terminal regions of a prokaryotic kleisin in complex with SMC heads suggest that this architecture is strictly conserved even in bacteria (Burmann et al., 2013; see Chapter 3.3).

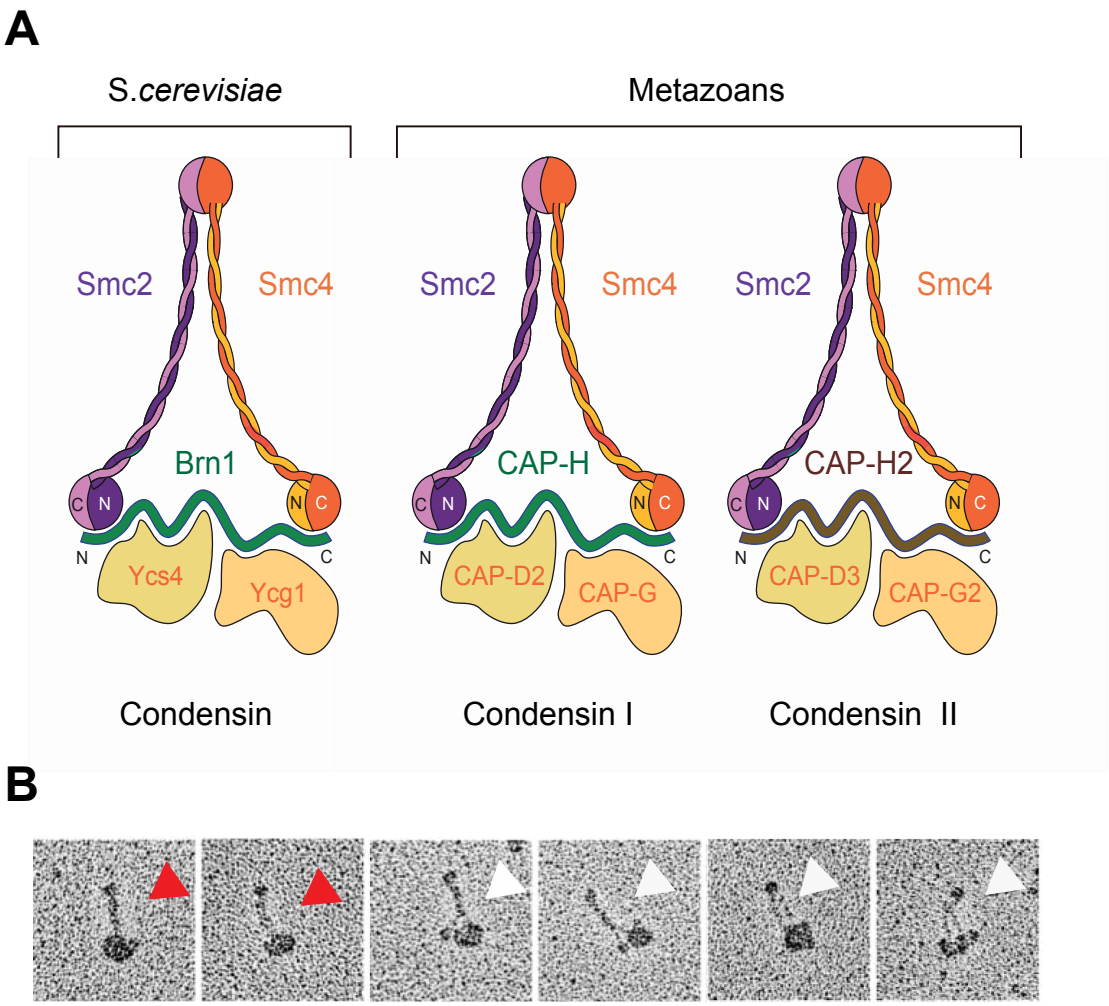

Figure 5. Condensin complexes and their subunits arrangements in eukaryotes. **A** Represented from the left to the right are the budding yeast condensin complex and its metazoan orthologs, condensin I and II. The core structure of the complex consists of five subunits assembled in a 1:1:1:1:1 stoichiometry. **B** Example images of rotary shadowed condensin complexes immunopurified from HeLa cells. Most images show the two coiled coiled domains of Smc2 and Smc4 in close proximity for most of their length (red arrows) producing the 'head-to-tail' conformation. Some images show the two coiled coil domains split apart (white arrows) Such conformations are presumably due to the loosening of interaction between the SMC heads and non-SMC subunit (images modified from Anderson et al., 2002).

3.2.2 Biological roles

Several studies in a range of model systems have demonstrated that condensin has a predominant role in the formation of structurally stable mitotic chromosomes and in their segregation during anaphase (Strunnikov et al., 1995; Saka et al., 1994; Bhat et al., 1996; Sutani et al., 1999; Gerlich et al., 2006; Cuylen et al., 2011).

Consistent with their role as organizers of mitotic chromosomes, condensins were found to associate with mitotic chromosomes in all species studied so far. In several eukaryotic model organisms, the inactivation by mutation or depletion of any of the condensin subunits lead to severe defects in chromosome condensation and chromosome segregation (Bhat et al., 1996; Hirota et al., 2004; Saka et al., 1994; Strunnikov et al., 1995; Hudson et al., 2009). Mitotic chromosome formation in *Xenopus* egg extracts was abolished by immunodepletion of condensin subunits (Hirano and Mitchson, 1994). However, knock-down of condensin subunits in human cells delayed prophase chromosome condensation but did not prevent the formation of apparently normal mitotic chromosomes. Neverthless, such condensin-depleted chromosomes are hypersensitive to mechanical stress (Ono et al., 2003) and fail to segregate correctly during anaphase, resulting in an increased frequency of chromosome bridges and irregular arm formations (Gerlich et al., 2006).

An increasing body of evidence suggests that, in addition to their role in shaping mitotic chromosomes, condensin complexes have also important functions in modulating chromosome architecture during interphase, with roles ranging from the maintenance of genomic integrity, compartimentalization of chromosomal domains to the regulation of gene expression.

Condensin complexes have also been reported to contribute to the maintenance of genomic stability by detecting and/or repairing DNA damage across the entire genome (reviewed in Wu and Yu, 2012). Indication that condensin plays a role in DNA damage repair pathways comes from the discovery that a temperature-sensitive mutant of the fission yeast kleisin subunit Cnd2 exhibited, in addition to the expected mitotic chromosome condensation defects, elevated sensitivity to hydroxyurea (HU)-induced replication fork stalling and UV-induced thymidine dimer formation (Aono et al., 2002). Consistently, depletion of condensin I or condensin II subunits in metazoan model systems caused a decrease in the efficiency to repair single or double strand DNA breaks, respectively (Kong et al., 2011; Schuster et al., 2013).

Condensin complexes were also found to promote the spatial organization of chromatin in the interphase nucleus. In both fission and budding yeast, condensin clusters DNA elements (e.g. Pol III genes) that are usually dispersed throughout the linear genome in different domains of the nuclear periphery (reviewed in Piazza et al., 2013). Clustering of these genes during interphase might be required for regulating their transcription (Iwasaki et al., 2010).

Consistent with the ability of condensin to determine the 3D organization of the genome, CAP-H2 over-expression in flies contributes to the formation of chromosome territories by promoting axial compaction of interphase chromosomes (Smith et al., 2013; Bauer et al., 2012).

Finally, increasing lines of evidence suggest that condensins play important roles in the regulation of gene expression (Machin et al., 2004; Rawlings et al., 2011; Dowen et al., 2013). This function might be particularly important in some organisms such as *C. elegans*, where specialized condensin complexes exist for this purpose (reviewed in Wood et al., 2010). Neverthless, transcription regulation by condensins is thought to be intimately linked to the role of condensins in the regulation of chromosome architecture in eukaryotes (Bhalla et al., 2002).

3.2.3 Chromosomal and subcellular localization of condensin complexes

An essential step towards a full understanding of how condensin complexes execute their many functions in genome dynamics and stability was achieved by the study of condensin localization in several model organisms, using chromatin immunoprecipitation analysis followed by microarray (ChIP-chip) or massive parallel sequencing analysis (ChIP-seq). These genome-wide analyses of condensin binding sites did not reveal any association of condensin with a specific DNA sequence, although a definite pattern of condensin distribution was observed across the genome of all examined organisms. In some cases, condensin was found to associate with promoter regions of highly transcribed genes (i.e. tRNA genes), but most condensin complexes bind preferentially centromeric, telomeric and rDNA regions, confirming that condensin distribution on chromosomes has a remarkable degree of evolutionary conservation (Wang et al., 2005; D'Ambrosio et al., 2008; Tanaka at al., 2012; Kim et al., 2013).

In vertebrates, condensins I and II display strikingly different spatiotemporal localization patterns. Immunofluorescence studies showed that they both bind along chromosome arm axes and to centromeres, but with a distinct binding pattern (Maeshima and Laemmli, 2003; Ono et al., 2004). Fluorescence Recovery After Photobleaching (FRAP) experiments with GFP-tagged kleisin subunits in HeLa cells showed that condensin I, which associates with chromosomes exclusively from the time of NEBD in prometaphase until the end of mitosis, dynamically exchanges on chromosomes throughout mitosis. In contrast, condensin II, which is nuclear throughout the cell cycle, is stabilised on chromatin at the onset of condensation in early prophase (Gerlich et al., 2006). The different localization dynamics of condensin I and II support the notion the two complexes contribute to different step of mitotic chromosome assembly. Condensin II is presumably required for

the early axial shortening of chromosome arms during prophase, whereas condensin I triggers the lateral compaction of chromosomes during prometaphase (Green et al., 2012; Shintomi and Hirano 2011).

Despite its sequence homology with condensin I, budding yeast condensin is localized into the nucleus throughout the cell cycle, similar to mammalian condensin II. On the other hand, fission yeast condensin is predominantly cytoplasmic during interphase and nuclear during mitosis (reviewed in Thadani et al., 2012).

Taken together, these findings suggest that the activity of condensin complexes and their localization on chromosomes need to be strictly controlled to allow proper condensin function. It has therefore been proposed that condensin function is largely regulated by cell-cycle dependent post-translational modifications (Bazile et al., 2010).

3.2.4 Regulation of condensin function

Condensin was reported to be constitutively phosphorylated (Hirano et al. 1997; Takemoto et al., 2004; Takemoto et al., 2006). Yet, the phosphorylation patterns differ significantly between interphase and mitosis, suggesting that phosphorylation may have a major role in condensin's specific localization and regulation over the course of the cell cycle (Takemoto et al., 2004; Takemoto et al., 2006). Multiple mitotic kinases, including Cyclin-dependent kinase 1 (Cdk1), Aurora B, Mps1 and Polo-like kinases (Plks) phosphorylate condensin, although their relative contributions seem to vary in different organisms (Bazile et al., 2010).

In budding yeast, the Cdk Cdc28 phosphorylates *in vitro* Smc4 and is thought to prime the non-SMC subunits of the condensin complex for hyperphosphorylation by the Polo-like kinase Cdc5 *in vivo* (St. Pierre et al., 2009). It has been proposed that mitotic Cdk activity triggers the supercoiling activity of condensin (see below) during anaphase (reviewed in Thadani et al., 2012). Similarly to yeast, Cdk has been shown to phosphorylate a threonine residue on the CAP-D3 subunit of condensin II in mitotic HeLa cells, priming the complex for hyperphosphorylation by PLK1 and ensuring the timely chromosome condensation during prophase (Abe et al., 2011). These findings support the emerging view that a single dominant kinase is not sufficient to regulate condensins function in any organism (Bazile et al., 2010). Consistent with this idea is the finding that phosphorylation of the Cut3 (Smc4) subunit by Cdc2 (Cdk) in fission yeast induces condensin localization to the nucleus upon entry into mitosis (Sutani et al., 1999), whereas its function onto mitotic chromosomes is subsequently regulated by Ark1 (Aurora B) kinase (Nakazawa et al., 2011).

In addition to its established role in creating unattached kinetochores during error correction and regulating mitotic spindle dynamics, Aurora B was found to modulate condensin function in several model organisms. While Aurora B-mediated phosphorylation of Ycg1 (CAP-G, see Table 1) is crucial for the correct segregation of the rDNA locus in budding yeast, condensin loading onto chromosome doesn't seem to be affected by inactivation of this kinase (Lavoie et al., 2004). In contrast, phosphorylation of the condensin I kleisin subunit by Aurora B in fission yeast and human cultured cells has been shown to regulate the loading of the complex onto mitotic chromosomes. Notably, specific inhibition of Aurora B activity abolishes recruitment of condensin to centromeres and on chromosome arms (Tada et al., 2011).

Recent work shows that also Mps1, a dual specifity kinase with an essential role in mitotic progression (Liu and Winey, 2012), phosphorylates a serine residue within the kleisin subunit of condensin II. This phosphorylation is similary required for condensin loading onto chromosomes and accurate chromosome condensation during early prophase (Kagami et al., 2014). It is therefore conceivable that phosphorylation of condensins may play a general role in regulating the loading of the complex onto chromosomes (see below).

3.2.5 Loading of condensin onto chromosomes

While the requirements for loading onto chromatin of cohesin complexes are well described, much less is known about condensin. The conserved structure of the SMC and kleisin subunits in both complexes suggest that there might be similarities in the way how condensin and cohesin bind to chromatin (Cuylen et al., 2011). Chromatin Immunoprecipitation (ChIP) experiments showed that condensin binding sites on budding yeast chromosomes overlap with those of the cohesin loading factor Scc2-Scc4 (D'Ambrosio et al., 2008). Even though there is no evidence that Scc2-Scc4 and condensin interact directly, their co-localization on chromosomes lead to the suggestion that Scc2-Scc4 might act as a chromosome loading factor for all SMC protein complexes. While inactivation of Scc2 indeed decreased condensin binding at tRNA genes (D'Ambrosio et al., 2008), it did not notably affect condensin's overall binding to chromosomes (Ciosk et al., 2000).

It is therefore conceivable that condensin might be recruited onto chromosomes by other factors. In budding yeast, the Replication Fork Barrier (RFB) sites at the 3' end of rDNA genes functions as *cis* element for condensin recruitment in a manner that depends on the RFB-binding protein Fob1 (Johzuka and Horiuchi, 2009). In vertebrates, Protein Phosphatase 2A (PP2A) was found to act as a non-catalytic scaffold for condensin II association with chromatin. Depletion of PP2A from mitotic chromosomes abolishes condensin II, but not condensin I, loading at the onset of mitosis, whereas expression of a

PP2A catalytic mutant rescues its chromosomal association (Takemoto et al., 2009). Condensin I is instead loaded onto chromosomes by the physical interaction with histones. A series of *in vitro* and *in vivo* experiments showed that Aurora B-dependent phosphorylation of the condensin I kleisin subunit triggers its interaction with the basic amino-terminal tails of histones H2A and H2A.Z, which is required for chromatin association of condensin during mitosis. This mechansim is conserved in both fission yeast and human cells (Tada et al., 2011).

However, an additional level of regulation is achieved in fission yeast, where condensin's enrichment at kinetochores and along chromosome arms depends on two region-specific recruiters, the monopolin homologue Pcs1–Mde4 and the Pol III transcription factor TFIIIC, respectively. This notion is based on the findings that the growth defect of a strain that harbours a condensin mutant that specifically fails to associate with chomosome arms is suppressed by a mutation in TFIIIC and that artificial tethering of condensin to centromeres suppresses the growth defect of a strain with defective Pcs1. The distinct localization of condensin to centromeres and chromosome arms may therefore reflect functionally separable pools of condensin (Tada et al., 2011).

In addition to the interaction with specific loading factors, condensin might make additional contacts with DNA itself. Recent biochemical studies with purified condensin subunits have revealed an unexpected *in vitro* DNA binding activity in the non-SMC subunits of the complex (see below). This activity correlates with the crucial role of the non-SMC subunits for the chromosomal loading of condensin in budding yeast and human cells (Piazza et al., 2014).

3.2.6 Condensin's interaction with DNA

Purified condensin complexes were found to bind different DNA substrates *in vitro* (Kimura and Hirano, 1997; Strick et al., 2004). While DNA binding was generally independent of ATP hydrolysis by the SMC subunits, addition of DNA increased the ATP turnover by condensin complexes more than 5-fold (Kimura and Hirano 1997; Kimura and Hirano, 2000). Interestingly, this stimulation was stricktly dependent on the presence of the non-SMC subunits (Kimura and Hirano, 2000; Piazza et al., 2014). It is therefore conceivable that the non-SMC subunits have a role in regulating condensin's interplay with DNA. Electrophoretic Mobility Shift Assays (EMSAs) of different DNA substrates in the presence of purified budding yeast non-SMC sub-complexes indeed showed that the non-SMCs bind to short double-stranded DNA (dsDNA) substrates. This DNA binding activity is presumably essential for condensin's loading onto chromosomes *in vivo*, since binding to chromosomes of yeast or human condensin complexes that contain only one HEAT-repeat subunit is strongly reduced (Piazza et al., 2014).

Even though condensin's ATPase activity seems to be intimately linked to the interaction of the complex with DNA, its precise ceullular function remains unclear. *In vitro* studies using isolated *Xenopus* condensin holocomplexes showed that high concentrations of condensin are capable of inducing ATP-dependent positive supercoiling of circular plasmid DNA in the presence of topoisomerase I (Kimura and Hirano 1997). Visualization via electron spectroscopic imaging of condensin-DNA complexes in presence of ATP suggested that a single condensin complex can wrap DNA in two (positive) gyres, which would result in the formation of compensatory (negative) supercoils in the protein-free region of the circular DNA (Bazett-Jones et al., 2002). This could serve as a mechanism to compact DNA. Consistent with the notion that condensin can compact naked DNA strands, purified condensin I was found to promote the compaction of linear double-stranded DNA in a magnetic tweezer setup. Notably, this reaction depended on ATP hydrolysis and could only be measured when condensin was isolated from mitotic extracts but not when it was isolated from interphase extracts (Strick et al., 2004).

The ability of condensin to alter DNA structure suggests that condensin might recognize and/or stabilize particular DNA conformations. The formation of positive knots in circular plasmid DNA by topo II in the presence of condensin *in vitro* (Kimura et al., 1999) could indeed be the result of a specific binding of condensin to DNA crossover regions. Condensin may therefore contribute to the structure and maintenance of mitotic chromosomes by stabilizing or actively re-configuring DNA topology in concert with topoisomerases (Baxter and Aragon, 2012). This is consistent with the observation that condensin and topo II are both required for the organization of mitotic chromosomes *in vitro* (Adachi et al., 1991) and *in vivo* (Cuvier and Hirano, 2003).

3.2.7 An emerging model for condensin's action on chromosomes

An alternative hypothesis for how condensins shapes mitotic chromosomes comes from the recent discovery that the integrity of the tripartite ring structure composed of the Smc2, Smc4 and Brn1 subunits is necessary for maintaining condensin's association with chromosomes and for the proper segregation of chromosome arms (Cuylen et al., 2011; Cuylen et al., 2013). By entrapping chromatin fibers inside its ring structure, condensin may thus act as a topological linker that fastens different regions of a chromosome arm (Fig. 6).

Consistent with this topological linker idea are *in vitro* biochemical analyses of the interaction between yeast condensin and circular minichromosomes, which show that DNA linearization or proteolytic opening of the condensin ring structure releases condensin's association with minichromosomes without affecting the interaction between the condensin ring subunits (Cuylen et al., 2011). Similarly to cohesin, condensin's primary mode of

binding to chromosomes might hence be of a topological nature. Since efficient dissociation of minichromosomes from condensin required five times higher salt concentrations than for cohesin release (Cuylen et al., 2011), condensin might make additional direct contacts with chromatin (see above).

How could chromatin fibers get entrapped within condensin rings? Recent work suggests the presence of distinct entry and exit gates for DNA in cohesin complexes. Sister chromatids are thought to enter the ring through the Smc1-Smc3 hinge interface (Gruber et al., 2006) and exits via the opening of the Smc3–kleisin interaction (Chan et al 2012; Buheitel and Stemmann, 2013; Eichinger et al., 2013). It is conceivable that similar entry and exit gates exist in condensin. The ATPase activity of the Smc2-Smc4 subunits may regulate the opening and closing of the condensin ring at either gate. Before the nature of DNA entry and exit can be addressed, however, it will be essential to first establish that DNA is indeed topologically entrapped within condensin rings.

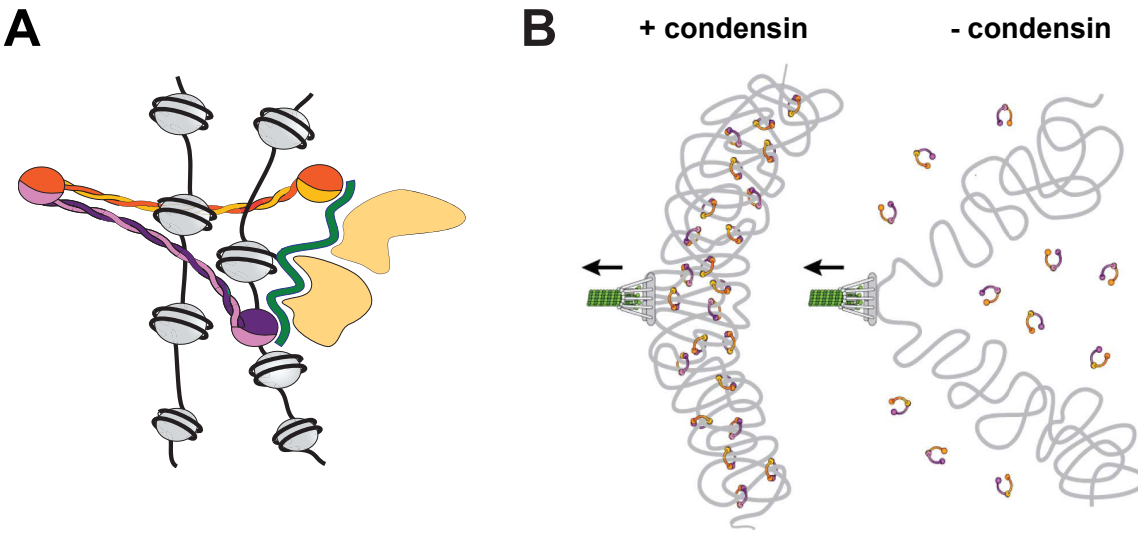

Figure 6. Condensin complexes structure mitotic chromosome through topological links. **A** The ring entrapment model predicts that condensin encircles different segment of DNA inside its ring structure. **B** Condensin complexes may structure chromosomes into rigid bodies that can be moved by mitotic spindle microtubules connected to a single kinetochore (left). Release of condensin would cause loss of chromosome rigidity, followed by stretching of chromosome arms and their lagging behind centromeres during segregation (right) (image adapted from Cuylen et al., 2011).

3.3. Prokaryotic SMC complexes and SMC-related complexes

Prokaryotes possess different SMC and SMC-related complexes. The best-studied complexes are the SMC-ScpAB complex from *Bacillus subtilis* and the MukBEF complex from *Escherichia coli*. They are often referred to as prokaryotic condensins due to the condensin-like phenotypes when either component of the complexes is inactivated. In both complexes, two identical SMC subunits (SMC or MukB) homodimerize via their hinge domains and then recruit two non-SMC subunits (ScpA and ScpB or MukF and MukE), which don't share any general sequence homology with eukaryotic non-SMC subunits (Niki et al., 1991; Moriya et al, 1998; Soppa et al., 2002).

In *B. subtilis*, the kleisin subunit ScpA binds to the SMC homodimer and interacts with ScpB at a stoichiometry of 1:2. ScpB molecules bind each other via their N-terminal WHD regions in a head-to-head orientation. Atomic resolution structures of the SMC-kleisin interaction reveal that ScpA binds to the two heads of the SMC homodimer in different orientations, thereby introducing asymmetry into the tripartite complex (Burmann et al., 2013). The C terminus of ScpA interacts with the ATPase region of one SMC head, while the N terminus of ScpA interacts with the coiled-coil adjacent to the other SMC head (Burmann et al., 2013; reviewed in Nolivos and Sherrat, 2014). In *E. coli*, the MukB homodimer is bridged by two molecules of the MukF kleisin subunit, which dimerize through their N-terminal WHD domains and α-helical bundles. Both MukF subunits contact the SMC heads through a second C-terminal WHD domain (Woo et al., 2009; Yamazoe et al., 1999) to produce a symmetric structure. The central region of each MukF kleisin is bound to a MukE homodimer. ATP-driven engagement by the MukB ATPase head domains is thought to re-arrange the SMC-kleisin interaction in a conformation similar to that of the asymmetric *B. subtilis* SMC-ScpAB complex (reviewed in Nolivos and Sherrat, 2014).

The study of prokaryotic SMC complexes has offered novel insight into how condensin complexes could work. Their ring-like architectures suggest that prokaryotic SMC complexes may encircle DNA similar to eukaryotic SMC complexes. In addition, prokaryotic SMC complexes have been suggested to form multimeric assemblies through the interaction of the non-SMC subunits, which might be physiologically relevant (Mascarenhas et al., 2005, Matoba et al., 2005). It is therefore possible that eukaryotic condensins may mediate long-range chromosomal interactions by the association of two (or more) condensin complexes, which each bind to different segments of a DNA strand. This suggestion is consistent with the cooperative behaviour of condensin I observed during the ATP-dependent compaction of DNA fibres in magnetic tweezer experiments (Strick et al., 2004).

In addition to the canonical SMC complexes, a family of pro- and eukaryotic SMC-like proteins with a role in DNA DSB repair, called Rad50, show architectural similarities with SMC complexes. Rad50 proteins form similarly long intra-molecular coiled coils with ABC ATPase head domains at one end and a dimerization domain at the other end. The Rad50 dimerization domain is, however, much smaller than the SMC dimerization domain and forms a so-called zinc-hook. The Rad50 ATPase head domains are bridged by the nuclease Mre11 (Lammens et al., 2011). In Rad50-Mre11 complexes, ATP-dependent head engagement causes a dramatic rearrangement within the complex, including a rotation of the coiled-coil domain with respect to the Mre11 dimer (Lammens et al., 2011). It is possible that ATP binding might cause similar large-scale structural rearrangements within condensin when its head domains are bound to the kleisin subunit.

In conclusion, the characterization of eukaryotic and prokaryotic condensin complexes has revealed a number of activities, including the ability to topologically encircle DNA, supercoil DNA, hydrolyse ATP and form higher order structures. It is reasonable that condensin's physiological functions require some or all of these activities, which might be regulated by post-translational modifications of the complex.

4. Aims of the PhD project

A growing body of evidence suggests that condensin is the key component for the formation and maintenance of mitotic chromosomes. The molecular basis for its role in structuring mitotic chromosomes is, however, not well understood. To gain insights into condensin's molecular mechanism of action, it will be necessary to first understand the interaction of the complex with its chromosomal substrate.

In the first part of this thesis, I will test the hypothesis that condensin complexes bind to chromosomes by encircling DNA strands topologically within the SMC-kleisin ring structure (Cuylen et al., 2011; Cuylen et al., 2013). I will describe the establishment of a modified *in vitro* biochemical binding assay, which had been originally developed to test the cohesin ring model (Ivanov and Nasmyth 2005; Haering et al., 2008). This assay depends on the isolation of condensin-bound minichromosome complexes from budding yeast, followed by the covalent circularization of condensin rings. If the topological model was correct, then the simultaneous closure of the SMC-kleisin structure should create a chemically circularized condensin ring that should remain bound to minichromosome DNA even after protein denaturation.

Assuming that condensin encircles chromosomal DNA, then this raises the questions how

the DNA enters and exists the condensin ring. It has been proposed that condensin loads onto and unloads from chromosomes through disengagement of one (or more) of the three interfaces between the subunits that form the ring. Covalent closure of the relevant interfaces should therefore prevent condensin loading onto or unloading from chromosomes. In the second part of this thesis, I will use different cross-linking approaches to selectively close condensin subunit interfaces *in vivo* to identify potential gates in the condensin ring. To achieve this goal, I will describe the use of novel protein-protein cross-linking technologies (Rutkoskwa et al., 2011).

In the third part of this thesis, I will describe a complementary study aimed at clarifying whether Scc2-Scc4, the budding yeast loading factor for cohesin, has also a role in the chromosomal turnover of condensin.

II Results

1. Testing the condensin ring hypothesis

Based on the finding that condensin's Smc2, Smc4 and Brn1 subunits form a tripartite ring structure, it has been proposed that condensin may form intra-chromosomal linkages by encircling chromatid segments within this ring. This hypothesis is supported by the findings that the interaction between budding yeast condensin complexes and small circular yeast minichromosomes is lost either by linearization of the DNA or by cleavage of the condensin ring (Cuylen et al., 2011). If the topological model was correct, the introduction of covalent connections between the Smc2-Smc4 hinge domains, the Smc2 head domain and the N terminus of Brn1 (Smc2-Brn1), and the C terminus of Brn1 and the Smc4 head (Brn1-Smc4) interfaces should create a chemically circularized condensin ring, which would have to encircle minichromosomes even after protein denaturation (Fig. 7A). A similar approach had been used previously for cohesin (Haering et al., 2008). In contrast, any non-topological association between condensin and circular minichromosome should be released under these experimental conditions (Fig. 7B).

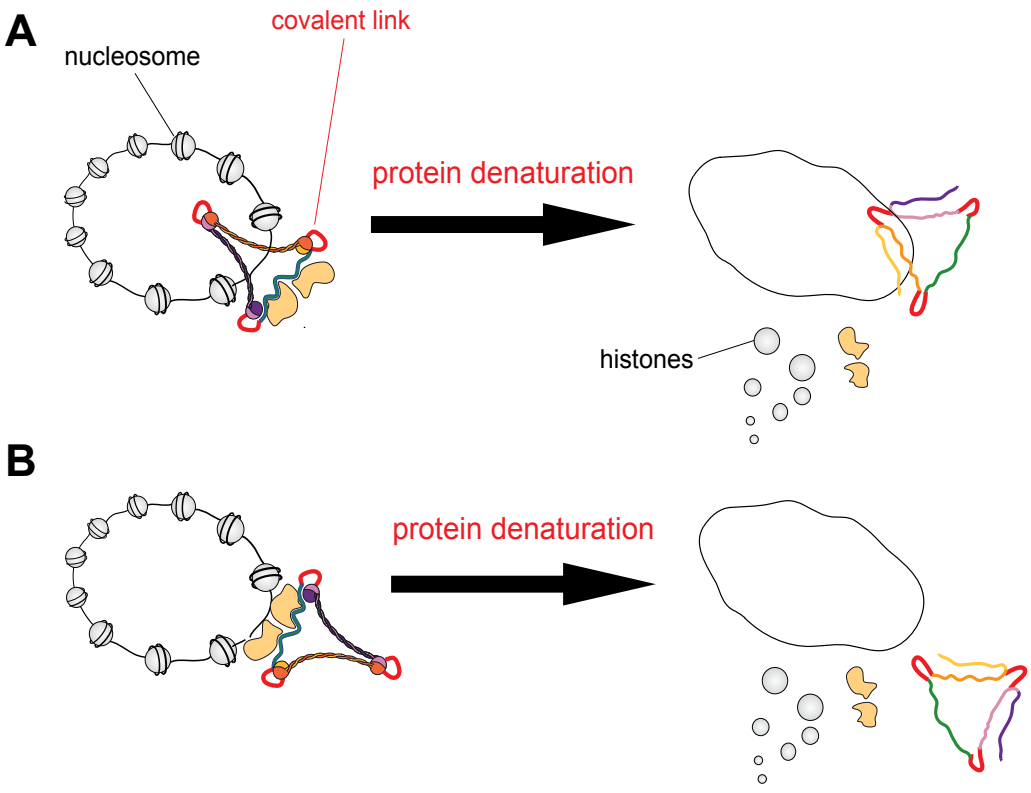

Figure 7. Analysis of condensin binding to circular minichromosomes upon covalent closure of condensin ring. **A** Circularization of the condensin ring prevents the release from minichromosomes upon denaturing conditions if the nature of condensin's interaction with minichromosomes is topological. **B** After protein denaturation, the interaction between covalently closed condensin rings and the circular minichromosomes would be lost if condensin bound to minichromosomes via a non-topological mechanism.

1.1. Chemical cross-linking of Smc2-Smc4 and Brn1-Smc4 interfaces

To connect the Smc2-Smc4 hinge and Brn1-Smc4 interfaces, I used the homo-bifunctional thiol-reactive chemical dibromobimane (bBBr), which can bridge two thiol groups at distances of 5-8 Å (Fig. 8). Based on the crystal structures of the *Thermotoga maritima* SMC hinge (Haering et al., 2002) and the *S. cerevisiae* Smc1 head bound to the C-terminal domain of Scc1 (Haering et al., 2004), homology models of the corresponding interfaces in the condensin complex were created. I identified two juxtaposed side chains of amino acid residues with the required distance constraints in two α-helices of the Smc2–Smc4 dimerization interface (Fig. 9A) and in a loop region between two predicted α-helices of Brn1's WHD and a β-strand in the ATPase head of Smc4 (Fig. 10A). I then used site-directed mutagenesis to replace the identified residues with cysteine residues in ectopic copies of the *SMC2*, *SMC4* and *BRN1* genes. The modified genes complemented the deletion of the essential endogenous genes when expressed from an ectopic copy under the control of the *SMC2*, *SMC4* and *BRN1* promoters in budding yeast (data not shown).

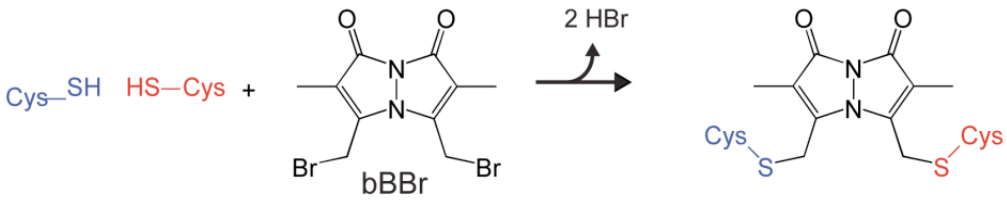

Figure 8. Covalent connection of adjacent cysteine residues by dibromobimane. Reaction schemes for crosslinking juxtaposed thiol groups with dibromobimane (bBBr). bBBr reacts mainly with thiol groups in an S_N2 mechanism to yield thioether linkages. Thiol groups of adjacent cysteine residues are depicted in red and blue.

To test whether cross-linking occurs between the modified condensin subunits, I immunoprecipitated the modified condensin holocomplexes from yeast cell extracts via an HA_6-tag fused to the Brn1 subunit. I then eluted the purified complex from the immunoprecipitation beads by Prescission protease cleavage of three copies of the Prescission protease cleavage sequence between the HA_6-tag and the Brn1 protein (Figures 9B and 10B, right scheme) and ran the eluted samples on an SDS PAGE gel to resolve all five subunits of the complex as individual bands, whose identity I could assign by mass spectrometry (data not shown).

As judged by Coomassie staining of the eluates, incubation of purified complexes with bBBr created an additional high-molecular weight band corresponding approximately in size to cross-linked Smc2-Smc4 or Brn1-Smc4 only when cysteine pairs were present at either the Smc2-Smc4 or the Brn1-Smc4 interfaces, but not when only one of the proteins contained a cysteine residue (Fig. 9B and Fig. 10B). To confirm the identities of the additional bands, I generated strains where I in addition fused Smc4 and Smc2 to different epitope tags. I then performed cross-linking of the immunopurified complexes directly on the beads and analyzed the cross-linked samples by Western blotting against each epitope tag. This confirmed that the high molecular weight bands must be cross-linked species of Smc2 and Smc4 (Fig. 9C) or Brn1 and Smc4 (Fig. 10C), respectively. I used the fluorescence signals of the semi-quantitative Western blot to estimate cross-linking efficiencies. While the cross-linking efficiency of the Smc2-Smc4 interface was ~65% (Fig. 9D), cross-linking at the Brn1-Smc4 interface was less than 20% (Fig. 10D).

I conclude that covalent connection of the Smc2-Smc4 and Brn1-Smc4 interfaces by bBBr cross-linking can be achieved, although cross-linking of the latter is only moderately efficient.

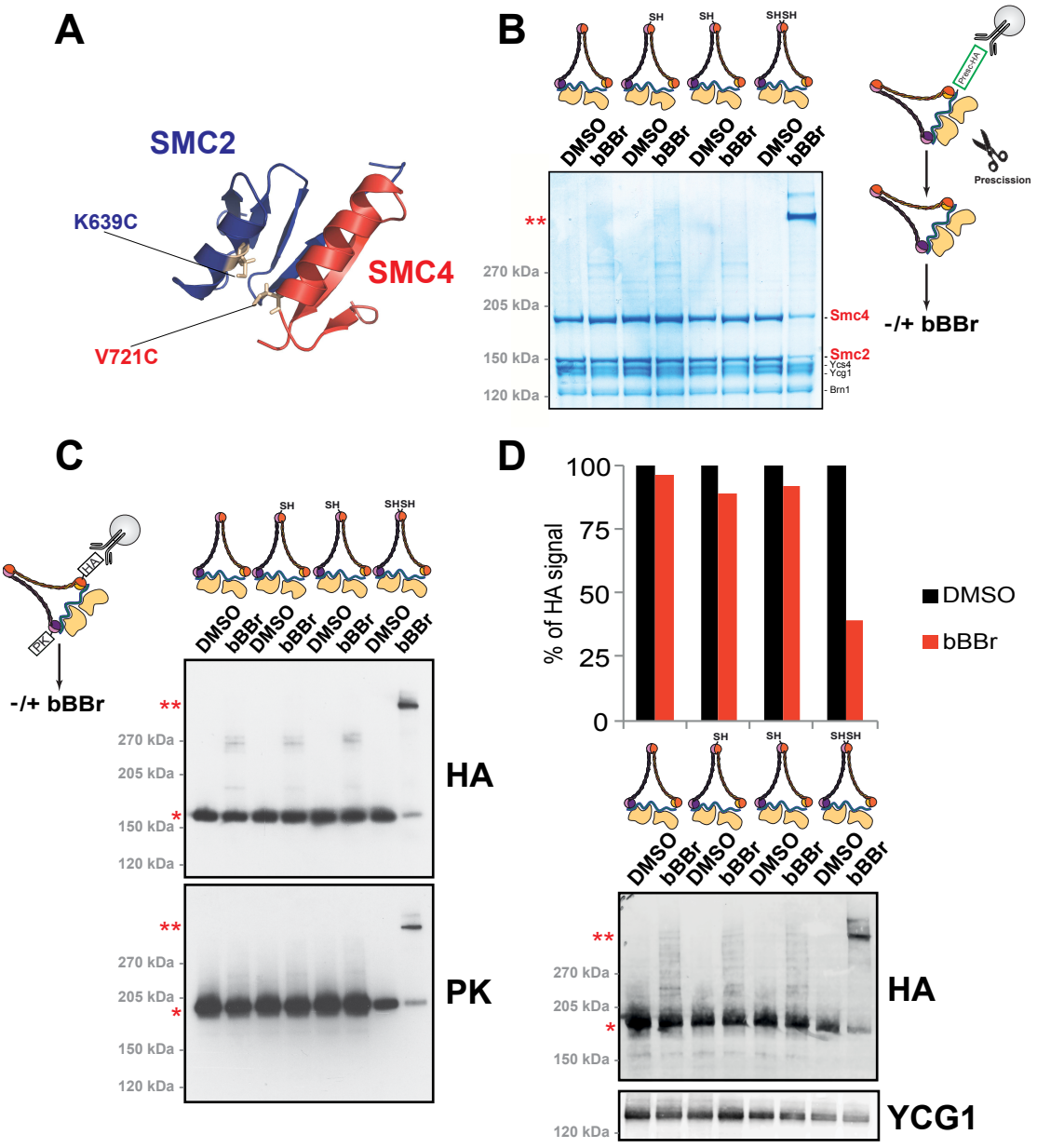

Figure 9. bBBr cross-linking of purified condensin holocomplexes: covalent closure of the Smc2-Smc4 hinge. **A** Homology model of the Smc2-Smc4 hinge interface using the homodimeric *Thermotoga maritima* structure. The introduced cysteine are represented as sticks (in wheat colour) in the outer helices of the hinge dimerization interface (Haering et al., 2002). **B** Eluted wild-type and cysteine mutant condensin complexes were treated with DMSO or bBBr for 10 minutes at 4°C. Samples were analyzed by SDS-PAGE and visualized by Coomassie staining. **C** Condensin mutants harboring an HA_6 or a PK_6 tag on Smc4 or Smc2, respectively, were immunoprecipitated from extracts with an anti-HA antibody, followed by incubation with DMSO or bBBr on the beads (cross-linking on the beads). After cross-linking, samples were split and analyzed by Western blotting against HA and PK epitopes. **D** Samples treated as in C were analyzed by semi-quantitative Western blotting using anti-HA and a polyclonal anti-Ycg1 antibody. Smc2-Smc4 efficiency of cross-linking was estimated by normalizing the signal of the monomeric band (*) in the HA blot to the Ycg1 banc intensity. High molecular weight products generated in presence of bBBr are indicated (**).

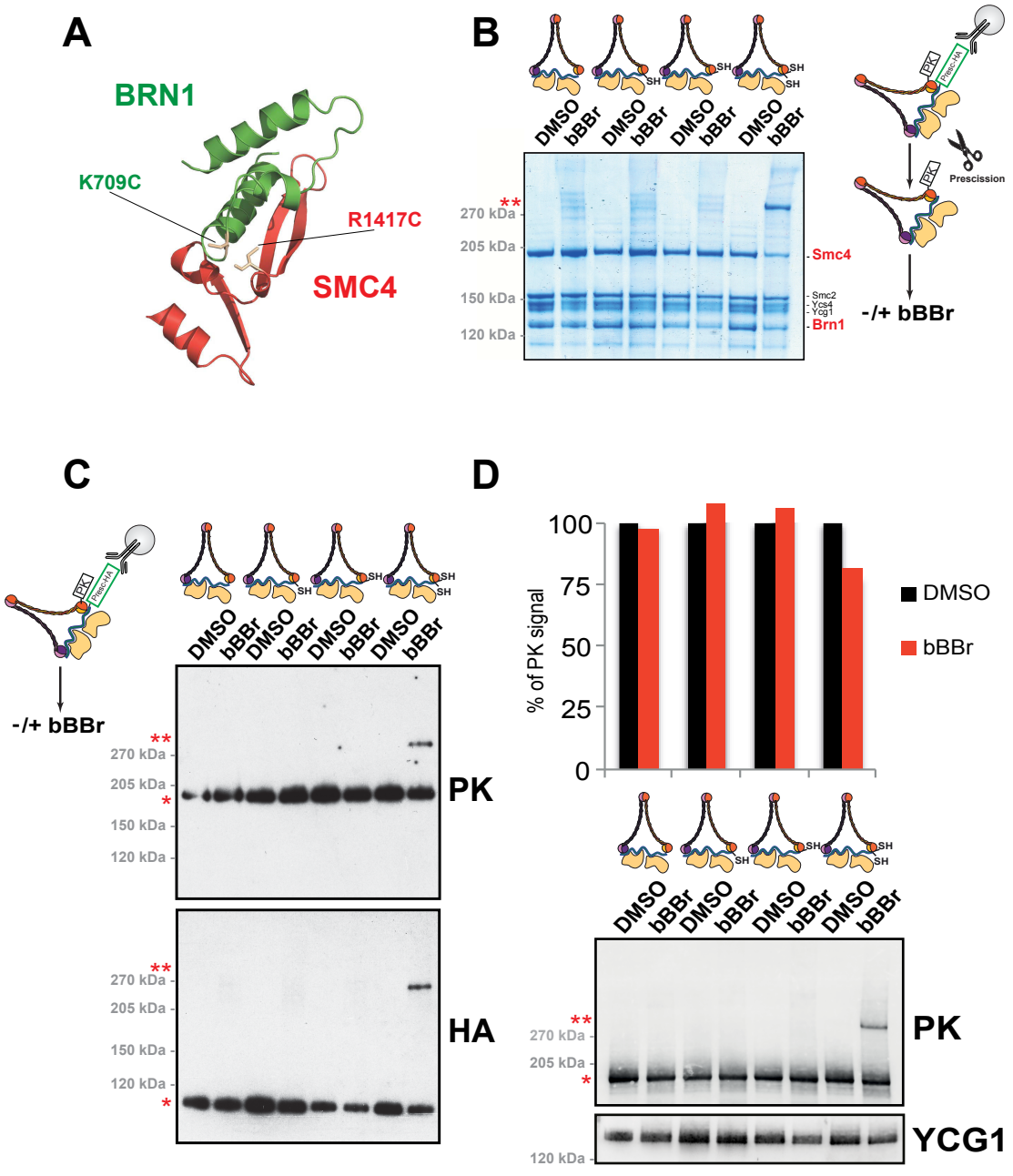

Figure 10. bBBr cross-linking of the Brn1-Smc4 interface. **A** A homology model of the Brn1-Smc4 interface using the Scc1-Smc1 yeast structure (Protein Data Bank 1W1W) identified two juxtaposed residues in a predicted loop region of the C-terminal WHD of Brn1 and the ATPase domain of Smc4 at a distance compatible with cross-linking when mutated to cysteine. **B and C** SDS–PAGE of purified complexes of wild-type and cysteine mutant condensin harboring a PK_6 tag on Smc4 after cross-linking in solution followed by Coomassie staining (B) or cross-linking on the beads followed by Western blot analysis (C). **D** Quantitation of Brn1-Smc4 cross-linking efficiency was performed by normalizing the signal of the monomeric band (*) in the PK blot to Ycg1 signal. High molecular weight products generated in presence of bBBr are indicated (**).

1.2. Smc2-Brn1 closure by fusing both proteins via a flexible peptide linker

Because no structural information was available for the Smc2-Brn1 interface, I decided to link Smc2 and Brn1 by creating a fusion protein. I used a flexible linker peptide sequence to connect the C terminus of Smc2 with the N terminus of Brn1 (Smc2-Brn1) to create a continuous peptide chain of the two proteins. Introduction of three Tobacco Etch Virus (TEV) cleavage sites in the linker sequence allows the cleavage of the peptide sequence (see scheme in Figure 11A).

I integrated the *SMC2-BRN1* fusion gene under the control of the *BRN1* promoter in diploid yeast cells heterozygous for *BRN1* and *SMC2* gene deletions. Tetrad dissection demonstrated that strains expressing the Smc2-Brn1 fusion protein were growing more slowly than strains expressing individual Smc2 and Brn1 proteins, even at 25°C. This suggests that fusion of the Smc2-Brn1 interface impairs condensin function. To test whether condensin complexes that contain the Smc2-Brn1 fusion protein associate with (mini)chromosomes, I immunopurified the complexes from yeast strains harboring a 4.0 kb circular minichromosome via the C-terminal HA-tag on Smc2-Brn1 and probed for minichromosome co-purification by Southern blotting (Figure 11B). Similar amounts of minichromosomes co-purified with condensin complexes containing the Smc2-Brn1 fusion protein as with condensin complexes without the Smc2-Brn1 fusion. This suggests that, at least at a temperature of 25°C, the Smc2-Brn1 fusion does not interfere with condensin loading onto (mini)chromosomes.

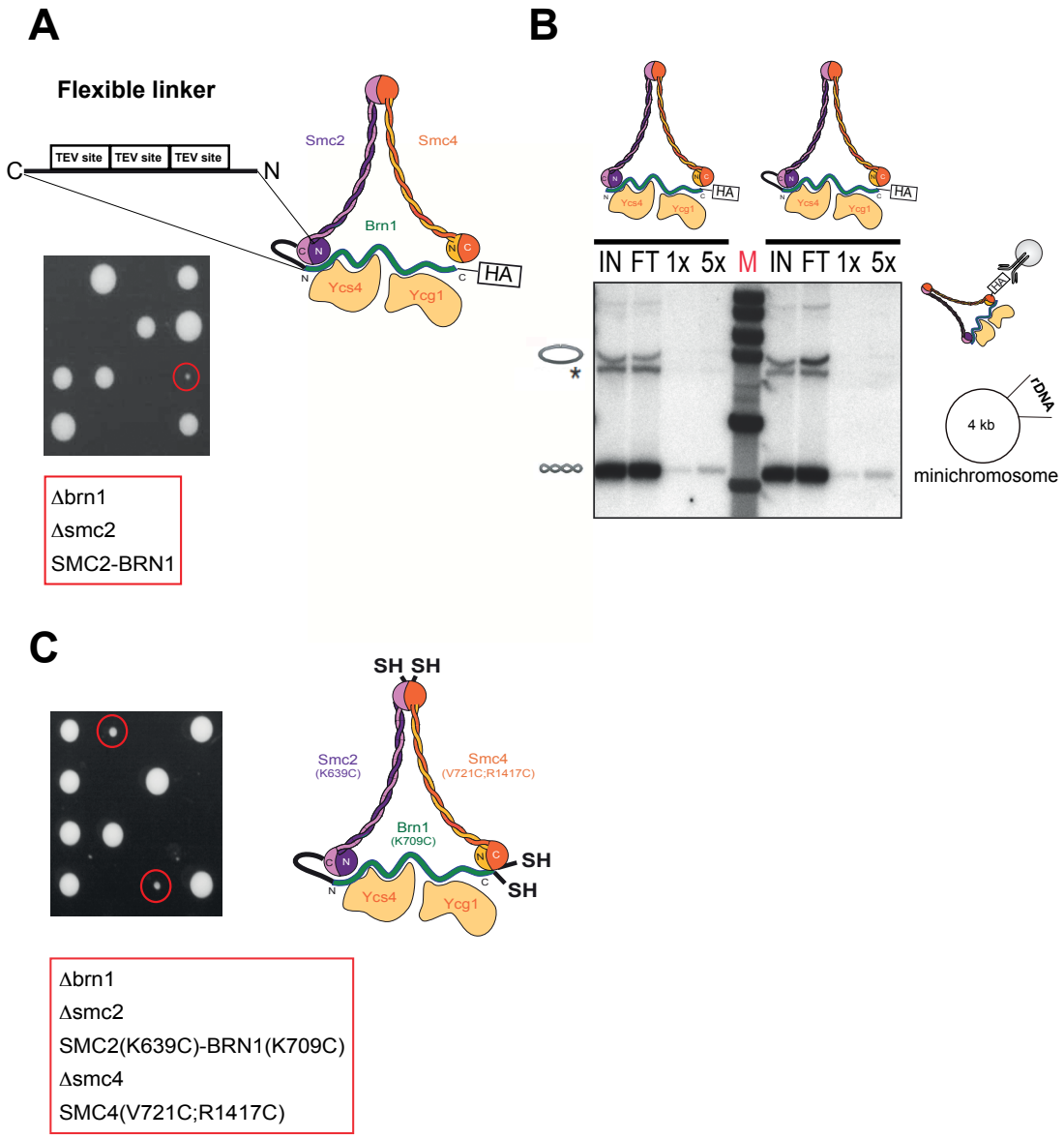

Figure 11. A Modified condensin complex that can be chemically circularized. **A** Smc2-Brn1 closure by fusing both proteins via a flexible peptide linker (scheme on the upper part). Tetrad dissection plate showing growth at 25°C of a strain harboring *SMC2-BRN1* and *SMC2*, *BRN1* deletions (red circle). **B** Co-immunoprecipitation of a 4.0 kb rDNA minichromosome (Cuylen et al., 2011) from extracts of asynchronous yeast cultures with condensin harboring Brn1-HA6 or condensin harboring Smc2-Brn1-HA6 was tested by Southern blotting of input (IN), flow-through (FT) and immunoprecipitated fractions (B, concentrated 1× or 5× relative to input). Relaxed (oval) or supercoiled (braided oval) monomers and supercoiled concatemers (*) are indicated (Cuylen et al., 2011). **C** Genotypes of spores from diploid yeast strains harboring cysteine residues in Smc2-Brn1 and Smc4 (MATa/α SMC2(K639C)-BRN1(K709C)-HA6/Dbrn1/Dsmc2 SMC4(V721C; R1417C)/Dsmc4) after dissection on YPAD at 25°C (red circled spores).

1.3. Creation of condensin complexes that can be covalently circularized

To produce a condensin ring that can, in addition to the Smc2-Brn1 fusion, be covalently connected at the other two interfaces by bBBr cross-linking, I introduced cysteine substitutions into the Smc2-Brn1 and Smc2-Smc4 interfaces. Ectopic expression of Smc2(K639C)-Brn1(K709C) and Smc4(V721C, R1417C) complemented deletion of the endogenous *SMC2*, *BRN1* and *SMC4* genes (Fig. 11C). Considering the cross-linking efficiencies of the individual interfaces, I estimate the fraction of condensin rings that are cross-linked simultaneously at the Smc2-Smc4 and Brn1-Smc4 interface to be ~12%.

1.4. Establishment of a new condensin-minichromosome binding assay

Isolated condensin-minichromosome complexes were reported to be a suitable system for investigating the nature of condensin's association with chromosomes (Cuylen et al., 2011). I decided to adapt this *in vitro* binding assay in order to test the condensin ring hypothesis.

To set up the conditions of the assay, I first used the condensin-related cohesin complex, for which topological entrapment of sister DNAs had been demonstrated by cross-linking of the tripartite ring formed by Smc3, Smc1 and Scc1 (Haering et al., 2008). The original assay relied on the enrichment of cohesed sister minichromosomes by gradient centrifugation, followed by cross-linking in solution. Since such an approach cannot be used later to enrich condensin-bound minichromosomes, I aimed for isolation of cohesin-minichromosome complexes by immunoprecipitation. I introduce the original 2.3 kb minichromosome or a 4.0 kb minichromosome, which contained part of the rDNA locus, into a yeast strain expressing versions of Smc1 and an Smc3–Scc1-HA_6 fusion protein that contained either cysteine pairs at both Smc1-Smc3 and Scc1-Smc1 interfaces or, as control, only single cysteine residues at each interface (Fig. 12A). I then isolated from extracts of asynchronous cells cohesin-minichromosome complexes by immunoprecipitation via the HA_6-tag on the Smc3-Scc1 fusion protein.

I incubated the immunoprecipitated samples either with bBBr or DMSO solvent only, quenched the reaction by addition of dithiothreitol (DTT), added SDS to a final concentration of 1%, and heat denatured the samples at 65°C. The last step also eluted the samples from the immunoprecipitation beads. I then tested whether cohesin-minichromosome complexes had been maintained by Southern blotting of the eluate fractions after agarose gel electrophoresis. If cohesin were still bound to minichromosome DNA after protein denaturation, I expected the presence of additional bands with lower electrophoretic mobility (Haering et al., 2008 and Figure 12A).

In the samples that contained cohesin rings with a single cysteine residue at each interface, I detected two major bands that correspond to supercoiled and relaxed (nicked) circular 2.3 kb minichromosome DNA, independent of whether the samples had been incubated with bBBr or DMSO only (Fig. 12B). The faster migrating species corresponds to supercoiled minichromosome monomers, the slower migrating species corresponds to a mixture of relaxed (nicked) monomers and supercoiled-supercoiled (catenated) dimers (see Haering et al., 2008). In addition, I detected minor bands that correspond to linear minichromosome DNA and supercoiled-relaxed dimers.

Incubation with DMSO of the samples that contained cohesin rings with cysteine pairs at each interface produced the same pattern of bands for the 2.3 kb minichromosome. Incubation with bBBr caused, in contrast, the appearance of two additional species (Fig. 12B). The more abundant DNA species migrated slightly more slowly than supercoiled monomers, whereas the less abundant species migrated slightly more slowly than supercoiled dimers and relaxed monomers. As shown before, these additional bands correspond to denatured cohesin complexes bound to supercoiled monomers or dimers, respectively (Haering et al., 2008).

Similarly, I observed the appearance of an additional band that migrated slightly more slowly than supercoiled monomers when I incubated with bBBr cohesin rings with cysteine pairs at both interfaces bound to the 4.0 kb minichromosome substrate (Fig. 12C). The band for the condensin-bound supercoiled dimers can presumably not be resolved from the free supercoiled dimers and relaxed monomers.

In conclusion, I established a biochemical assay for cross-linking of cohesin-minichromosome complexes after immunoprecipitation, which could next be applied to condensin-minichromosome complexes.

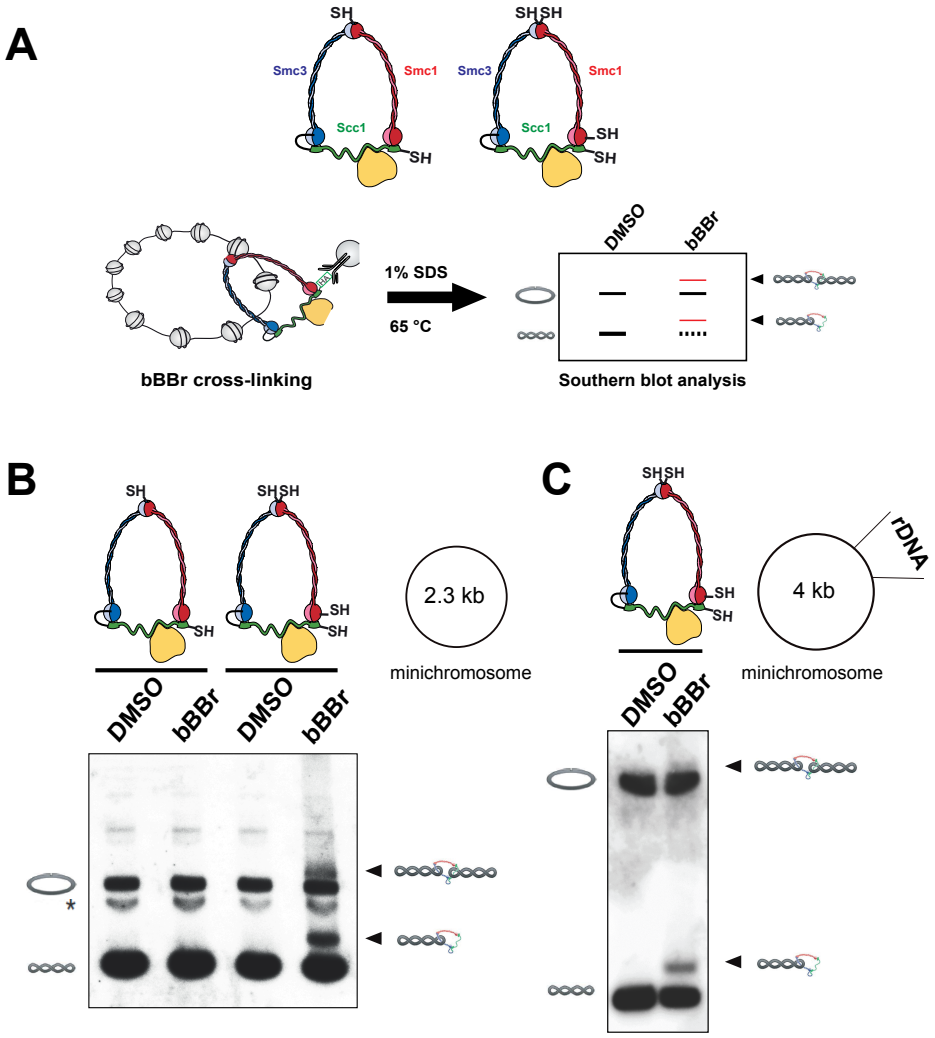

Figure 12. A new *in vitro* biochemical assay to test the ring entrapment model. **A** Schematic representation of the *in vitro* assay. Upper part: strains expressing a modified Smc3-Scc1 fusion protein and Smc1 with different subsets of cysteines were used for setting up the assay. Bottom part: cohesin-minichromosome complexes were isolated from yeast extracts and cross-linked on the beads. After elution, minichromosome bands were detected by Southern blot analysis using a specific radiolabelled probe against the minichromosome DNA. Only samples in which all three cohesin ring subunit interfaces have been covalently linked should contain additional slower migrating bands (red lines). **B** and **C** Minichromosome band analysis of cross-linked cohesin immunoprecipitations with a 2.3 kb minichromosome (B) or a 4.0 kb rDNA minichromosome (C)**.** Relaxed (oval) or supercoiled (braided oval) monomers and supercoiled concatemers (*) are shown. SDS-resistant cohesin-minichromosome complexes are indicated by black arrowheads.

1.5. Crosslinking of cohesin- and condensin-minichromosome complexes

To test whether condensin binds minichromosomes in a topological fashion, I isolated from asynchronous cell extracts condensin-minichromosome complexes by immunoprecipitation via the HA_6-tag on the Smc2-Brn1 fusion protein and compared its association with that of cohesin-minichromosome complexes, which I isolated in an analogous manner. Since condensin has been reported to bind with higher efficiency to minichromosomes containing rDNA regions (Cuylen et al., 2011), I used the 4.0 kb minichromosome for these experiments. I then added bBBr or DMSO solvent only to the immobilized protein-minichromosome complexes and processed the samples for Western and Southern blot analysis (Fig. 13A).

Western blot analysis demonstrated successful cross-linking of Smc3-Scc1 to Smc1 in cohesin and Smc2-Brn1 to Smc4 in condensin. In the case of cohesin, I observed the appearance of additional bands that might be the result of separase cleavage within Scc1 in asynchronous cell (Gruber et al., 2006; Fig. 13B). As already seen before (Fig. 12C), Southern blotting revealed the appearance of an additional band in samples treated with bBBr for cohesin, which corresponds to denatured cohesin complexes still bound to monomeric supercoiled minichromosomes (Fig. 13C). Strikingly, incubation of the condensin samples with bBBr, but not with DMSO solvent, created an additional band that migrated with similar electrophoretic mobility (Fig. 13C). The abundance of the two additional DNA species was consistent with the overall cross-linking efficiency of cohesin (~30%, see Haering et al., 2008) and condensin rings (~12%, see above): cohesin circularization shifted ~26% of the supercoiled monomers, condensin circularization shifted ~10% of the supercoiled monomers (Fig. 13D). The formation of the slower migrating species is therefore directly proportional to the efficiency of chemical circularization of the ring structures formed by the different SMC-kleisin subunits.

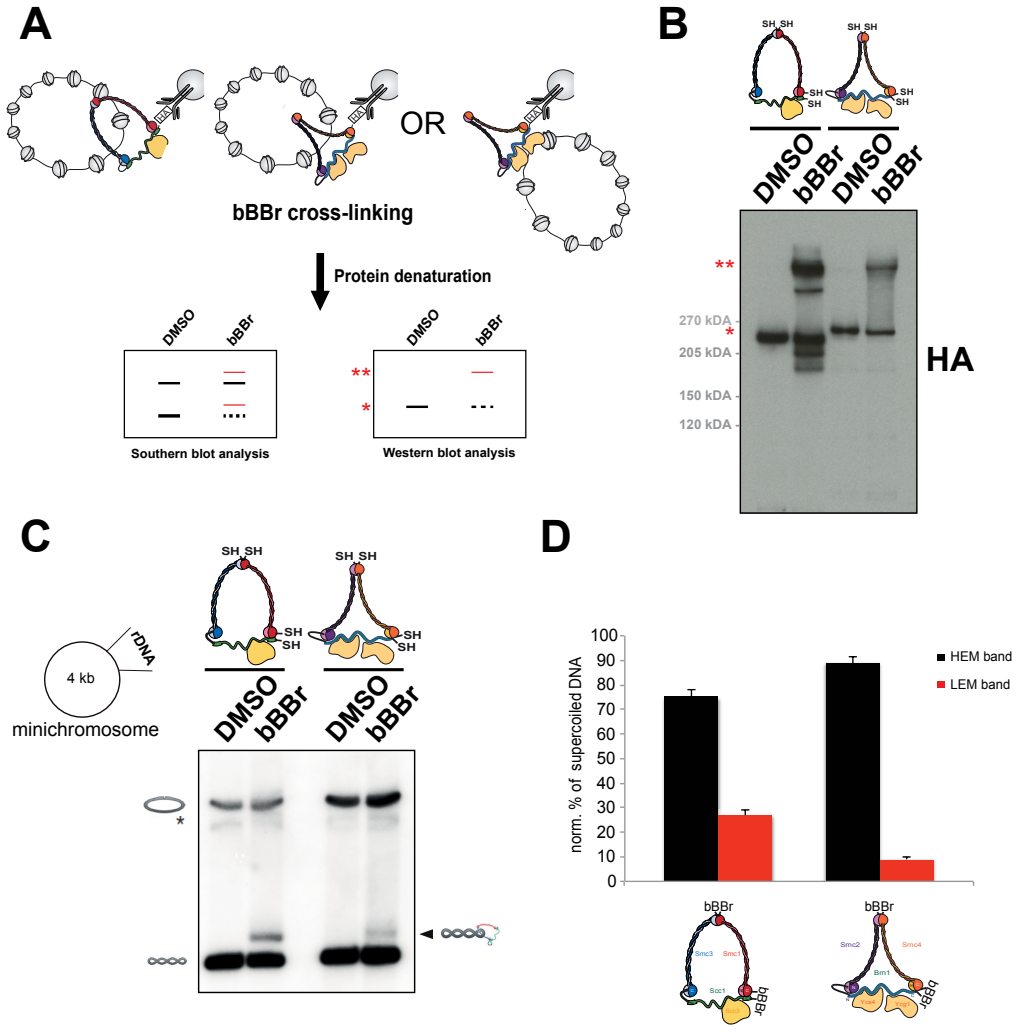

Figure 13. Chemical circularization of cohesin and condensin ring produces SDS-resistant DNA species. **A** Schematic representation of the *in vitro* assay for isolated cohesin- and condensin-minichromosome complexes. Condensin binding to minichromosomes is depicted by two different cartoon models, one for a topological interaction (left) and the other for a direct interaction (right). After cross-linking and protein denaturation, samples were split and analyzed by Western blot or by Southern blot analysis. **B** Smc3-Scc1-HA$_6$ and Smc2-Brn1-HA$_6$ were probed by Western blotting of DMSO or bBBr treated samples. The monomeric band of the fusion protein and the main high molecular weight product generated in presence of bBBr, are indicated (* and **, respectively). **C** Cohesin and condensin co-immunoprecipitated minichromosomes were assayed by Southern blotting after incubation with DMSO or bBBr. **D** Quantitation of supercoiled minichromosome band intensities in bBBr treated samples. High electrophoretic mobility bands (HEM) and low electrophoretic mobility bands (LEM) intensities were normalized against the total amount of supercoiled monomeric DNA in the sample. The average of three independent experiments is shown; error bars indicate standard deviations.

1.6. Formation of SDS-resistant condensin-minichromosome complexes requires covalent connection of all three interfaces of the condensin ring

To test whether the appearance of the slower migrating band depends on the covalent circularization of condensin rings, which the topological model predicts, I generated yeast strains harboring modified condensin subunit with none or only a single cysteine pairs at either the Smc2-Smc4 or the Brn1-Smc4 interface. To furthermore assay whether also higher order condensin-minichromosome complexes would form, I transformed these yeast strains with the 2.3 kb instead of the 4.0 kb minichromosome. I then isolated from the extracts of asynchronous cells condensin-minichromosome complexes by immunoprecipitation, cross-linked as described before, and probed by Southern blotting for the appearance of additional bands (Fig. 14A).

Importantly, incubation of minichromosomes bound by condensin complexes that contained no or only a single cysteine pair with bBBr produced the same bands as incubation with DMSO only (Fig. 14A). However, incubation of minichromosomes bound by condensin complexes that contained cysteine pairs at both Smc2-Smc4 and Brn1-Smc4 interfaces produced an additional band equivalent to the additional band observed with the 4.0 kb minichromosome before (Fig. 13C). This result proofs that the generation of SDS-resistant species is due to the simultaneous cross-linking of Smc2-Smc4 and Brn1-Smc4 interfaces (Fig. 14A). Unlike for the cohesin cross-linking experiments (Fig. 12B), I could not observe a cross-linked supercoiled dimer band in these experiments (see also below).

If the formation of an SDS-resistant supercoiled minichromosome species indeed depended on the circularization of condensin rings, I would expect that opening the condensin ring by TEV protease cleavage of the Smc2-Brn1 linker peptide after cross-linking should result in the loss of this species (Fig. 14B). I therefore incubated cross-linked condensin-minichromosome complexes with TEV protease or buffer only before denaturing the samples. While incubation of cross-linked condensin-minichromosome complexes with buffer did not influence the presence of the slower migrating band, incubation with TEV protease resulted in its disappearance (Fig. 14C).

In conclusion the production of SDS-resistant condensin-minichromosome complexes depends on the formation of covalently circularized condensin rings, as predicted by the topological model.

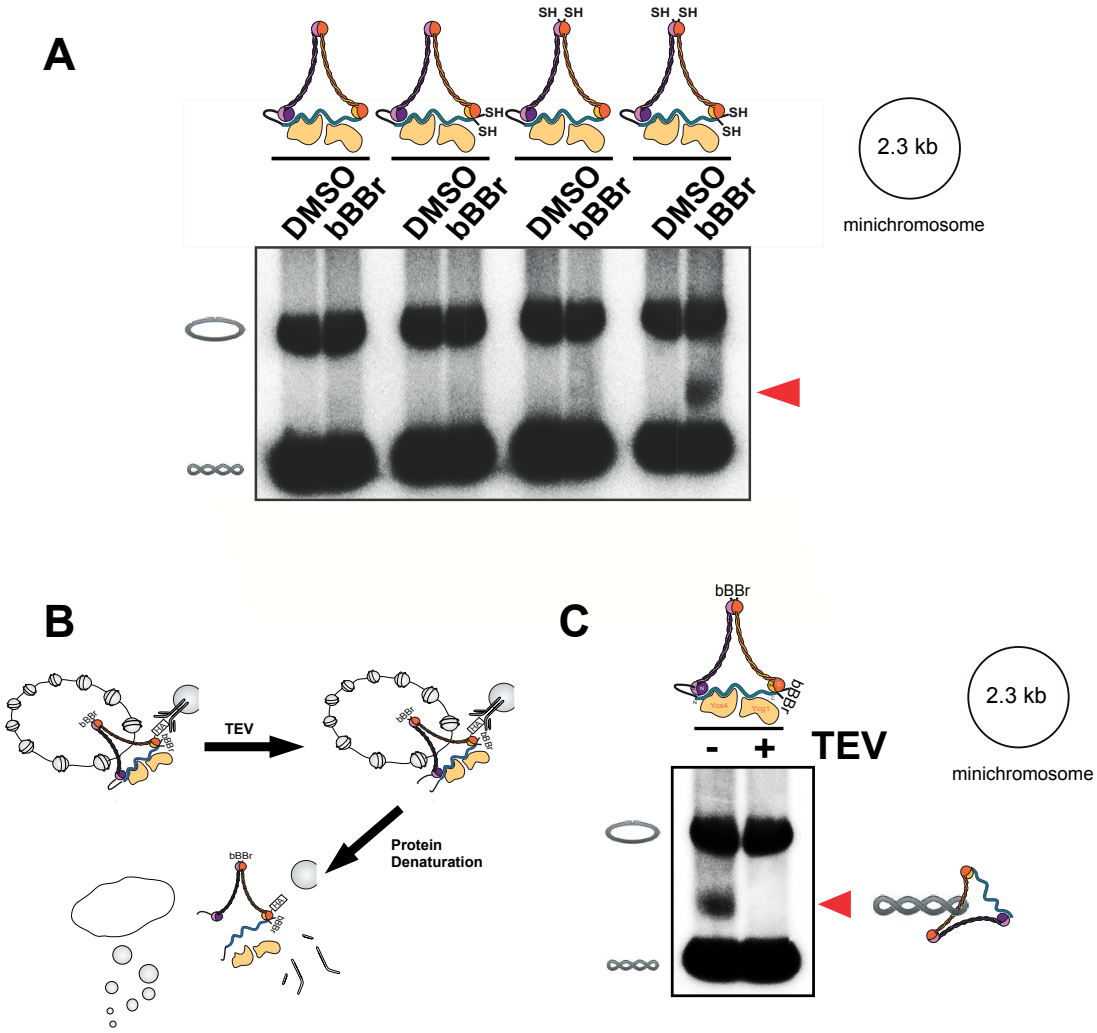

Figure 14. Closure of condensin ring produces SDS-resistant condensin-minichromosome complexes. **A** 2.3 kb minichromosomes were co-purified with condensin complexes harboring Smc2-Brn1-HA$_6$ and Smc4 with none or different subsets of cysteine pairs. After cross-linking, minichromosome bands were analyzed by Southern blotting. **B** If SDS-resistant DNA bands were produced by covalently closed condensin rings still bound to minichromosomes, then opening of the condensin ring by TEV cleavage followed by protein denaturation should release the minichromosome and eliminate the formation of the additional band. **C** Crosslinked minichromosome samples were incubated at 30°C for 1 hrs with or without TEV protease before denaturation. The slower migrating band corresponding to condensin-bound supercoiled monomers disappeared upon TEV incubation, thus confirming that this SDS-resistant species is formed by entrapment within condensin rings as indicated by the red arrowhead.

1.7. Condensin rings encircle only single minichromosomes

My experiments demonstrated that condensin encircles minichromosome DNA. To test whether condensin encircles individual minichromosomes or might link two (sister) minichromosomes similar to cohesin (Fig. 15A; Haering et al., 2008), I investigated more closely the minichromosome band pattern after chemical circularization of condensin or cohesin rings bound to replicated 2.3 kb minichromosomes.

To purify SMC complexes bound to replicated minichromosomes, I arrested cells in a mitotic-like state by addition of nocodazole (Ivanov and Nasmyth, 2005 and 2007) before extract preparation and immunoprecipitation. Consistent with the notion that sister minichromosome DNAs are entrapped within the same cohesin ring, cross-linking of cohesin-minichromosome complexes produced an upshifted band of supercoiled dimeric minichromosomes. The intensity of this band considerably increased in minichromosome samples isolated from nocodazole-arrested cells compared to minichromosomes samples isolated from asynchronous cells (Fig. 15B), to approximately the same intensity as the upshifted monomer band. I then repeated the cross-linking experiments with condensin-minichromosome complexes isolated from nocodazole-arrested cells. While chemical circularization of the condensin ring created a clearly identifiable upshifted monomeric band, I could not detect an upshifted dimeric band (Fig. 15C). This suggests that condensin encircles only individual but not duplicated chromatin fibers within its ring, which is consistent with the notion that condensin plays no role in sister chromatid cohesion (Guacci et al., 1997; Michaelis et al., 1997; Cuylen et al., 2011).

In conclusion, chemical circularization of condensin ring produced only monomeric SDS-resistant condensin-DNA species even when condensin is in complex with sister minichromosomes.

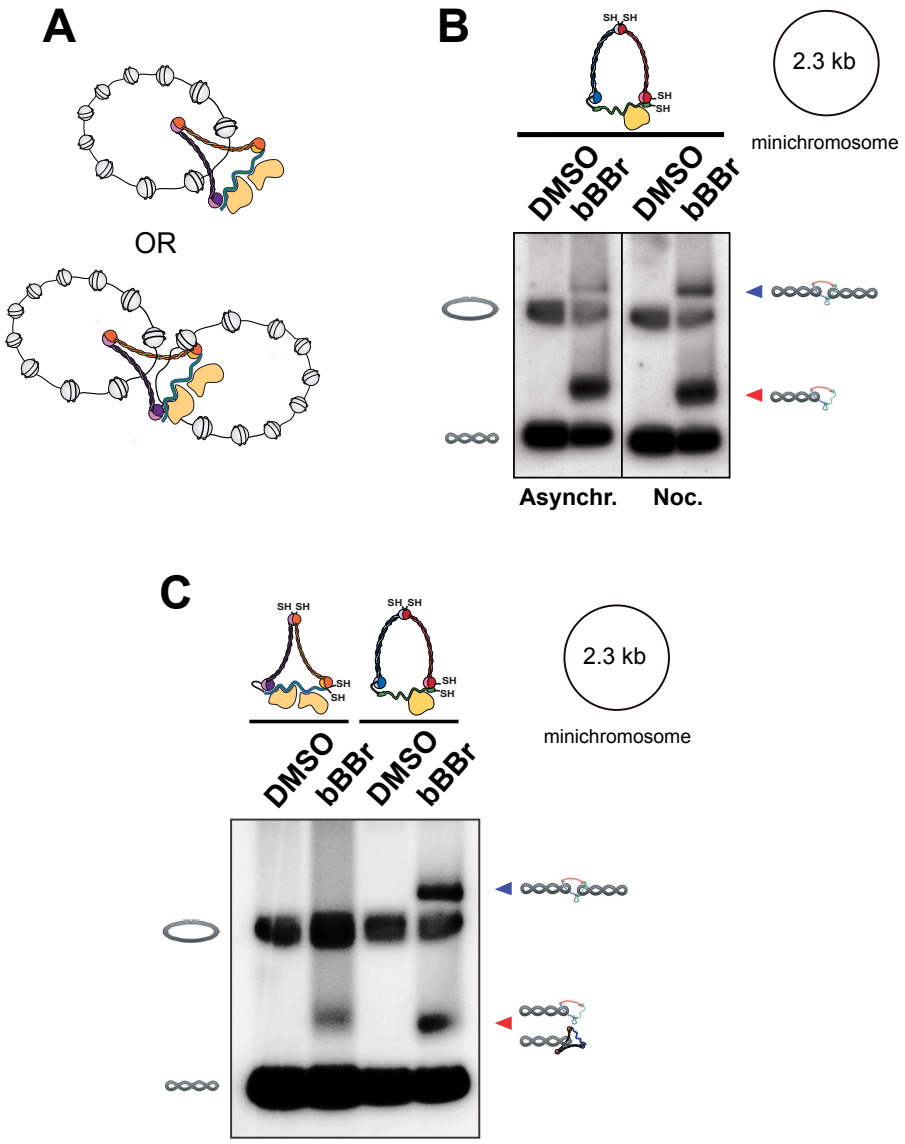

Figure 15. Simultaneous closure of condensin rings does not produce SDS-resistant dimeric minichromosomes. **A** Schematic model depicting condensin encircling either one or two minichromosomes within its ring structure. **B** Isolated cohesin-(2.3 kb) minichromosome complexes from non-mitotic or mitotic extract were cross-linked and analyzed as described previously. As shown in the Southern blot, cross-linking of mitotic cohesin-minichromosome complexes produced an increase in the formation of dimeric supercoiled minichromosomes that are resistant to protein denaturation (upper cartoon). **C** Condensin- or cohesin-minichromosome complexes were immunoprecipitated from mitotic extracts. After cross-linking, minichromosome bands were analyzed by Southern blotting. Unlike for cohesin, chemical circularization of condensin rings produced monomeric but not dimeric SDS-resistant minichromosomes in the presence of bBBr.

2. Covalent closure of condensin rings *in vivo*

In the first part of this thesis, I provided evidence that condensin rings encircle chromosomal DNA inside the tripartite structure formed by the Smc2-Brn1-Smc4 subunits. Since most condensin exists as pre-assembled rings even when it is not bound to chromosomes (Onn et al., 2007), DNA must entry or exit condensin rings by the opening of one or more of the three interfaces between the subunits that form the ring. To test which of the three possible 'gates' is involved in condensin loading onto and unloading from chromosomes, respectively, I devised a plan to close each of the three 'gates' in living cells.

2.1. Which condensin ring interface might act as gate for DNA?

It has been suggested that ATP hydrolysis by the SMC head domains produces the temporary opening of cohesin ring (Arumugam et al., 2003; Weitzer et al., 2003), presumably at the Smc1-Smc3 hinge interface (Gruber et al., 2006), to allow the entry of chromosomal DNA. It is therefore possible that the Smc2-Smc4 hinge functions in an analogous manner in condensin rings. However, the observation that condensin complexes defective in ATP hydrolysis can still associate with mitotic chromatin argues against this hypothesis (Hudson et al., 2008).

Recent reports suggest that another gate is involved in the release of cohesin from chromosomes. Artificial blockage of the Smc3-Scc1 interface in flies and human cells was found to increase the stability of cohesin binding to mitotic chromosomes (Eichinger et al., 2013; Buheitel and Stemman 2013). Consistent with the hypothesis that dissociation of the Smc2-Brn1 interface in condensin might be physiologically important, I found that closure of this interface by expression of an Smc2-Brn1 fusion protein affected the growth of budding yeast cells, even at 25°C (see Chapter 1.2 of the Results Section and Fig. 16A).

To test whether dissociation of the Brn1-Smc4 interface might similarly be necessary for condensin function, I generated a diploid yeast strain with heterozygous *BRN1* and *SMC4* deletions, where I expressed Brn1 and Smc4 as a fusion protein by connecting the C terminus of Brn1 with the N terminus of Smc4 via a TEV-cleavable peptide linker (Fig. 16A). Tetrad dissection after sporulation of the diploid strains produced viable spores that expressed the Brn1-Smc4 fusion protein over *BRN1* and *SMC4* deletions. In contrast to the cells that expressed the Smc2-Brn1 fusion protein, cells that expressed the Brn1-Smc4 fusion protein were growing similar to wild-type cells.

To test whether SMC-kleisin fusions affect merely sporulation or also mitotic cell growth, I spotted different dilutions of mitotically growing cells onto plates at different temperatures and compare their growth to that of a wild-type strain. While the growth of the Brn1-Smc4 fusion strain was undistinguishable from that of the wild-type strain at all temperatures tested, growth of the Smc2-Brn1 strain was considerably slower at 25°C and 30°C and almost completely abolished at 37°C (Fig. 16B).

In conclusion, these results suggest that covalent closure of the Smc2-Brn1 interface, but not of the Brn1-Smc4 interface, interferes with condensin function. I cannot rule out at this point that the effect of the Smc2-Brn1 fusion might be due to a lower expression of the fusion protein compared to the expression of the individual Smc2 and Brn1 subunits, although in Western blot analysis the levels of Brn1-Smc4 and Smc2-Brn1 are approximately similar to the level of Brn1 expressed alone (Fig. 16C). I therefore decided to start investigating whether the Smc2-kleisin interface functions as a potential gate for DNA entry into or exit from condensin rings (Fig. 16D).

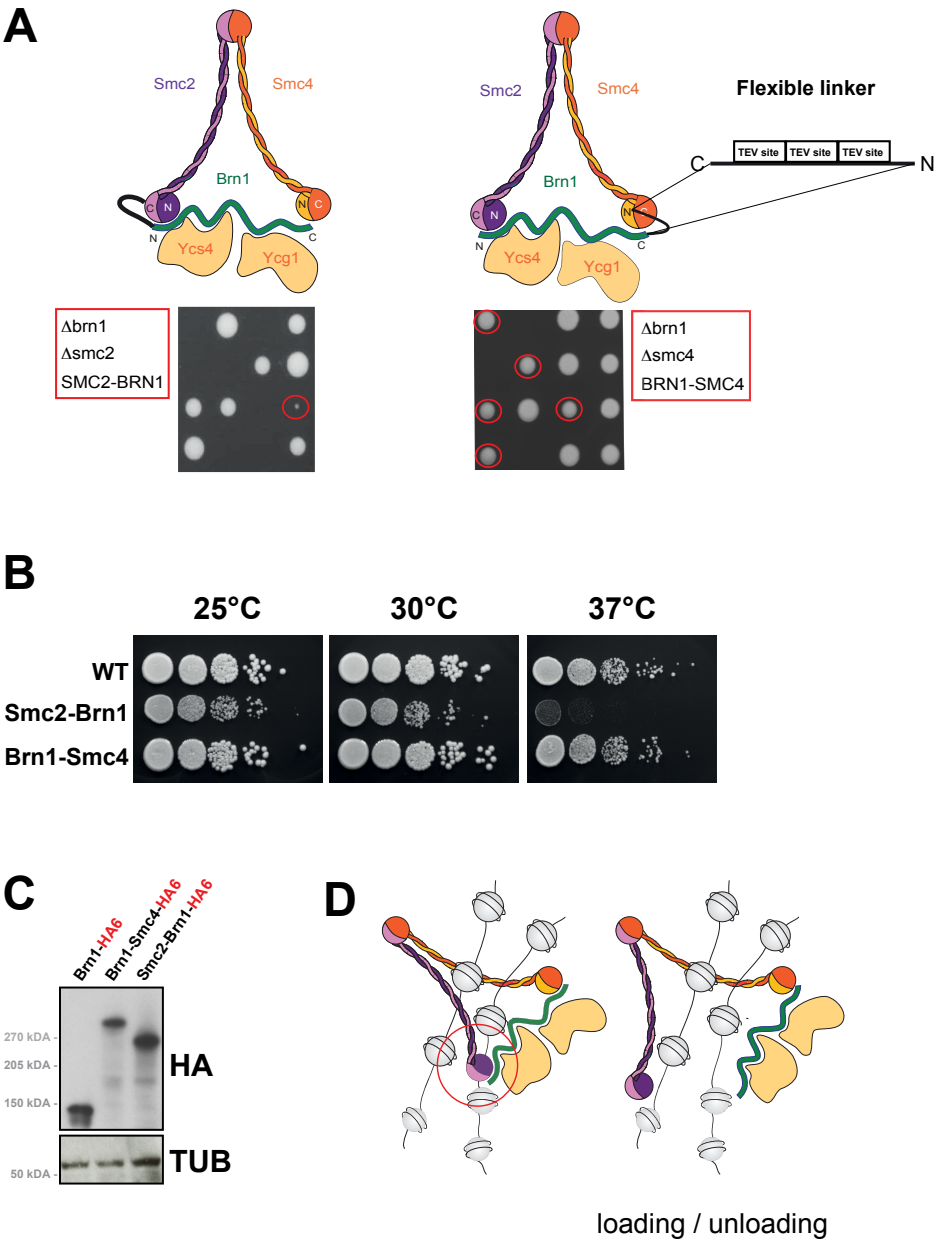

Figure 16. Brn1-Smc2 but not Brn1-Smc4 interfaces has a role in condensin function. **A** BRN1-SMC4 spores harboring *BRN1* and *SMC4* gene deletions were grown after dissection on YPAD at 25°C (right panel). Tetrad dissection plates were compared with the SMC2-BRN1 plates (left of the panel). Fusion of Brn1-Smc4 interfaces produced more viable spores than Smc2-Brn1. **B** 10-fold serial dilutions of yeast cultures were spotted onto the same YPAD plate and tested for their ability to grow for 2 days at 25°C, 30°C and 37°C in comparison with a wild-type (WT) strain. **C** Total extracts obtained from haploid strain harboring either Brn1 fusion construct were analyzed by Western blotting against the HA epitope (as indicated). Detection of tubulin (TUB) was used as loading control. **D** A model for the role of the Smc2-Brn1 interface in regulating condensin's chromosomal turnover.

2.2. Cross-linking of the SMC2-kleisin interface in mammalian cells

To test whether the SMC2-kleisin interface is involved in condensin's turnover on chromosomes, I decided to establish a system to close this interface in living cells. Since assays to measure condensin turnover had been successfully developed in mammalian cells (Gerlich et al., 2006), I decided to use the same model system for my experiments. The mammalian condensin I complex associates with chromosomes exclusively from the time of nuclear envelope breakdown (NEBD) until the end of mitosis. It should therefore be possible to test whether blocking of the SMC2-kleisin interface of condensin I results in a failure of condensin I to associate with chromosomes upon NEBD or a failure to dissociate from chromosomes upon exit from mitosis.

To close the interface between SMC2 and the condensin I kleisin CAP-H, I decided to use the hetero-bifunctional cross-linker BG-CrAsH (Fig. 17A; Rutkowska, Haering and Schultz, unpublished), which is based on the homo-bifunctional cross-linker xCrAsH (Rutkowska et al, 2011). In contrast to xCrAsH, which covalently connects two tetracysteine (4cys) peptide motifs, BG-CrAsH forms covalent bonds between a 4cys motif and a SNAP tag (Keppler et al., 2004; Jansen et al., 2007) in living cells. If placed at the SMC2 and CAP-H interface, *in vivo* hetero-dimerization of the SNAP and 4cys tags should close the SMC2-CAP-H interface of human condensin I complexes (Fig. 17B).

2.2.1 Generation of a stable cell line expressing SMC2-SNAP and 4cys-CAP-H

In collaboration with Ania Rutkowska, I generated stable cell lines that can be induced to express siRNA-resistant (denoted by an asterisk; see details in the legend of Figure 18A) versions of SMC2 fused at its C terminus to a SNAP-EGFP tag and of CAP-H fused at its N terminus to a $FLAG_3$-4cys tag (Fig. 18A). I used Flp-In™ T-REx™ 293 cells for targeted integration of SMC2*-SNAP-EGFP and $FLAG_3$-4cys-CAP-H* genes separated by a 'self-cleaving' picornavirus peptide sequence (2A peptide) into the single FRT site present at a transcriptionally active genomic locus. This enabled tetracycline-induced expression of the modified subunits after knockdown of the endogenous SMC2 and CAP-H genes (Szymczak-Workman et al., 2013; Fig. 18A-C).

Western blot analysis of cell lysates showed that SMC2*-SNAP-EGFP and $FLAG_3$-4cys-CAP-H* were expressed to detectable levels after doxycycline induction (Fig. 18C). The same analysis of cell lysates 72 hours after siRNA transfection revealed that expression of the transgenes was resistant to knockdown, whereas both endogenous proteins were efficiently depleted by the siRNAs (Fig. 18D). However, doxycycline-induced expression

of the SMC2*-SNAP-EGFP and FLAG$_3$-4cys-CAP-H* transgenes was considerably lower than expression of the endogenous SMC2 and CAP-H proteins, even after siRNA knockdown of the latter (Figure 18E).

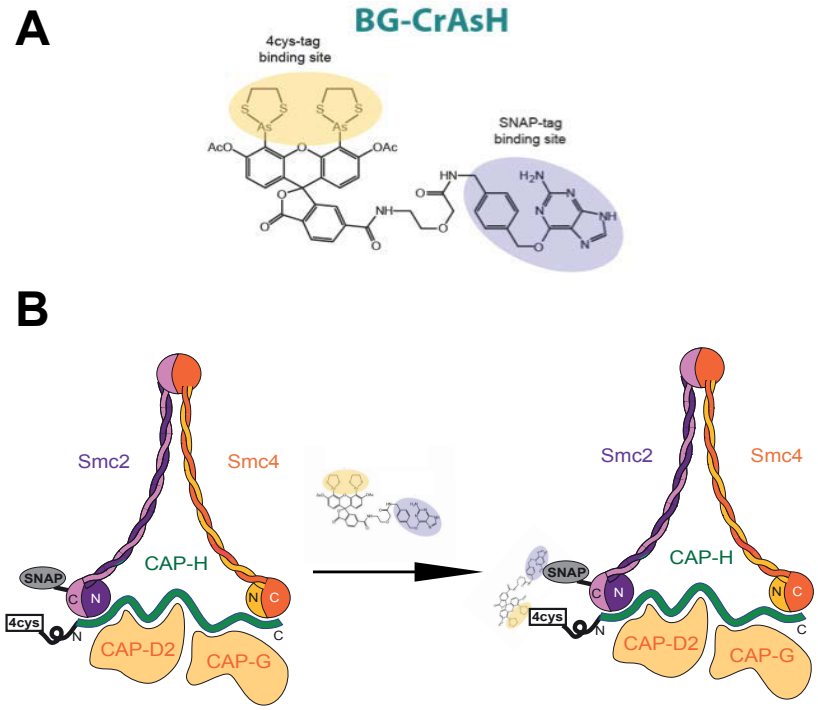

Figure 17. BG-CrAsH heterodimerization of modified SMC2 and CAPH condensin subunits. **A** Chemical structure of the BG-CrAsH cross-linker, showing the benzo-guanidin group (grey) and bi-arsenic derivative of carboxy-fluorescein (in yellow) that allow BG-CrAsH to bind to SNAP and 4cys tags, respectively. **B** Schematic model of how BG-CrAsH induces cross-linking of the SMC2-CAP-H interface in condensin I.

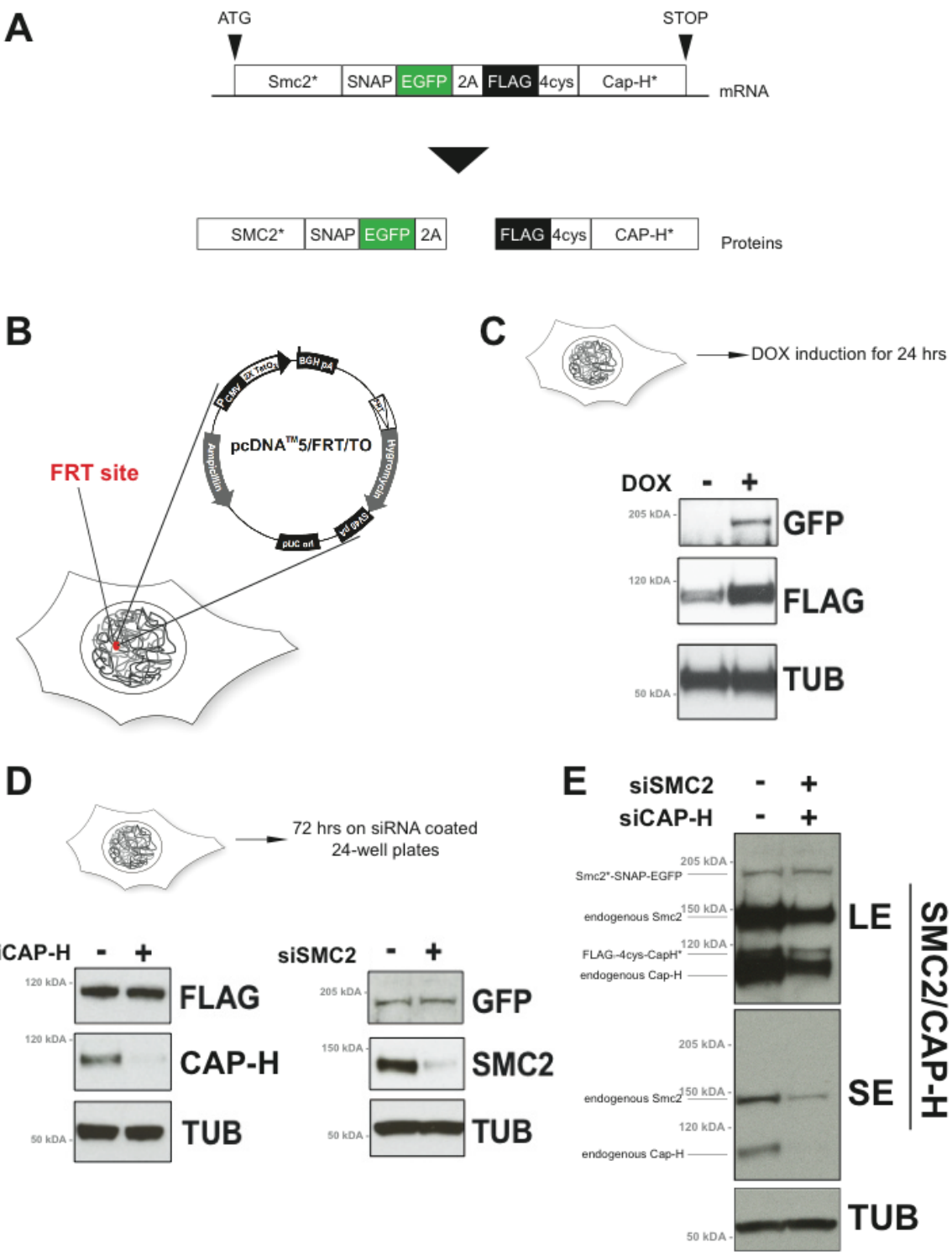
A
ATG
STOP
Smc2*
SNAP
EGFP
2A
FLAG
4cys
Cap-H*
mRNA
SMC2*
SNAP
EGFP
2A
FLAG
4cys
CAP-H*
Proteins
B
FRT site
pcDNA™5/FRT/TO
C
DOX induction for 24 hrs
DOX - +
205 kDA
GFP
120 kDA
FLAG
50 kDA
TUB
D
72 hrs on siRNA coated 24-well plates
siCAP-H - +
120 kDA
FLAG
120 kDA
CAP-H
50 kDA
TUB
siSMC2 - +
205 kDA
GFP
150 kDA
SMC2
50 kDA
TUB
E
siSMC2 - +
siCAP-H - +
205 kDA
Smc2*-SNAP-EGFP
endogenous Smc2
150 kDA
FLAG-4cys-CapH*
120 kDA
endogenous Cap-H
LE
205 kDA
endogenous Smc2
150 kDA
120 kDA
endogenous Cap-H
SE
SMC2/CAP-H
50 kDA
TUB

Figure 18. HEK 293 stably expressing SNAP and 4cys tagged SMC2 and CAP-H subunits. **A:** Generation of siRNA-resistant SMC2 (SMC2*) and CAP-H (CAP-H*) cDNAs was achieved by introduction of three silent mutations into the siRNAs target regions**.** A single ORF was designed with SMC2*-SNAP-EGFP and $FLAG_3$-4cys-CAP-H* separated by a 2A sequence. Ribosome skipping at the 2A sequence (Szymczak-Workman et al., 2013) will produce an upstream protein (Smc2-SNAP-EGFP) with C-terminal tail of 18 aa (2A) and a down-stream protein (FLAG-4cys-CAP-H) with a proline at the N terminus. **B** The pcDNA™ 5/FRT/TO vector contains a single FRT (Flippase Recognition Target) site immediately upstream of the hygromycin resistance gene that allow the Flp recombinase-mediated integration and selection of the pcDNA™ 5/FRT/TO plasmid following co-transfection of the vector into Flp-In™ T-REx™ mammalian host cells. The expression of SMC2*-SNAP-EGFP-2A-$FLAG_3$-4cys-CAP-H* was controlled by the strong CMV immediate early enhancer/promoter, into which 2 copies of the tet operator 2 ($TetO_2$) sequence have been inserted in tandem. Insertion of these $TetO_2$ sequences into the CMV promoter confers regulation by tetracycline (or its analogs) to the promoter N terminus. **C** After 24 h incubation in presence or absence of doxycycline (DOX) (tetracycline analog), cycling cells were harvested and lysed. Extracts were analysed for the expression of the ectopic SMC2 or CAP-H by Western blotting against GFP of FLAG tags, respectively. **D** A stable cell line was seeded on siRNA-coated dishes (see Methods) in presence of DOX. Western blot analysis of cell lysates 72 h after seeding revealed that the SMC2 and CAP-H mutant versions were resistant to knock-down (GFP and FLAG blot), whereas both endogenous versions were efficiently depleted as showed in the SMC2 and CAP-H blot, respectively. **E** Transgenic Hek293 lines were transfected with siRNAs (like in D) against the indicated endogenous condensin subunits and incubated for 3 days in the presence of transgene-inducing doxycycline. After cell lysis, levels of endogenous versus ectopic subunits were estimated by simultaneous detection of samples with SMC2 and CAP-H antibodies by Western blotting. In all the experiments, tubulin protein band signals (TUB) were used to check equal loading of samples.

2.2.2 Are the SMC2*-SNAP-EGFP and FLAG$_3$-4cys-CAP-H* transgenes functional?

One reason for the low protein levels of SMC2*-SNAP-EGFP and FLAG$_3$-4cys-CAP-H* might be that these proteins could fail to assemble into condensin I complexes. I therefore performed immunoprecipitation experiments using anti-FLAG or anti-EGFP antibodies and tested by Western blotting for the co-purification of the other condensin I subunits (Fig. 19A). FLAG$_3$-4cys-CAP-H* co-precipitated significant amounts of endogenous SMC2 and CAP-D2 (Fig. 19B). SMC2*-SNAP-EGFP precipitated barely detectable amounts of CAP-D2 and CAP-H (Fig. 19C), presumably due to the significantly lower expression levels of the modified SMC2.

I then analyzed whether SMC2*-SNAP-EGFP and FLAG$_3$-4cys-CAP-H* assembled with mitotic chromosomes by performing chromatin fractionation experiments. I separated chromatin-enriched and cytoplasmic fractions from either asynchronous cells or cells arrested in a prometaphase-like state with nocodazole and analyzed the fractions by immunoblotting against the EGFP and FLAG tags. I could detect both SMC2*-SNAP-EGFP and FLAG$_3$-4cys-CAP-H* subunits in the chromatin fraction specifically in nocodazole-arrested cells (Fig. 19D), suggesting that both modified proteins can load onto mitotic chromosomes. To test whether they would also dissociate from mitotic chromosomes upon exit from mitosis, I released cells from the nocodazole arrest into G1 phase (2 hours after nocodazole wash-out; Cui et al., 2010) and again probed chromatin and cytoplasmic fractions by Western blotting. This showed that the levels of SMC2*-SNAP-EGFP and FLAG$_3$-4cys-CAP-H* in the chromatin fraction were strongly reduced in the extracts from G1 phase cells (Fig. 19E), suggesting that condensin I complexes that contain the modified SMC2 and CAP-H subunits correctly unload from chromosomes.

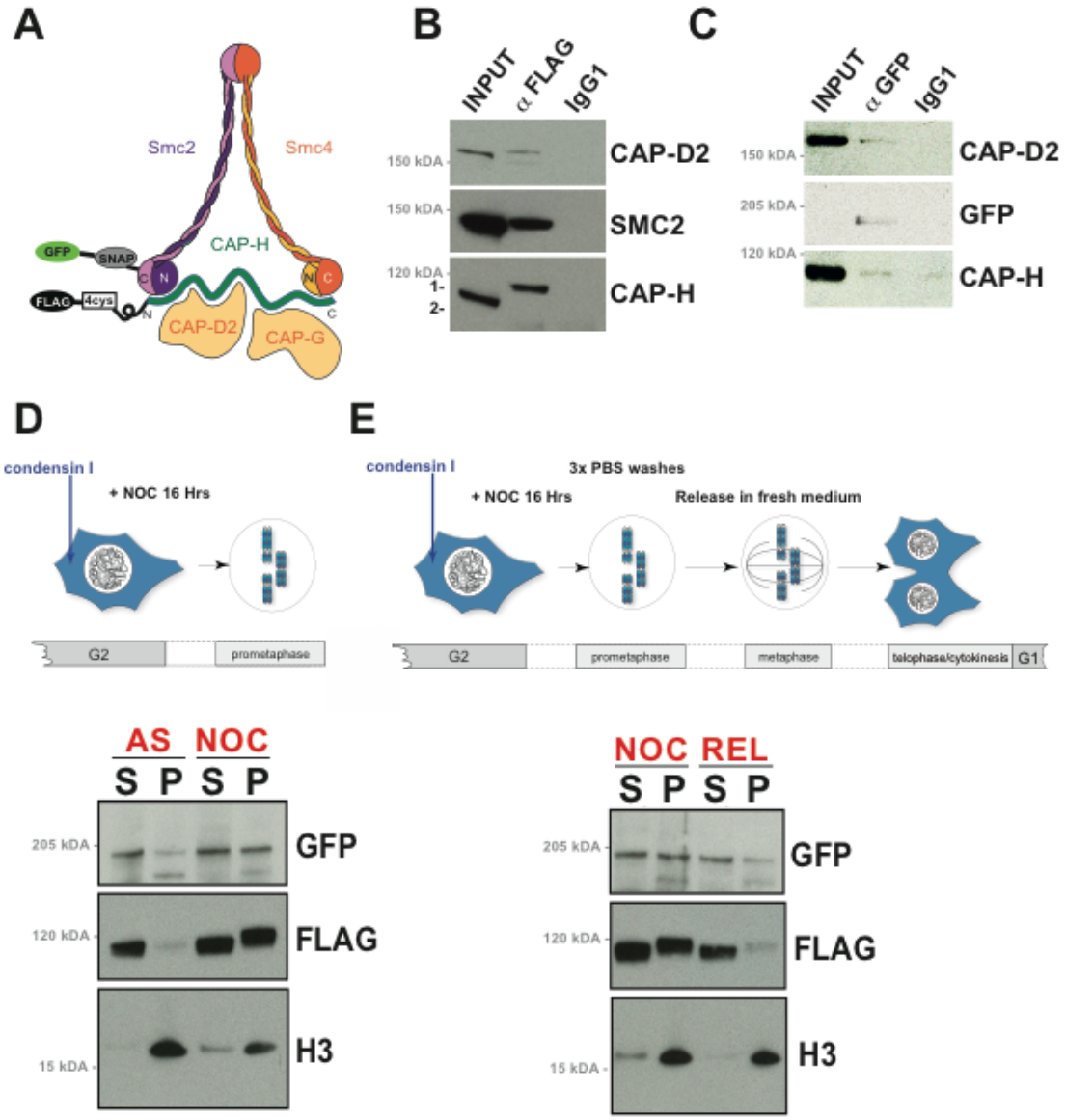

Figure 19. Modified ectopic SMC2 and CAP-H assembled with condensin I complexes. **A** Cartoon illustration of the condensin I complex harboring SMC2*-SNAP-EGFP and FLAG-4cys-CAP-H subunits. **B and C** After 24 h of doxycycline induction, cell were lysed and extracts were prepared for immunoprecipitation (IP) with anti-FLAG (αFLAG) (B) or anti-GFP antibodies (αGFP) (C). Western blots for SMC2 or CAP-D2 and CAP-H or CAP-D2 that were performed with sampled from FLAG or GFP immunoprecipitations, respectively, revealed the co-purification of ectopic subunits with the endogenous condensin I components. GFP and CAP-H immunoblots show the protein level of immunoprecipitated ectopic subunits in relation to the 5% of the whole cell extracts (INPUT). A control IP was performed by incubating extracts with IgG1 antibodies. **D and E** Cytosolic (S) and chromatin (P) fractions were prepared from doxycycline-induced cells incubated in presence (NOC) or absence (AS) of nocodazole for 16 h (D) and cell arrested in nocodazole or released (REL) for 2 hrs in fresh medium after extensive PBS washout of the drug (Cui et al., 2010) (E). Chromatin and cytosolic fractions were probed by histone H3 (H3) immunoblotting. 1 or 2 represent $FLAG_3$-4cys-CAP-H and endogenous CAP-H, respectively.

2.2.3 Can SMC2*-SNAP-EGFP and $FLAG_3$-4cys-CAP-H* be cross-linked *in vivo*?

To test whether SMC2*-SNAP-EGFP and $FLAG_3$-4cys-CAP-H* can be efficiently cross-linked with BG-CrAsH in live cells, I incubated asynchronous cells that had been induced with doxycycline with increasing concentrations of BG-CrAsH for 2 hours (Fig. 20A). I then lysed the cells, immunoprecipitated condensin I complexes via the $FLAG_3$ tag, and probed for cross-linking by Western blotting using anti-SMC2 and anti-FLAG antibodies.

Immunoblotting showed that already at the lowest concentration of BG-CrAsH used (1 μM), I could detect cross-linking between SMC2*-SNAP-EGFP and $FLAG_3$-4cys-CAP-H* (Fig. 20B). Based on the intensities of cross-linked and non-cross-linked SMC2*-SNAP-EGFP bands, I estimate that about half of the condensin complexes containing the modified SMC2 subunit had been cross-linked (Fig. 20C). However, less than 10% of $FLAG_3$-4cys-CAP-H* had been cross-linked (Fig. 20B and data not shown). The reason for this might be the significantly lower expression levels of SMC2*-SNAP-EGFP in comparison to $FLAG_3$-4cys-CAP-H*. $FLAG_3$-4cys-CAP-H* might therefore mostly assemble into condensin complexes with endogenous SMC2.

I also tested whether SMC2*-SNAP-EGFP and $FLAG_3$-4cys-CAP-H* turnover on chromosomes was affected by BG-CrAsH cross-linking. I used the stable inducible cell line in live imaging experiments to follow the localization of SMC2*-SNAP-EGFP during the cell cycle after BG-CrAsH treatment. Unfortunately, the experiments were not conclusive due to the very low EGFP signal in the cells.

In summary, both modified condensin subunits, although expressed at low levels, are incorporated into condensin complexes that associate with mitotic chromosomes and can be cross-linked *in vivo* by BG-CrAsH. To overcome the low expression, I plan to introduce the SNAP and 4cys tags into the endogenous SMC2 and CAP-H genomic loci using zinc finger nuclease technology (Urnov et al., 2005; Moehle et al., 2007).

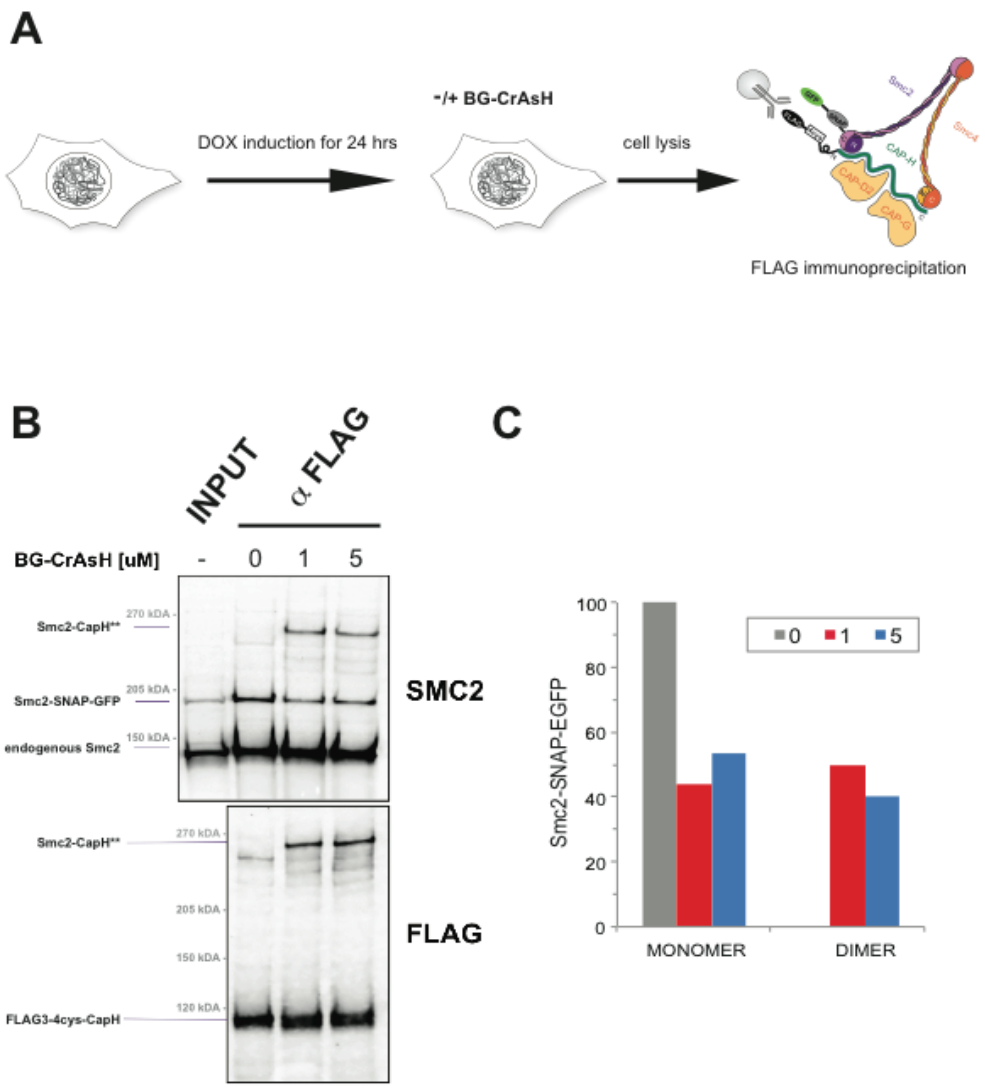

Figure 20. BG-CrAsH produces covalent closure of Smc2-CapH interface *in vivo*. **A** Schematic illustration of the *in vivo* cross-linking experiment with BG-CrAsH. Cycling cells were induced with doxycycline (DOX) for 24 h to allow incorporation of modified SMC2 and CAP-H into condensin I complexes. Before cell lysis, BG-CrAsH was added to the culture medium for 2 hrs at 37°C. To check whether the SMC2-CAP-H interface had been cross-linked, condensin I complexes were then isolated by FLAG immunoprecipitation. **B** INPUT and FLAG immunoprecipitates (αFLAG) were analysed by SDS-PAGE and Western blotting with αFLAG and αGFP antibodies. The identities of the bands in the Western blot are indicated. Bands representing cross-linked products (SMC2-CAP-H, **) were visible only in IP samples from cell treated with 1 µM and 5 µM BG-CrAsH. **C** Band intensities of SMC2-SNAP-EGFP (monomer) and the SMC2-SNAP-EGFP-FLAG$_3$-4xcys-CAP-H band (dimer) were quantified.

3. Does the Scc2-Scc4 complex have a role in loading condensin complexes onto chromosomes?

The molecular players involved in the loading onto and unloading from chromosomes of the condensin-related cohesin complex have been well characterized. Much less is known about condensin. However, the finding that condensin and cohesin associate with DNA using a similar topological mechanism (Cuylen et al., 2011 and Part 1 of the Results Section) suggests that they may share factors involved in their chromosomal turnover.

In favor of this notion is a recent genome-wide analysis of condensin binding sites on budding yeast chromosomes, which showed that condensin binding sites coincide with those of the cohesin loading factor Scc2-Scc4 (D'Ambrosio et al., 2008). This raises the possibility that Scc2-Scc4 might play a role also in condensin loading. To test this possibility, I decided to measure by ChIP-qPCR the levels of condensin bound to chromosomes after depletion of Scc2.

3.1. Anchoring-away Scc2 from chromatin

Temperature-sensitive (ts) mutants have extensively been used for functional studies in *Saccharomyces cerevisiae*. However, the use of ts mutants does present several problems. For example, some ts mutants have a leaky response to the temperature shift, resulting in only a partial inactivation of the target protein. Moreover, the exact mechanism of inactivation of the mutant protein at the nonpermissive temperature is rarely clear. Finally, ts mutants frequently show pleiotropic phenotypes. This applies in particular to the *scc2-4* mutant used in most previous studies (Ciosk et al., 2000; Lindroos et al., 2006; D'Ambrosio et al., 2008). For these reasons, I decided to explore a new tool for the conditional inactivation of the Scc2-Scc4 complexes in budding yeast.

A technology for *S. cerevisiae* developed by the Laemmli lab, named 'anchor away' (AA; Haruki et al., 2008), sequesters the target protein from the nucleus in a ligand-dependent manner by conditional tethering it to an abundant ribosomal subunit, which shuttles from the nucleus to the cytoplasm. The tethering reaction relies on the hetero-dimerization of the human FKBP12 domain to the FRB domain of human mTOR in the presence of the small molecule rapamycin (Belshaw et al., 1996; Chen et al., 1995).

To apply the AA technique for my purpose, I fused an FRB domain to the C terminus of the endogenous *SCC2* gene using PCR-tagging in a yeast strain that expresses an HA_6-tagged version of the kleisin subunits of either of condensin (Brn1) or cohesin (Scc1). Measuring cohesin binding to chromosomes will serve as a positive control to evaluate if

Scc2 function can be abolished by depleting it from the nucleus. I then crossed these strains with a rapamycin-resistant strain harboring an FKBP12-tagged version of Ribosomal Protein of the Large subunit 13A (RPL13A, Fig. 21A).

To test whether anchor-away interferes with Scc2's essential function in cell division, I checked for the ability of strains with FRB-tagged versions of Scc2, the cohesin kleisin Scc1, or the condensin subunit Smc2 to grow on media containing rapamycin. Strikingly, all three strains were unable to grow in the presence of rapamycin (Fig. 21B), indicating that anchor-away interfered with the function of the Scc2-Scc4 loading complex in a similar way as it interfered with the function of cohesin or condensin. Introduction of an additional untagged copy of Scc2 into the Scc2-FRB strain restored its ability to grow on rapamycin plates, as did introduction of an additional copy of Smc2 in an Smc2-FRB strain (Fig. 21B). This demonstrates that the observed growth defects were specific to the FRB-tagged versions of the target proteins.

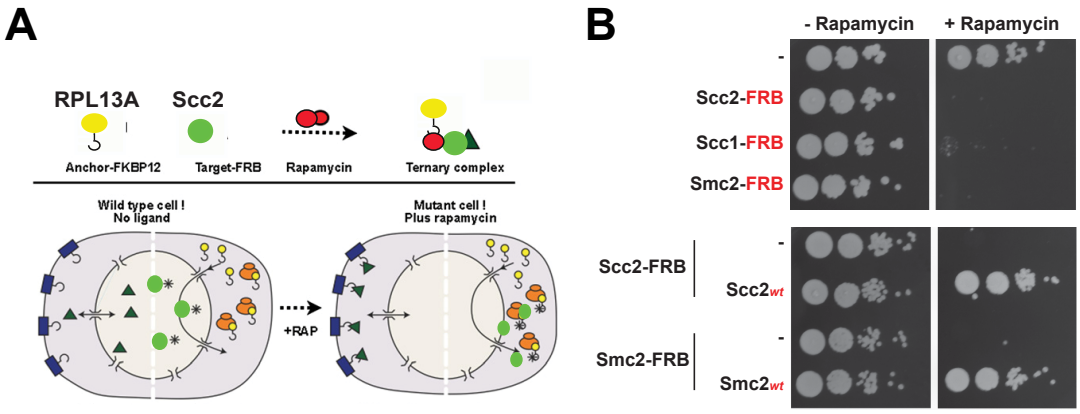

Figure 21. A new conditionally inactivable Scc2 allele. **A** Schematic representation of the anchor away system (AA) applied to Scc2 (modified from Haruki et al., 2008). The anchor and target were fused to the FKBP12 and FRB domains, respectively. A ternary complex would form upon addition of rapamycin. The scheme in the right half of the depicted cells shows as the AA system by using as anchor the ribosomal protein RPL13A-FKBP12, take advantage of the large flux of ribosomal proteins transiting the nucleus during their assembly process to the 40S and 60S particles (in orange) to deplete Scc2 (in green) from the nucleus (Haruki et al., 2008). **B** Yeast cultures were spotted in 5 serial dilutions onto YPAD plates with or without rapamycin to test the viability of the indicated FRB-tagged strains in the absence (upper part) or presence of wild-type versions of the genes (bottom part). Smc2-FRB and Scc1-FRB strains were used as positive controls for the AA system in the spot assays (Haruki et al., 2008).

3.2. Assaying condensin binding to chromosomes after Scc2 depletion

To monitor condensin binding to chromosomes, I selected two different chromosomal binding sites based on available ChIP-on-chip data (Wang et al., 2005; D'Ambrosio et al., 2008). These sites were the 5'UTR of the yeast ribosomal DNA repeat (rDNA) on chromosome 12 and the centromeric region of chromosome 4 (CEN4). I added rapamycin for 2 hours to logarithmically growing Scc2-FRB cells and then processed the cells for ChIP-qPCR at the CEN4 and rDNA loci using the HA_6 tag on the Brn1 or Scc1 subunits of condensin or cohesin, respectively.

Addition of rapamycin caused a ~70% reduction of the amount of DNA that co-immunoprecipitated with the HA_6-tagged Scc1 cohesin subunit at both loci tested (Fig. 22A). The decrease in binding was specific to the presence of the FRB tag on Scc2. In contrast, rapamycin addition had little to no effect on the amounts of DNA that co-immunoprecipitated with the HA_6-tagged Brn1 condensin subunit at the rDNA locus, while the co-immunoprecipitated amounts of DNA even increased at the CEN4 locus (Fig. 22B). These experiments suggest that Scc2 has no role in loading condensin onto chromosomes or might even counteract efficient condensin loading.

To rule out that the effects I observed were not due to the prolonged rapamycin-induced sequestering of Scc2 in cycling cells, which might result in loss of chromosome cohesion, I repeated the experiment in cells arrested in a metaphase-like state with nocodazole (Ciosk et al., 2000; D'Ambrosio et al., 2008). Once cells had arrested, I added rapamycin for 2 hours and measured cohesin and condensin levels at the CEN4 and rDNA loci by ChIP-qPCR (Fig. 23A).

Consistent with the previous finding that most cohesin loading occurs before mitosis, the reduction in cohesin binding to chromosomes upon anchor-away of Scc2 was less pronounced than before, resulting in a reduction of the amount of DNA that co-immunoprecipitated with cohesin of ~30% at both CEN4 and rDNA loci (Fig. 23B). Consistent with what I had observed in asynchronous cells, anchor-away of Scc2 in mitotically arrested cell had no notable effect on the amount of co-immunoprecipitated DNA with condensin at the rDNA locus (Fig. 23C). Also under these conditions, the amounts of DNA that co-precipitated with condensin at the CEN4 locus increased, but less pronounced than in asynchronous cells (~20% in nocodazole-arrested cells compared to ~50% in asynchronous cells). I conclude that the increase in condensin binding at the centromeric locus might be an effect of the potential reduction in cohesin binding and hence impaired sister chromatid cohesion at this site.

A possible explanation why depletion of Scc2 by anchor-away does not reduce condensin binding and only partially reduces cohesin binding could be that Scc2-Scc4 turnover on

chromosomes might be slow. The pool of chromosome-bound Scc2-Scc4 might in turn be refractory to anchoring away. In order to test directly the efficiency of Scc2-Scc4 depletion from chromosomes under the conditions of the assay, I measured by ChIP-qPCR in nocodazole-arrested cells the amount of Scc2-Scc4 bound to chromosomes using an HA_6-tagged version of Scc4 (Ciosk et al., 2000). Addition of rapamycin reduced the amounts of DNA that co-immunoprecipitated with Scc4 to background levels at the rDNA locus and to ~10% at the CEN4 locus (Fig. 23D). This demonstrates that Scc2 can be efficiently depleted from the nucleus using the anchor-away technique.

Taken together, these results show that depletion of the Scc2-Scc4 complex from the budding yeast nucleus effectively reduces cohesin binding to chromosomes, but has little to no effect on condensin's association with chromosomes. Scc2-Scc4 might therefore not act as a general chromosome loading factor for all SMC protein complexes

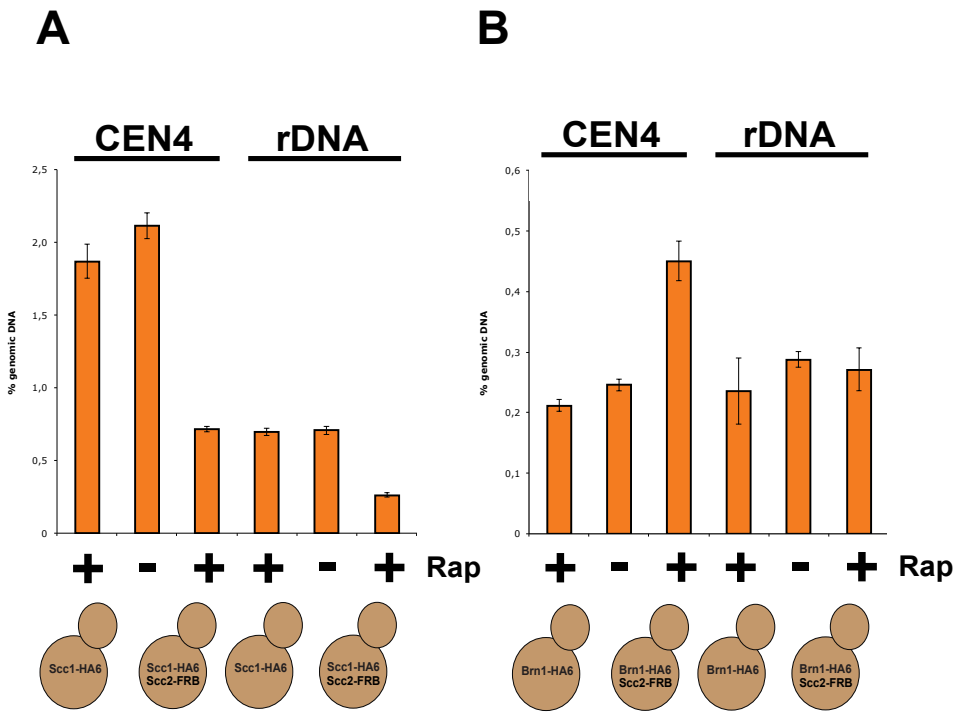

Figure 22. Measuring cohesin and condensin binding to chromosomes upon depletion of Scc2. **A** Chip-qPCR analysis of cohesin binding at CEN4 and rDNA loci after 2 hrs rapamycin (Rap) treatment of asynchronous yeast cultures. **B** Condesin levels at CEN4 and rDNA were measured as described in A. The values in the histograms represent the mean ± s.d. of three independent experiments. A strain not containing an Scc2-FRB allele was used to measure whether rapamycin addition influenced the level of cohesin and condensin at CEN4 and rDNA loci (Tsang et al., 2007).

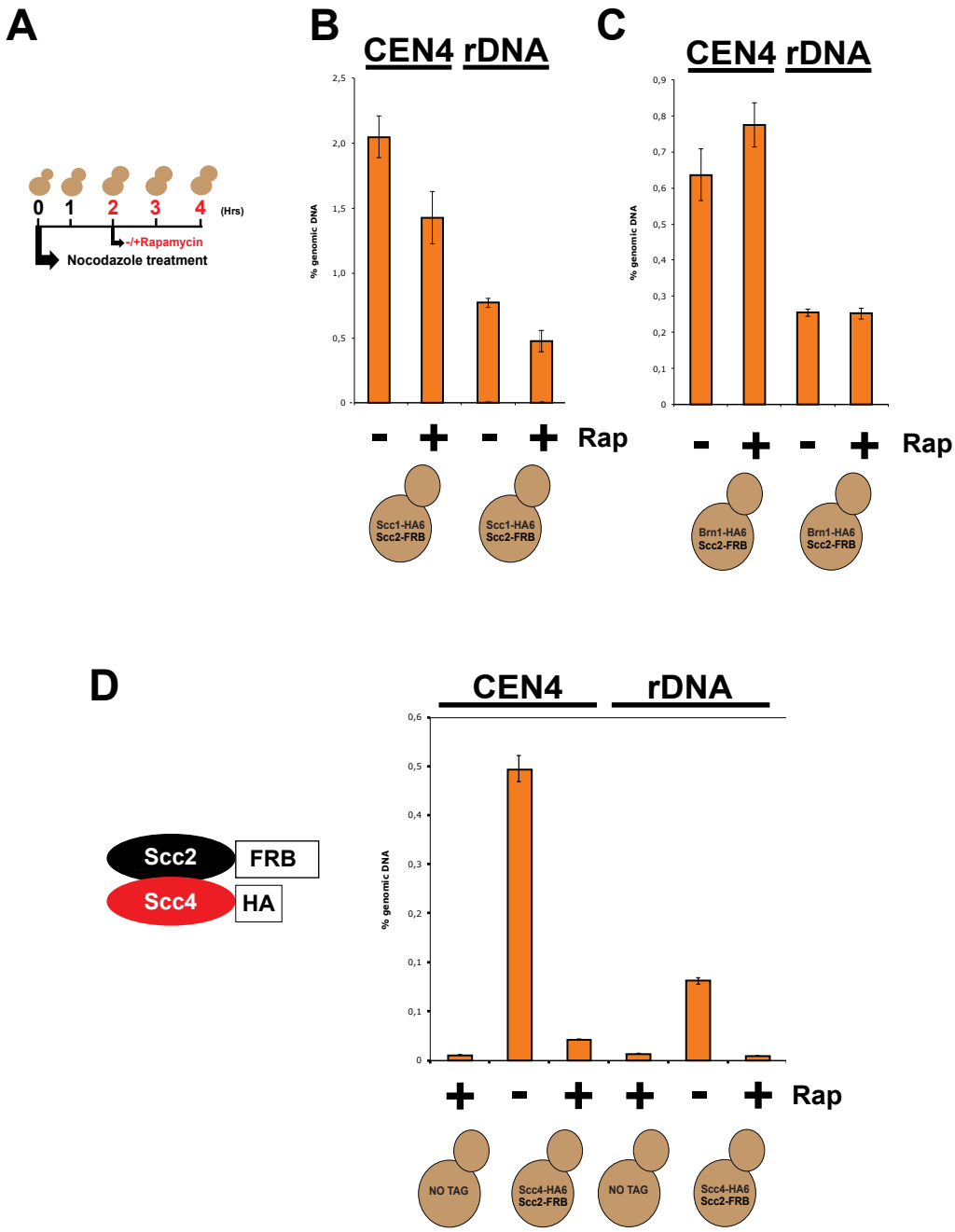

Figure 23. Condensin binding to mitotic chromosomes is not affected by depletion of the Scc2-Scc4 complex. **A** Schematic representation of the experimental set up. Esponentially growing yeast cultures were first arrested with nocodazole and then treated with rapamycin for the indicated times. **B** and **C** CEN4 and rDNA loci were monitored by ChIP-qPCR for binding of cohesin (B) or condensin (C) after treating cells as described in A. **D** Representantion of the Scc2-Scc4 complex harboring Scc2-FRB or Scc4-HA_6 (left). Using the same experimental condition of A, the amount of Scc4-HA_6 levels at CEN4 and rDNA loci was measured and compared to a control strain without HA tag (NO TAG) (right). Values in the histograms indicate the mean ± s.d. of three independent experiments.

III Discussion

1. The nature of condensin's binding to chromosomes

While requirement for condensin complexes in the formation of mitotic chromosomes has been well established, their mechanism of action and their contribution to chromosome condensation has remained a major unanswered question.

Recent studies in *Saccharomyces cerevisiae* provided important insight into this question. by demonstrating that the integrity of the condensin ring was necessary for its cellular functions (Cuylen et al., 2011; Cuylen et al., 2013). This lead to the proposal that condensin might function by topologically embracing DNA, similar to the entrapment of sister chromatids by cohesin rings (Gruber et al., 2003; Ivanov and Nasmyth, 2005; Haering et al., 2008). However, structural and biochemical studies argued against this idea. EM images showed that the Smc2/Smc4 coiled coils were associated along their entire length, resulting in a 'lollipop'-like appearance (Fig. 5B; Anderson et al., 2002) that was similar to the 'head-to-tail' structure obtained in electron-spectroscopic imaging (Bazett-Jones et al., 2002). These structures were in striking contrast to the ring-like appearance of cohesin (Fig. 3B; Anderson et al., 2002), making it hard to believe that chromatin could pass between the associated coiled coils. In addition, early electrophoretic mobility shift experiments (Kimura & Hirano, 1997; Sakai et al., 2003) suggested that condensin contacts DNA directly, presumably by interaction with the Smc2-Smc4 head domains or the non-SMC subunits. In support of the latter hypothesis are recent experiments, which showed that the condensin non-SMC subunits are not only important for the correct association of the complexes with mitotic chromosomes in yeast and human cells but also for their DNA-dependent ATPase activity (Piazza et al., 2014).

To test whether the topological model is indeed valid for condensin, I used different biochemical approaches to understand how the large tripartite ring structure formed by Smc2, Brn1 and Smc4 contributes to the interaction between condensin and chromatin.

1.1. Cross-linking analysis of condensin interfaces

In first set of experiments, my cross-linking data using bBBr showed that I could specifically connect the Smc2-Smc4 (hinge) and Brn1-Smc4 interfaces of purified condensin holocomplexes *in vitro* (Results, Chapters 1.1 and 1.2). However, the cross-linking efficiency of the Brn1-Smc4 interface was 3-times lower than that of the Smc2-Smc4 hinge domains (Fig. 9B–D and 10B–D). A possible explanation for this result might be in a higher accuracy of the structural model generated for the Smc2-Smc4 hinge interface than the model generated for the Brn1-Smc4 interface.

The crystal structure of the bacterial SMC hinge domains (Haering et al., 2002) shows high resemblance with the crystal structure of the mouse condensin hinges (Griese et al., 2010),

suggesting that topology of this domain is highly conserved even between pro- and eukaryotic SMC complexes. However, the latter structure shows an open and presumably not biologically relevant conformation of the hinge caused by the use of a too short coiled-coil domain in the crystallized construct (Griese et al., 2010). For this reason, only the bacterial structure was used for building the budding yeast homology model.

Consistent with the conclusion that the yeast Smc2-Smc4 hinge model is very accurate, three different cysteine pairs combination tested in the outer helices of the predicted dimerization interface all resulted in specific cross-links between Smc2 and Smc4 (data not shown). I selected one of the three combinations (K639C/V721C; Fig. 9A), which was not affecting yeast growth.

In contrast, of six cysteine pair combinations tested at adjacent positions in the predicted loop region of the C-terminal WHD of Brn1 and the ATPase domain of Smc4, which would be at a distance compatible with bBBr crosslinking (data not shown), only one produced cross-links; and this only with low efficiency. I obtained similar results using BMOE, a more flexible thiol-reactive cross-linker able to link cysteine residues at longer distances than bBBr (data not shown). Since the Brn1-Smc4 homology model was produced based on the yeast Smc1-Scc1 interface structure (Haering et al., 2004), it is possible that sequence differences might have produced this apparently low accuracy of the model. However, since the overall structural organization of this interface is conserved even in prokaryotic SMC complexes, as revealed by comparison of yeast cohesin structure with crystal structure of the SMC–ScpA interface of *B.subtilis* SMC complexes (Burmann et al., 2013), it is likely that all SMC proteins complexes assemble this interface in a similar way. Why then should Brn1-Smc4 be different? A possible explanation comes from the discovery that DNA binding by condensin's HEAT-repeat subunits stimulates the SMC subunit ATPase activity (Piazza et al., 2014). This suggests that the presence of Ycs4 and Ycg1 in the holocomplex might produce structural changes in the SMC head domains that are necessary for their activation (Introduction, Chapter 3). Such rearrangement could, for example, account for different geometries at SMC-kleisin interfaces. Consistent with this idea, it has been proposed that the auxiliary cohesin subunit Wapl could modulate the opening of the cohesin ring structure by making contact with the SMC3 head domain, to allow its unloading from chromosomes (Chatterjee et al., 2013; Buheitel and Stemman, 2013). Presumably X-ray crystallographic analysis of condensin would be ideal for obtaining detailed structural information about the SMC-kleisin interface of condensin. Since the information provided by this method will, however, be limited to sub-complexes of minimal interaction domains, alternative approaches like mass spectrometry followed by cross-linking of condensin holocomplexes (Leitner et al., 2010; Leitner et al., 2012) would be helpful in identifying inter-subunit contacts in the context of the condensin holocomplex.

1.2. Establishment of a new minichromosome-binding assay

In this thesis, I described the establishment of a biochemical assay that is based on the cross-linking of cohesin- and condensin-minichromosome complexes after immunoprecipitation. By combining a one-step immunopurification protocol with direct cross-linking on the beads, I was able to isolate protein-DNA complexes from yeast extracts in good yields and, in contrast to other protocols that are based on sucrose gradient preparation of minichromosome fractions (Haering et al., 2008), cross-link the SMC-kleisin structures without the need for additional steps (Results, Chapters 1.4 and 1.5). For example, the presence of dithiols like DTT quenches the bBBr reaction and therefore its removal is crucial for efficient cross-linking of cysteine pairs. Having condensin-minichromosome complexes immobilized on beads allowed me to remove DTT from the immunoprecipitated samples by a simple washing step, eliminating the need for salt dialysis. Using this new biochemical assay, I obtained results consistent with previous reports (Haering et al., 2008; Farcas et al., 2011). In fact, cross-linking of cohesin-minichromosome complexes (used as a positive control) produced a fraction of SDS-resistant cohesin-minichromososome species consistent with the overall cross-linking efficiency of the two interfaces in cohesin (Results, Chapter 1.5).

1.3. Condensin rings are encircling individual (mini)chromosomes

By using the cysteine cross-linking approach on purified condensin-minichromosome complexes (see above), I demonstrated that condensin binds to DNA by encircling it within the tripartite ring structure formed by its Smc2, Smc4 and Brn1 subunits (Results, Chapters 1.5 and 1.6). I first showed in the newly established in *vitro* system (see above) that the covalent closure of condensin rings produces SDS-resistant condensin-minichromosome complexes in a similar manner as cohesin-minichromosome complexes (Fig. 13C). The efficiency of formation of the SDS-resistant species was low, but nevertheless directly proportional to the circularization efficiency of condensin ring structures formed by simultaneous crosslinking of both interfaces (Results, Chapter 1.3; Fig. 13C–D). This finding proofs beyond doubt that the molecular mechanism of condensin's interaction with circular (mini)chromosomes must be of topological nature.

Furthermore, I showed that the production of SDS-resistant condensin-minichromosome complexes depends on the integrity of covalently circularized condensin rings (Fig. 14A). Consistent with this notion, the SDS-resistant interaction is lost by opening the one of the covalently connected ring interfaces by TEV cleavage after cross-linking (Fig. 14B–C), as predicted by the ring hypothesis.

The fact that condensin binds to DNA via a topological mechanism opens the possibility

that the complex might not be able to discriminate between different chromosomes and simply randomly encircles any DNA strand that comes into close proximity. For example, it was suggested that inter-sister linkages generated by condensin could be the reason for the tight association between certain sister loci, which had been lost in some condensin mutants (Lam et al., 2006). It is therefore possible that condensin, like cohesin, entraps both sister chromatids inside its ring (Fig. 15A). However, my cross-linking experiments argue against this hypothesis. Covalently circularized condensin rings in complex with replicated minichromosomes produced only monomeric SDS-resistant condensin-DNA species (Fig. 15C). Future experiments will now have to test whether the same chromatid fibre passes once or twice through a single condensin ring.

While my data unambiguously support a topological mode of condensin binding to chromosomes, they do not rule out the existence of direct contacts between the condensin protein subunits and the chromosomal DNA fibre. Several lines of evidence in fact suggest the presence of direct DNA binding sites for ssDNA or dsDNA in the Smc2-Smc4 hinge domain or the non-SMC subcomplex, respectively (Griese et al., 2010; Piazza et al., 2014). Why would condensin require additional sites for direct binding to DNA? These DNA binding sites might, for example, be important for directing the loading of condensin complexes onto chromosomes. Alternatively, recognition of ssDNA intermediates might be necessary in condensin's roles in telomere maintenance and DNA damage repair (Burrack et al., 2013; see Introduction, Chapter 3.2.2).

2. A possible gate within condensin rings

The findings that condensin encircles (mini)chromosomes raises the question of how DNA enters and exits condensin rings. Since most condensin exists as pre-assembled rings even when it is not bound to chromosomes (Onn et al., 2007), DNA must enter or exit condensin by a transient opening of the ring at one or more of the three interfaces between the subunits. The discovery that cohesin loading onto chromosomes in yeast cells is abolished by the artificial connection (by rapamycin-induced dimerization of FKBP12 and FRB domains) of Smc1 and Smc3, but not by fusion of Smc3-Scc1 or Scc1-Smc1, suggests that the Smc1-Smc3 hinge domains need to transiently dissociate to let DNA pass into cohesin rings (Gruber et al., 2006). It has furthermore been proposed that ATP hydrolysis by the SMC head domains results in the temporary opening of the cohesin ring (Arumugam et al., 2003; Weitzer et al., 2003) at the Smc1-Smc3 hinge interface (Gruber et al., 2006). Although the observation that condensin ATPase mutants are still able to bind mitotic

chromatin argues against a similar mechanism in the condensin loading reaction (Hudson et al., 2008), further characterization of these mutants will be required to figure out whether they are still able to bind DNA topologically or merely associate with chromatin in a non-topological manner.

The finding that covalent closure of the Smc2-Brn1 interface, but not of the Brn1-Smc4 interface, affected the growth of budding yeast suggests that opening of the former interface might be physiologically important for condensin function (Results, Chapters 1.2 and 2.1). In line with this finding is the recent report that the same interface (Smc3-Scc1) is crucial for the first step release of cohesin complexes from chromosomes during mitotic prophase (Eichinger et al., 2013; Buheitel and Stemman, 2013). Smc2-Brn1 may be involved in condensin's turnover on chromosomes in an analogous way. The fact that, in contrast to cohesin, no cell cycle dependent proteolytic cleavage of any condensin subunit has been reported strongly suggests that the transient opening of condensin interfaces is the only mechanism that ensures chromosomal turnover of the condensin complex. If this is the case, why forcing Smc2-Brn1 closure in vivo does not produce cell lethality in yeast?

One possibility is that different condensin gates might have functional redundancy. While the highly conserved architectural organization of condensin, cohesin and prokaryotic SMC rings suggests that all SMC complexes might use the same molecular mechanisms for loading onto and unloading from chromosomes, this does not necessarily need to be the case. For example, a recent crystallographic study of the *E. coli* SMC complex MukBEF showed that the ATP-dependent engagement of MukB (SMC) head domains leads to the dissociation of one of the two bound MukF kleisin subunits, thereby transiently opening MukBEF rings at the SMC-kleisin interface instead of the SMC hinge interface (Woo et al., 2009). It might therefore be possible that condensin uses the Smc2-Brn1 in combination with one of the other gate for its chromosomal turnover. To test this hypothesis, I'm planning to close two interfaces at the same time by using the FRB-FKBP system mentioned above in combination with either Brn1-Smc4 or Smc2-Brn1 fusion protein.

A second hypothesis comes from the finding that condensin is localizes to the budding yeast nucleus (Freeman et al., 2000) and binds to chromosomes (D'Ambrosio et al., 2008) throughout the cell cycle. It is therefore possible that, under normal growth conditions, its chromosomal turnover is very slow. Condensin rings might therefore not need to open frequently in yeast cells. Notably, it has been reported that the residence time on chromosomes of cohesin complexes during oocyte growth in mice is longer than 2 weeks (Tachibana-Konwalsky et a., 2010). This makes the possibility of slow turnover a valuable option for condensin. Moreover, the evidence that yeast strains expressing the Smc2-Brn1 fusion are not viable at 37°C is consistent with the idea that the fusion of this gate becames critical for condensin function under stress conditions (Fig. 16B). Future FRAP analysis to

measure condensin's chromosomal turnover will be important for understanding this aspect.

2.1. A new tool for selective closure of condensin interfaces *in vivo*

To reveal the physiological contribution of the individual interfaces in the chromosomal turnover of condensin, I have started to selectively close one or multiple ring subunit interfaces *in vivo*. I used mammalian cells for this purpose, since condensin's turnover on chromosomes had been well characterized and could be easily monitored by live cell imaging (Gerlich et al., 2006).

I established in collaboration with Ania Rutkowska a system to induce the closure of the Smc2-kleisin interface of condensin I in live cells. By cross-linking ectopic SMC2*-SNAP-EGFP and $FLAG_3$-4cys-CAP-H* via the hetero-bifunctional cross-linker molecule BG-CrAsH (Rutkowska, Haering and Schultz, unpublished; Fig. 17A), I tested whether blockage of the Smc2-kleisin interface prevents the association of condensin I with chromosomes upon NEBD or its dissociation from chromosomes upon exit from mitosis (Gerlich et al., 2006; Introduction, Chapter 3.2.3).

The strategy for Smc2-kleisin cross-linking using BG-CrAsH turned out to be very successful, since I observed that 50% of the condensin I complexes that contained both modified subunits had been cross-linked (Fig. 20C). Unfortunately, the modified subunits were expressed only at very low levels, making attempts to follow the localization of SMC2*-SNAP-EGFP after BG-CrAsH treatment by live cell imaging impossible (data not shown). SMC2*-SNAP-EGFP and $FLAG_3$-4cys-CAP-H* were in fact barely detectable by Western blotting when compared with endogenous SMC2 and CAP-H in total lysates, even after knockdown of the endogenous genes (Fig. 18D–E). Nevertheless, both ectopic proteins were still able to incorporate into condensin complexes that could associate with mitotic chromosomes (Fig. 19B–E). Despite the production from of a single SMC2*-SNAP-EGFP-2A-$FLAG_3$-4cys-CAP-H* mRNA (Fig. 18A–B), the two proteins were expressed in non-equimolar ratios, with ectopic SMC2 being apparently much less abundant than ectopic CAP-H (Results, Chapter 2.2.2; Fig. 19B–C). Consistent with this notion, only a small fraction of $FLAG_3$-4cys-CAP-H* incorporated in the condensin I complex and could hence be cross-linking (Fig. 20C).

A possible explanation for the low and non-stoichiometric expression of the modified subunits might be the presence of the SNAP-EGFP or FLAG-4cys tags, which could determine different protein stabilities of SMC2 and CAP-H at the cellular level. Intriguingly, when I tried to express from transiently transfected vectors either SMC2-

SNAP-EGFP or SMC2 without tags, I observed the same low expression, whereas I noted expression of FLAG-4cys-CAP-H or untagged CAP-H constructs at levels similar to the endogenous CAP-H protein (data not shown). These observations suggest that the presence of the tag does not affect the stability of the ectopic proteins and at the same time that SMC2 expression in the cell is apparently more tightly regulated than the expression of CAP-H. In line with the idea that the expression of the SMC2 subunits is tightly controlled are recent experiments, which suggested that in order to perform their known biological functions and correctly assemble functional cohesin complexes, SMC1 and SMC3 levels need to be strictly balanced. Paucity of either one of the human SMC proteins caused the mislocalization of the leftover SMC and degradation of the kleisin subunit (Laugsh et al., 2013). Notably, after simultaneous knockdown of endogenous SMC2 and CAP-H, also $FLAG_3$-4cys-CAP-H* was reduced, whereas SMC2*-SNAP-EGFP signal remained stable (Fig. 18E). These data suggest that knockdown of endogenous SMC2 also affected the other condensin I subunits. Consistent with this hypothesis is the fact that only SMC2 knockdown caused down-regulation of the other condensin I subunits, including the ectopic CAP-H. CAP-H knock-down in contrast had no effect (data not shown). The fact that even the ectopic CAP-H was down regulated together with endogenous condensin I subunits rule out the possibility that this effect was due to a negative feedback on the gene expression, but rather that SMC2-specific depletion triggers degradation of the other subunits. Although further analysis using proteasome inhibitors should clarify this point, these results show that the SMC2 level in the cell needs to be stably maintained for the stable assembly of stoichiometric condensin complexes.

To overcome the problem discussed above, I'm currently using genome editing technologies in collaboration with Birgit Koch to modify the endogenous SMC2 and CAP-H genes in HeLa cells.

3. Scc2-Scc4 is not a general loading factor for all SMC complexes

Since I showed that condensin and cohesin bind DNA using a similar topological mechanism, I tested whether the cohesin loader Scc2-Scc4 might act as chromosome loading factor for both complexes. To answer this question, I generated a yeast strain in which I could specifically sequester Scc2 from the nucleus by anchoring it to a ribosomal protein (Haruki et al., 2008; Fig. 21). I then compared by ChIP-qPCR condensin and cohesin binding to chromosomes after Scc2 'anchor-away'. I determined the efficiency of

Scc2-Scc4 depletion from chromosomes based on the reduction of the chromosomal levels of Scc4 at two chromosomal loci (CEN4 and rDNA) and measured a depletion of 90-100% within 2 hours after rapamycin addition (Results, Fig. 23D). To confirm the depletion efficiency of Scc2-Scc4, I'm planning to probe chromatin pellets from cells treated with rapamycin by Western blotting.

By using the anchor-away system to sequester Scc2 from the budding yeast nucleus, I demonstrated that Scc2-Scc4 is essential for cohesin's binding to chromosomes but not for condensin's association with DNA (Results, Chapter 3.2). The ChIP-qPCR measurements of chromosomal condensin levels revealed that, under condition where Scc2-Scc4 is efficiently removed from chromosomes (Fig. 23D), condensin level at CEN4 or rDNA were not noticeably reduced (Fig. 23C). Although I cannot exclude the possibility that condensin binding to other chromosome regions is affected (i.e. tRNA loci; D'Ambrosio et al., 2008), this notion is consistent with earlier studies, which showed that the overall levels of condensin bound to chromatin were not obviously affected after inactivation of Scc2 by mutation in budding yeast (Ciosk et al., 2000) or by depletion of Scc4 in human cells (Watrin et al., 2006b). Chromatin immunoprecipitation followed by massive parallel sequencing (ChIP-seq) analysis of the genome-wide distribution of budding yeast condensin should be able to show whether removal of Scc2-Scc4 from chromosomes affects condensin targeting to other chromosome sites.

However, a recent study proposed that mitotic rDNA condensation is defective after inactivation of Scc2, which somewhat reduced condensin binding at this locus (D'Ambrosio et al., 2008). In contrast, my Chip-qPCR data showed no significant reduction of condensin binding at this locus after removal of Scc2-Scc4 from the nucleus (Fig. 23C, Right panel). This result imply that condensin loading and/or activity at the rDNA locus does not depend on Scc2-Scc4 and might instead depend on additional factors (see Introduction, Chapter 3.2.5).

My ChIP experiments for cohesin recapitulate published data on the importance of Scc2-Scc4's role in loading cohesin onto chromosome (Ciosk et al., 2000; Arumugam et al., 2003; Hu et al., 2011; Fig. 22A) and further extend this analysis. It has been shown that cohesin becomes more stably attached to chromosomes during replication (Gerlich et al., 2006). Stabilization and establishment of sister chromatid cohesion depends on the acetylation of Smc3 (Sutani et al., 2009). These previous findings suggest that, after cohesion has been established, Scc2-Scc4 might not be required anymore for cohesin loading. Consistent with this hypothesis, my data show that cohesin binding is more refractory to complete removal of Scc2-Scc4 from chromosomes in metaphase-arrested cells (Fig. 23B).

Taken together, these results indicate that Scc2-Scc4 does not act as a general loading factor for all SMC protein complexes. While stimulation of cohesin's ATPase activity by Scc2-Scc4 might be required for efficient chromosome loading of cohesin (Murayama and Uhlmann, 2014), this role might have been taken over by the HEAT-repeat subunits in condensin (Piazza et al., 2014). Consistent with this hypothesis is the finding that the ATPase activity of condensin holocomplexes is higher than that of the Smc2–Smc4 subcomplex and increases in the presence of DNA (Stray et al., 2003; Piazza et al., 2014).

4. A mechanistic model for condensin's role in chromosome organisation

I showed that condensin binds to (mini)chromosomes by entrapping individual DNA fibres within its ring structure. How could this topological mode of binding result in the organisation of mitotic chromosomes? By fastening different regions of a chromosome arm, condensin may produce the necessary chromosomal stiffness to resist the pulling forces of the microtubule spindle. Since the condensin ring structure would have a diameter of ~35 nm if the Smc2-Smc4 coiled coils were separated, which is in principle sufficiently large to enclose one (see Results, Part 1) or even two 10-nm chromatin fibres, such linkages can be made either (a) by entrapping both chromosome segments within the same condensin ring (Fig. 24A) or (b) by the interaction of two (or multiple) rings that each topologically bind one chromatin fibre (Fig. 24B).

That the first option is indeed possible is supported by the evidence that cohesin rings are able to entrap both sister chromatids within the same ring structure (Haering et al., 2008). However, the fact that release of cohesin rings from minichromosomes is more salt-sensitive than that of condensin rings suggest that chromatin fibres encircled by condensin rings may still make additional direct contacts with condensin subunits while they pass through the condensin ring (Introduction, Chapter 3.2.7; Cuylen et., 2011).

In support of the second option is the proposal that bacterial SMC complexes form oligomers *in vitro* (Matoba et al., 2005; Woo et al., 2009) and *in vivo* (Badrinarayanan et al., 2012). It is therefore conceivable that also eukaryotic condensins use similar multimerization mechanisms. Consistent with this hypothesis is the proportional increase observed in the mobility shift of protein-DNA complexes produced by increasing concentrations of recombinant budding yeast non-SMC subcomplexes, which might be a result of oligomerization of the non-SMC subcomplexes bound to DNA (Piazza et al., 2014).

Since both model are compatible with the evidence that condensin is able to physically compact DNA *in vitro* (Strick et al., 2004), none of them can currently be ruled out.

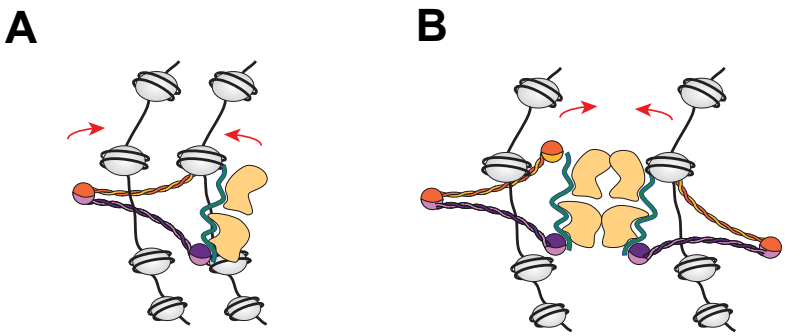

Figure 24. Possible models of how condensin links different segments of the same chromatin fiber. **A** Condensin rings may connect distant segments of the same chromatin fibre by encircling them within the ring structure. **B** Alternatively, linkages could be the result of the association between condensin rings that each entrap a single chromatin fibre. Red arrows indicate the two 10 nm chromatin fibres being held together.

How does condensin load onto chromosomes? My work proofs that condensin and cohesin are binding to chromosome with a similar topological mechanism. However, I showed that at least the mechanism of the first loading step has to be different, since the cohesin loader Scc2-Scc4 is not involved in the loading of condensin onto chromosomes. Instead, my data support the idea that condensin's HEAT-repeat subunits take over the role of Scc2-Scc4 (Fig. 25; Piazza et al., 2014). Recent data suggest that cohesin is able to topologically bind DNA, although with low efficiency, independently of Scc2-Scc4 (Murayama and Uhlmann, 2014). SMC complexes might therefore be able to topologically bind DNA without the need for a loader.

My experiments furthermore suggest that the opening of the ring through the Smc2-Brn1 interface could form a gate for DNA to enter (or exit) the condensin ring. It is possible that the opening reaction is regulated by the binding of DNA to the HEAT-repeat subunits (Fig. 25) or a yet unknown factor. Investigating further how the topological loading of

condensin onto chromosomes is regulated represents a new exciting challenge for understanding how this complex participates in the organization and maintenance of genomic architecture.

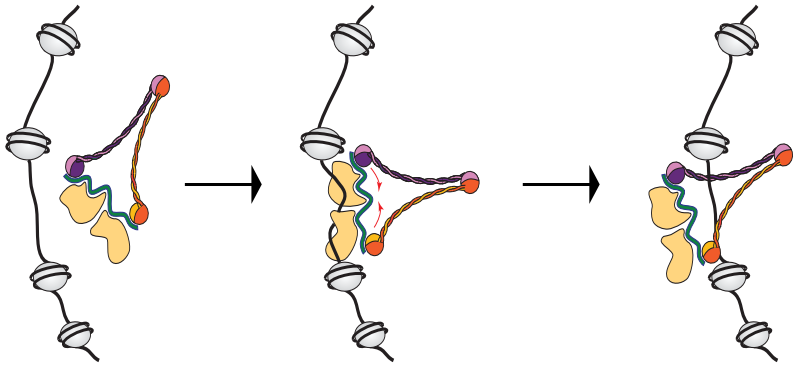

Figure 25. Potential mechanism of condensin's loading onto chromosomes. Condensin may first load onto DNA by direct contacts with the non-SMC subunits. After DNA binding, the SMCs ATPase activity (red arrows) triggers DNA entry through one or multiple interface of the ring structure.

IV Materials and Methods

1. Materials

1.1 Laboratory equipment

Standard biology equipment

Agarose gel chambers	Invitrogen (Darmstadt, DE)
Nanodrop	Thermo Scientific (Wilmington, US)
PCR machine	DNAEngine, BioRad (München, DE)
SDS gel chambers	Invitrogen (Darmstadt, DE)
Western blotter	Amersham Bioscience (Freiburg, DE)
Phosphoimager	FLA3000, Fujifilm (Düsseldorf, DE)
Imaging plate	BAS-MS, Fujifilm (Düsseldorf, DE)

ChIP-qPCR instruments

qPCR machine	ABI 7500, Applied Bioscience (Darmstadt, DE)
Bioruptor	UCD-200, Diagenode (Liege, BE)

Yeast equipment

Dissection microscope	MSM 400, Singer (Wachet, UK)
Spectrophotometer	Amersham Bioscience (Freiburg, DE)
Vibrax	IKA Werke (Staufen, DE)
FastPrep	MP Biomedical (Santa Ana, US)
Freezer mill,	SPEX SamplePrep (Metuchen, US)

Centrifuges

Small	Eppendorf (Wesseling, DE)
Middle	Multifuge 3SR+, Heraeus (Newport, UK)
Big	Avanti J-20 XP, Beckmann (Brea, US)

Software

Clustal X	EBI (Hinxton, UK)
Illustrator CS3	Adobe (San Jose, US)
Multi gauge	Fujifilm (Düsseldorf, DE)
Office 2008	Microsoft (Unterschleißheim, DE)
Photoshop CS3	Adobe (San Jose, US)
SnapGene 2	GSL Biotech LLC (Chicago,US)
SDS software	Applied Biosystems (Darmstadt, DE)
PyMol	DeLano Scientific

1.2 Consumables

Cuvettes for transformation	Biorad (München, DE)
3 mm filter paper	Whatman (Dassel, DE)
1 mm filter paper	Roth (Karlsruhe, DE)
Glass beads 0.25-0.5 mm	Roth (Karlsruhe, DE)
24-well dishes	Nunc (Waltham, US)
PVDF membrane	Biorad (München, DE)
Southern membrane Immobilon-NY+	Millipore (Schwalbach, DE)
KODAK BioMax MR Film	Sigma-Aldrich (Steinheim, DE)
NuPAGE 4-12% Bis-Tris Mini Gels	Invitrogen (Darmstadt, DE)
NuPAGE 3-8% Tris-Acetate Mini Gels	Invitrogen (Darmstadt, DE)
Nick columns	GE Healthcare (Freiburg, DE)
Nitrocellulose membrane	Perkin Elmer Life Science (Boston, US)
Filter membrane	Millipore (Darmstadt, DE)

1.3 Chemicals and media components

Ampicillin	Calbiochem (San Diego, US)
Agarose, for routine use	Sigma-Aldrich (Steinheim, DE)
Agarose ultrapure	Upstate (Lake Placid, US)
α-32P Adenosinetriphosphate	Hartmann Analytic (Braunschweig, DE)
Dextran	Amresco (Solon, US)
Galactose	Biosynth (Staad, CH)
Geneticine sulfate G418	Gibco (Paisley, UK)
HEPES	Biomol (Hamburg, DE)
Nocodazole	Acros Organics (Geel, BE)
NP-40	Fluka (Buchs, CH)
Phenylmethylsulfonylfluoride (PMSF)	Applichem (Darmstadt, DE)
Raffinose	Biosynth (Staad, US)
Sodiumdodecylsulfate (SDS)	Serva (Heidelberg, DE)
Dibromobimane (bBBr)	Invitrogen (Darmstadt, DE)
BG-CrAsH	self made
ECF	GE Healthcare (Freiburg, DE)

All other common chemicals were obtained from companies Sigma (München, DE), Merck AG (Darmstadt, DE) and Roth (Karlsruhe, DE) in p. A. quality. Media components were ordered from Becton Dickinson (Heidelberg, DE) and amino acids from Roth (Karlsruhe, DE), Sigma (München, DE) and Fluka (Buchs, CH).

1.4. Biological reagents

1.4.1 Reagents and kits

Bovine Serum Albumin (BSA)	New England Biolabs (Ipswich, US)
Deoxyribonucleotides (dNTPs)	Fermentas (St. Leon-Rot, DE)
Fish sperm DNA	Roche (Mannheim, DE)
Gel extraction kit	Qiagen (Hilden, DE)
Min elute gel extraction kit	Qiagen (Hilden, DE)
PCR purification kit	Qiagen (Hilden, DE)
Protein A dynabeads	Invitrogen (Darmstadt, DE)
Protein G dynabeads	Invitrogen (Darmstadt, DE)
GFP-Trap	Chromotek (Planegg-Martinsried, DE)
Anti-FLAG M2 affinity gel	Sigma-Aldrich (Steinheim, DE)
Quick change II XL kit	Stratagene (La Jolla, US)
Lumi-Light	Roche (Mannheim, DE)
Random primer labeling kit	Stratagene (La Jolla, US)
Rapid DNA ligation kit	Takara (Otsu, JP)
SYBR green PCR master mix	Applied Biosystems (Foster City, US)

1.4.2 Enzymes

Calf intestinal phosphatase (CIP)	New England Biolabs (Ipswich, US)
Klenow polymerase	Fermentas (St. Leon-Rot, DE)
KOD DNA polymerase	Novagen (Madison, US)
Lyticase	Sigma-Aldrich (Steinheim, DE)
Polynucleotide kinase (PNK)	Fermentas (St. Leon-Rot, DE)
Proteinase K	Merck AG (Darmstadt)
Restriction endonucleases	New England Biolabs (Ipswich, US)
RNase	Roche (Mannheim, E)
TEV protease	self-made
TopTaq DNA polymerase	Qiagen (Hilden, DE)
Zymolyase T-100	Seikagaku Corporation (Tokyo, JP)
Prescission protease	self-made

1.4.3 DNA and protein size markers

1 kb DNA ladder	New England Biolabs (Ipswich, US)
100 bp DNA ladder	New England Biolabs (Ipswich, US)
PageRuler prestained protein ladder	Fermentas (St. Leon-Rot, DE)
PageRuler prestained protein ladder	Fermentas (St. Leon-Rot, DE)
HiMark prestained protein marker	Invitrogen (Darmstadt, DE)

1.4.4 Antibodies

Anti-FLAG M2	mouse monoclonal	Sigma-Aldrich (Steinheim, DE)
Anti-V5 tag	mouse monoclonal	AbD Serotec (Düsseldord, DE)
12CA5	mouse monoclonal	self made
16B12	mouse monoclonal	Covance (Princton, US)
Anti-mouse AP	goat polyclonal	GE Healthcare (Freiburg, DE)
Anti-rabbit AP	goat polyclonal	GE Healthcare (Freiburg, DE)
Anti-SMC2	goat polyclonal	Sigma-Aldrich (Steinheim, DE)
Anti-CAPH	goat polyclonal	Bethyl (Montgomery,US)
Anti-CAPD2	goat polyclonal	Bethyl (Montgomery,US)
Anti-SMC4	goat polyclonal	Bethyl (Montgomery,US)
Anti-GFP	goat polyclonal	Roche (Mannheim, DE)
Anti-rabbit HRP	goat polyclonal	Dianova (Hamburg, DE)
Anti-mouse HRP	goat polyclonal	Dianova (Hamburg, DE)

1.5 Plasmids

Table 2: Plasmids used in this study

Fusion constructs		
No	**Name**	**Reference**
849	YIplac211 SMC2-TEV3-BRN1-myc18	Haering Lab
850	YIplac211 BRN1-TEV3-SMC4-myc18	Haering Lab
1612	YIplac211 SMC2-TEV3-BRN1-Presc3-HA6	Haering Lab
1613	YIplac211 SMC2-TEV3-BRN1(K709C)-Presc3-HA6	Haering Lab
1614	YIplac211 SMC2(K639C)-TEV3-BRN1-Presc3-HA6	Haering Lab
1615	YIplac211 SMC2(K639C)-TEV3-BRN1(K709C)-Presc3-HA6	Haering Lab
1629	YIplac211 SMC2-TEV3-BRN1-Presc3-HA6	Haering Lab
	YIplac211 BRN1-TEV3-SMC4-Presc3-HA6	this study

Brn1 constructs		
No	**Name**	**Reference**
1432	Ylplac211 BRN1-PK6	Haering Lab
1601	YIplac128 BRN1-Presc3-HA6	Haering Lab
1603	YIplac128 BRN1(K709C)-Presc3-HA6	Haering Lab
1659	YIplac211 BRN1(K709C)-Presc3-HA6	Haering Lab
1677	YIplac211 BRN1(SpeI_115, K709C)-Presc3-HA6	Haering Lab
1737	YIplac128 BRN1 Presc PK6 KanMX	Haering Lab

Smc4 constructs		
No	**Name**	**Reference**
1045	YIplac128 SMC4-PK6	Haering Lab
1497	YIplac211 SMC4-HA6	Haering Lab
1559	YIplac211 SMC4(V721C)-HA6	Haering Lab
1585	YIplac211 SMC4(R1417C)	Haering Lab
1616	YIplac128 SMC4(V721C)	Haering Lab
1617	YIplac128 SMC4(R1417C)	Haering Lab
1618	YIplac128 SMC4(V721C; R1417C)	Haering Lab
	YIplac211 SMC4(R1417C)-PK6	this study
	pRS303 SMC4(V721C;R1417C)	this study

Smc2 constructs		
No	**Name**	**Reference**
1340	YIplac128 SMC2-PK6	Haering Lab
1562	YIplac128 SMC2(K639C)-PK6	Haering Lab
1658	pRS303 SMC2(K639C)	Haering Lab

Minichromosome constructs		
No	**Name**	**Reference**
1110	Minichromosome 2.3 Kb	Haering Lab
1211	Minichromosome-rDNA	Haering Lab

Other constructs		
No	**Name**	**Reference**
1985	pcDNA5-CAP-E*-SNAP-EGFP-2A-FLAGx3-4xCys-CAP-H*	this study
1709	pFA6a-L(12)-FRB-hph	Euroscarf

1.6 Oligonucleotides

Table 3: Oligonucleotides used in this study

Quick change primers to introduce cysteine mutations in Brn1, Smc2 amd Smc4		
No	**Sequence 5´to 3´**	**Name**
609	GTATTCGGATGATACACTATGCGACATTTCAACAAGCTTTTGTTTTATA	BRN1 (K709C)
610	GCTTGTTGAAATGTCGCATAGTGTATCATCCGAATACATTTTAC	BRN1 (K709C)
613	CATAGATATCTTAAACTGTACTTAGTAAGCATGCGGTACCAAGC	SMC4 (R1417C)
614	CCGCATGCTTACTAAGTACAGTTTAAGATATCTATGTTTTTAATCG	SMC4 (R1417C)
137	TGTGAAGATCCGGAAACAGCATGTAAAATTACCTTCCATCCAAAG	SMC2 (K639C)
138	CTTTGGATGGAAGGTAATTTTACATGCTGTTTCCGGATCTTCACAG	SMC2 (K639C)
139	ATGATGTCGTGGTTGATACTTGTGAATGTGCGCAACACTGCATCG	SMC4 (V721C)
140	CGATGCAGTGTTGCGCACATTCACAAGTATCAACCACGACATCATC	SMC4 (V721C)

Primers for C-terminal tagging of Scc2 with FRB		
No	**Sequence 5´to 3´**	**Name**
YF-1	CGATTTGGTGTCCCTACTCA	Checking 1
YF-2	CTCGTCCGAGGGCAAAGGAA	Checking 2
YF-3	CTCGTCCGAGGGCAAAGGAA	Checking 3
YF-4	GCCGCTCCGAAAACCGTATT	Checking 4
YF-5	CATCAAATGGCAAGCTTCTTACATATTTTAGAAAACACGTGAA GGATACGGGTGGCGGTTCTGGTGGAAT	FRB cassette
YF-6	AATGCAAAATGATTATTAATACTATGTATATTTTAAGTGCAAT ATATTATTCCTTTGCCCTCGGACGAG	FRB cassette
156	CTCAACGGAGGTAAGAATGATG	tor1-1
157	GGATATCCAAATGTCTCTTGAAAC	tor1-1

Primers for cloning HA6 and PK6 into Brn1-Smc4 and Smc4 respectively		
No	**Sequence 5´to 3´**	**Name**
YF-7	AAAACGACGGCCAGTGAATTCATGGTA	Brn1-Smc4 (EcoRI)
YF-8	GCGACTAGTCATCTTATATAACTACCTGCTGGTT	Brn1-Smc4 (SpeI)
YF-9	TTGACTGTACTCGATCAGGAATACCGGTCC	Smc4 (AgeI)
YF-10	GAGCGGCCGCtAGTACAGTTTAAGATATCTATGTTTT	Smc4 (NotI)

Primers for qPCR		
No	**Sequence 5´to 3'**	**Name**
SC-41	GACAGAGAGGGCAAAAGAAAA	rDNA
SC-42	TTTCTGCCTTTTTCGGTGAC	rDNA
SC-77	TGGTGTGGAAGTCCTAATATCG	CEN4
SC-78	TGCATGATCAAAAGGCTCAA	CEN4

Quick change primers to introduce silent mutation in SMC2 and CAP-H		
No	**Sequence 5´to 3´**	**Name**
AR-124	CAAGTCCTATGCTCAGAGGACCGAGGTGAACGGTTTTGACCC CCTCTT	SMC2(A)
AR-125	GCATTGAAGAGGGGGTCAAAACCGTTCACCTCGGTCCTCTGA GCATA	SMC2(A)
AR-126	GATGGCCCAGGGCCATAGGGTCGAAACCGAGCATTATGAAG AAATTG	CAP-H(B)
AR-127	CTTCAATTTCTTCATAATGCTCGGTTTCGACCCTATGGCCCTG GGCCA	CAP-H(B)

Primers to test for integration of *LEU2*, *URA3*, *TRP1*, *HIS3*		
No	**Sequence 5´to 3´**	**Name**
39	TCATGACATTAACCTATAAAAATAGGCG	YIp
40	CGTCATCACCGAAACGCGCG	YIp
41	CAAAGAAGGTTAATGTGGCTGTGG	URA3
42	CGTCATTATAGAAATCATTACGACCG	URA3
43	GTCACCTTACGTACAATCTTGATCCGG	TRP1
44	CAATCAATCAAAAAGCCAAATGATTTAGC	TRP1
45	GCCGAGCGGTCTAAGGCGCC	LEU2
46	CCTTCTTGATAAATGTATGTAGATTGCG	LEU2
96	TTGTTTGGCCGAGCGGTCTAAG	LEU2
97	CGACTACGTCGTTAAGGCCGTTTC	LEU2
153	GTGGGAAAAACTTATCGAAAGATGACG	HIS3
154	GAATACCACTTGCCACCTATCACC	HIS3
155	GCATCTGTGCGGTATTTCACACC	RS

Primers for cloning SMC2*-SNAP-EGFP-2A-FLAG34cys-CAP-H*		
No	**Sequence 5´to 3´**	**Name**
609	CTAGCGGCAGTGGAGAGGGCAGAGGAAGTCTGCTAACATGC GGTGACGTCGAGGAGAATCCTGGCCCAATGA	T2A
610	CCGGTCATTGGGCCAGGATTCTCCTCGACGTCACCGCATGTT AGCAGACTTCCTCTGCCCTCTCCACTGCCG	T2A
AR-128	CAGGTACCTGGAAGCGGCTCCGGATTCACCATGGACAAAGA CTGCGAAATGAAGCGCACCACC	SNAP (NotI)
AR-129	CAGGTACCTGGAAGCGGCTCCGGATTCACCATGGACAAAGA CTGCGAAATGAAGCGCACCACC	SNAP (KpnI)
AR-131	CTAGCGCTACCGATCGCCACCATGACCGGTTTCCTGAACTGC TGCCCTGGCTGCTGTATGGAACCGCT	4cys- (BsrGI)
AR-132	GTACAGCGGTTCCATACAGCAGCCAGGGCAGCAGTTCAGGA AACCGGTCATGGTGGCGATCGGTAGCG	4cys- (BsrGI)
AR-137	CCGGTGACTACAAAGACCATGACGGTGATTATAAAGATCAT GATATCGATTACAAGGATGACGATGACAAGT	$FLAG_3$ (AgeI)
AR-138	CCGGACTTGTCATCGTCATCCTTGTAATCGATATCATGATCTT TATAATCACCGTCATGGTCTTTGTAGTCA	$FLAG_3$ (AgeI)
AR-164	TGACCGGTGTGAGCAAGGGCGAGGAGCTGTTCAC	GFP (AgeI)
AR-165	GTCCCGGGCCCTCCACTGCCGCTAGCCTTATACAGCTCGTCC ATTC	GFP (XmaI)
AR-133	GATCTCGAGCTTAAGCCACCATGCATATTAAGTCAATTATTC TAGAG	SMC2 (AflII)
AR-122	ATGCGGCCGCTCAGCCCAGGCTTGCCCAGTCTGTGG	SMC2 (Not I)

1.7 Yeast and Bacterial strains

Table 4: Bacterial strains used in this study

Name	Genotype	Reference
E. coli DH5 α	fhuA2 Δ (argF-lacZ)U169 phoA glnV44 80 Δ (lacZ)M15 gyrA96 recA1 relA1 endA1 thi-1 hsdR17	Hanahan, 1983
E. coli XL-10 gold	Tetr Δ (mcrA)183 Δ (mcrCB-hsdSMR-mrr)173 endA1 supE44 thi-1 recA1 gyrA96 relA1 lac Hte [F′ proAB lacIqZ Δ M15 Tn10 (Tetr) Amy Camr]*	Stratagene (Palo Alto, US)

Table 5: Yeast strain used in this study

No	Genotype	Reference
2452	MATa smc3::HIS3 scc1::kanMX ura3::SMC3(E570C)-3xNoTEVlinker-SCC1(A547C)-3xTEV HA6::URA3	Haering Lab
2459	MATa leu2:SMC1(G22C, K639C)-myc9::LEU2 smc1::kanMX4 smc3::HIS3 scc1::kanMX ura3::SMC3(E570C)-3xNoTEVlinker-SCC1(A547C)-3xTEV HA6::URA3	Haering Lab
3197	MATα smc2::HIS3 leu2::SMC2(K639C)-PK6::LEU2 smc4::natMX ura3::SMC4(V721C)-HA6::URA3	this study
3355	MATa brn1::natMX smc2::HIS3 smc4::natMX leu2::SMC4(V721C, R1417C)::LEU2 ura3::SMC2(K639C)-TEV3-BRN1(K709C)-Prec3-HA6::URA3	Haering Lab
3361	MATα tor1-1 fpr1::loxP-LEU2-loxP RPL13A-2×FKBP12::loxP-TRP1-loxP	Euroscarf
3363	MATα tor1-1 fpr1::NAT RPL13A-2xFKB12::TRP1 SCC1-FRB::kanMX6	this study
3388	MATa brn1::natMX smc2::HIS3 smc4::natMX leu2::SMC4(V721C, R1417C)::LEU2 ura3::SMC2(K639C)-TEV3-BRN1(K709C)-Prec3-HA6::URA3 Minichromosome-rDNA	this study

No	Genotype	Reference
3444	MATα tor1-1 fpr1::IoxP-LEU2-IoxP RPL13A-2xFKBP12::IoxP-TRP1-IoxP BRN1-HA6::HIS3	this study
3457	MATα tor1-1 fpr1::loxP-LEU2-loxP RPL13A-2×FKBP12::loxP-TRP1-loxP SCC2-FRB:: hghMX	this study
3474	MATa tor1-1 fpr1::IoxP-LEU2-IoxP RPL13A-2xFKBP12::IoxP-TRP1-IoxP BRN1-HA6::HIS3 SCC2-FRB:: hghMX	this study
3477	MATa tor1-1 fpr1::IoxP-LEU2-IoxP RPL13A-2xFKBP12::IoxP-TRP1-IoxP SCC1-HA6::HIS3 SCC2-FRB:: hghMX	this study
3576	MATa tor1-1 fpr1::loxP-LEU2-loxP RPL13A-2×FKBP12::loxP-TRP1-loxP SCC2-FRB::hphMX SCC4-HA6::HIS3	this study
3682	MATα smc2::HIS3 brn1::natMX ura3::SMC2(K639C)-TEV3-BRN1(K709C)-Prec3-HA6::URA3 Minichromosome rDNA	this study
3685	MATα dbrn1::HIS3 leu2::BRN1-Presc3-HA6:::LEU2	this study
3687	MATα dbrn1::HIS3 leu2::BRN1(K709C)Presc3-HA6:::LEU2	Haering Lab
3689	MATa smc2::hphMX4 his3::SMC2 K639C:::HIS3	Haering Lab
3691	MATa smc4::natMX leu2::SMC4(V721C)::LEU2 BRN1(Presc3)-PK6 KanMX::BRN1	this study
3694	MATα smc4::natMX his3::SMC4 (V721C; R1417C):: HIS3	this study
3698	MATα smc4::natMX ura3::SMC4(R1417C)::URA3 dbrn1::HIS3 leu2::BRN1 Presc3-HA6:::LEU2	this study
3700	MATα Brn1(Presc3)-PK6::KanRMX his3::SMC2K639C:::HIS3 dsmc2::hghMX leu2::SMC4(V721C)::LEU2 smc4::natMX	this study

No	Genotype	Reference
3911	MATα brn1::HIS3 smc4::natMX ura3::BRN1-SMC4-HA6::URA3	this study
3939	MATa Brn1(Presc3)-PK6::kanRMX his3::SMC2K639C:::HIS3 smc2::hghMX	this study
3941	MATα Brn1(Presc3)-PK6::kanRMX his3::SMC2K639C:::HIS3 smc2::hghMX leu2::SMC4V721C::LEU2 smc4::natMX Minichromosome rDNA	Haering Lab
3942	MATα Brn1(Presc3)-PK6::kanRMX his3::SMC2K639C:::HIS3 smc2::hghMX leu2::SMC4V721C::LEU2 smc4::natMX Minichromosome 2.3 kb	this study
3955	MATa smc2::HIS3 brn1::natMX ura3::SMC2(K639C)-TEV3-BRN1-Presc3-HA6::URA3 smc4::natMX leu2::SMC4(V721C)::LEU2 Minichromosome rDNA	this study
3956	MATa smc2::HIS3 brn1::natMX ura3::SMC2-TEV3-BRN1(K709C)-Presc3-HA6::URA3 smc4::natMX leu2::SMC4(R1417C)::LEU2 Minichromosome rDNA	this study
3957	MATa smc2::HIS3 brn1::natMX ura3::SMC2-TEV3-BRN1(K709C)-Presc3-HA6::URA3 smc4::natMX leu2::SMC4(R1417C)::LEU2 Minichromosome 2.3 kb	this study
3958	MATa smc2::HIS3 brn1::natMX ura3::SMC2(K639C)-TEV3-BRN1-Presc3-HA6::URA3 smc4::natMX leu2::SMC4(V721C)::LEU2 Minichromosome 2.3 Kb	this study
3977	MATa ura3:: SMC4 (R1417C)- PK6::URA3 smc4::natMx	this study
3978	MATα ura3:: SMC4 (R1417C)- PK6::URA3 smc4::natMx	this study

No	Genotype	Reference
3996	MATα ura3:: SMC4 (R1417C)- PK6::URA3 smc4::natMx brn1::HIS3 his3:: BRN1(K709C) Presc-HA6::HIS3	this study
3997	MATa ura3:: SMC4 (R1417C)- PK6::URA3 smc4::natMx brn1::HIS3 leu2:: BRN1(K709C) Presc-HA6::LEU2	this study
3998	MATα ura3:: SMC4 (R1417C)- PK6::URA3 smc4::natMx brn1::HIS3 leu2:: BRN1 Presc-HA6::LEU2	this study
4017	MATα brn1::HIS3 leu2::BRN1-Presc3-HA6:::LEU2 SMC4-PK6::kanMX	this study
4019	MATα brn1::HIS3 leu2::BRN1(K639C)-Presc3-HA6:::LEU2 SMC4-PK6::kanMX	this study
4038	MATα Smc2-Pk6::kanMx smc4::natMx ura3::Smc4 V721C-HA6:::URA3	this study
4039	MATa Smc2-Pk6::kanMx smc4::natMx ura3::Smc4 V721C-HA6:::URA3	this study
4055	MATa brn1::natMX smc2::HIS3 smc4::natMX leu2::SMC4::LEU2 ura3::SMC2-TEV3-BRN1-Presc3-HA6::URA3 Minichromosome 2.3 kb	this study
4056	MATa brn1::natMX smc2::HIS3 smc4::natMX leu2::SMC4::LEU2 ura3::SMC2-TEV3-BRN1-Presc3-HA6::URA3 Minichromosome rDNA	this study
4085	MATα smc2::hphMX4 ura3::SMC2-PK6:URA3	Haering lab
4086	MATa smc2::hphMX4 ura3::SMC2-PK6:URA3	this study

1.8 Buffers and solutions

1.8.1 Standard DNA techniques

6x DNA loading buffer	30% (v/v) Glycerol 25 mM EDTA 0.1% (w/v) Bromphenol blue 2 M TRIS
50x TAE	5.75% (v/v) Glacial acetic acid 50 mM EDTA pH 8.0
Southern blotting solution	0.4 M NaOH 1 M NaCl
20x SSC	3 M NaCl 0.3 M Sodium citrate pH 7.0 3 M NaCl
Hybridisation solution	10.8% (w/v) Dextran 1.1% (v/v) SLS 6.36x SSC
5x Oligo annealing buffer	200 mM TRIS pH 7.5 100 mM $MgCl_2$ 250 mM NaCl

1.8.2 Standard protein techniques

5x SDS sample buffer	250 mM TRIS-HCl pH 6.8 10% (w/v) SDS 0.5% (w/v) Bromphenol blue 50% (v/v) Glycerol 0.5 M DTT
20x MES/SDS running buffer	50 mM MES 50 mMTris base 0.1% SDS 1 mM EDTA
20x MOPS/SDS running buffer	1 M MOPS 1 M TRIS base 2 % (w/v) SDS 20 mM EDTA

20x Tris-Acetate running buffer	50 mM Tricine 50 mM TRIS-base 2 % (w/v) SDS 20 mM EDTA
Towbin buffer	25 mM TRIS base 192 mM Glycine 0.01% (w/v) SDS 10% (v/v) Methanol
Colloidal Coomassie	0.1 % (w/v) Coomassie Brilliant Blue G250 2 % (w/v) ortho-phosphoric acid 10 % (w/v) ammonium sulfate
TBS (10x)	1.4 M NaCl 30 mM KCl 250 mM TRIS-HCl pH 7.4

1.8.3 Yeast minichromosome assay, immunoprecipitation and cross-linking

Yeast lysis buffer	50 mM TRIS pH 8.0 100 mM NaCl 2,5mM $MgCl_2$ 0.25% (v/v) TritonX-100
Pellet washing buffer	50 mM TRIS pH 8.0 100 mM NaCl 2.5 mM $MgCl_2$
Reaction buffer	25 mM NaPI pH 7.5 100 mM NaCl 10 mM MgSO4 50 mM $MgCl_2$ 0.25% (v/v) TritonX-100
Elution buffer	50 mM TRIS pH 8.0 100 mM NaCl 1 mM MgSO4

1.8.4 Mammalian cell lysis, immunoprecipitation and chromatin fractionation

HNTG	50 mM Hepes pH 7.5 150 mM NaCl 5 mM EGTA 10% glycerol 1% (v/v) TritonX-100
Buffer A	10 mM Hepes pH 7.9 10 mM KCl 1.5 mM $MgCl_2$ 10% glycerol 0.34 M sucrose
Buffer B	3mM EDTA 0.2 mM EGTA 1.5 mM $MgCl_2$
Imaging buffer	20 mM Hepes, pH 7.4, 115 mM NaCl, 1.2 mM $CaCl_2$, 1.2 mM $MgCl_2$, 1.2 mM K_2HPO_4, 2 g /l D-glucose

1.8.5 ChIP-qPCR

Fixative	50 mM TRIS-HCl pH 8.0 100 mM NaCl 0.5 mM EGTA 1 mM EDTA 30% (v/v) Formaldehyde
HEMS	100 mM HEPES-KOH pH 7.5 1 mM EGTA 1 mM $MgSO_4$ 1.2 M Sorbitol
Lysis buffer	50 mM HEPES-KOH pH 7.5 140 mM NaCl 1 mM EDTA 1% (v/v) Triton X-100 0.1% (w/v) Sodium deoxycholate

Wash buffer	10 mM TRIS pH 8.0 0.25 M Lithium chloride 0.5% (v/v) NP-40 0.5% (w/v) Sodium deoxycholate 1 mMEDTA
TE buffer	10 mM TRIS-HCl pH 8.0 1 m EDTA
TES buffer	50 mM TRIS-HCl pH 8.0 10 mM EDTA 1% (w/v) SDS

1.8.6 Solutions for yeast work

Drop out for yeast media	2 g/l Arginine 1 g/l Histidine 6 g/l Isoleucine 6 g/l Leucine 4 g/l Lysine*H2O 1 g/l Methionine 6 g/l Phenylalanine 5 g/l Threonine 4 g/l Tryptophan	one or more amino acids were left out for a certain drop out
SCE buffer:	1 M Sorbitol 0.1 M Na-Citrat pH 5.8 10 mM EDTA pH 7.6	
SDS lysis buffer:	2% (w/v) SDS 100 mM TRIS-HCl pH 9.0 50 mM EDTA	

1.9. Culture media

1.9.1 Culture media for bacteria

LB	EMBL media kitchen, standard protocol, If required, supplemented with ampicillin (100 mg/l)
SOC	EMBL media kitchen, standard protocol

1.9.2 Culture media for yeast

YPAD	EMBL media kitchen, standard protocol If required supplemented with geneticin (200 mg/l) or hygromycin (300 mg/l)
SD-minimal plates	8 g/l Yeast nitrogen base without amino acids 22g/l Agar 2% (w/v) Glucose after autoclaving
YEP	11 g/l Yeast extract 22 g/l Peptone 55 mg/l Adenine
SpoVB plates	8,2 g/l Sodium acetate 1.9 g/l Potassium chloride 350 mg/l Magnesium sulfate 1.2 g/l Sodium chloride 15 g/l Agar
-TRP	55 mg/l Tyrosine 55 mg/l Adenine 55 mg/l Uracil 11 g/l C.A.A vitamin assay 0.5% (w/v) Leucine after autoclaving 2% (w/v) Glucose after autoclaving (22 g/l Agar)
-URA	55 mg/l Tyrosine 55 mg/l Adenine 11 g/ C.A.A vitamin assay 0.5% (w/v) Leucine after autoclaving 0.5% (w/v) Tryptophan after autoclaving

	2% Glucose after autoclaving (22 g/l Agar)
-LEU	55 mg/l Tyrosine 55 mg/l Adenine 55 mg/l Uracil 1x -LEU drop out (see Materials and Methods 1.8.5) 2% (w/v) Glucose after autoclaving (22 g/l Agar)
-HIS	55 mg/l Tyrosine 55 mg/l Adenine 55 mg/l Uracil 1x -His drop out (see Material and Methods 1.8.5) 2% (w/v) Glucose after autoclaving 22 g/l Agar)

2 Methods

2.1 Standard molecular biology methods

2.1.1 Isolation of plasmid DNA, concentration measurement

Plasmid DNA was isolated from bacteria using the QIAprep Spin Miniprep Kit according to the manufacturer's protocol. DNA concentration was measured at 260 nm by UV spectroscopy using a NanoDrop spectrophotometer.

2.1.2 Agarose gel electrophoresis

Agarose gel electrophoresis was used for identification, separation and purification of nucleic acids. DNA samples were diluted in 6x DNA loading buffer prior to loading. Depending on the amount and the expected size of DNA samples different gels varying in size and agarose concentration (0.8% - 2% (w/v) agarose in 1x TAE) were run. SYBR safe (1x) or ethidium bromide (0.5 µg/ml) was mixed into the liquid gel and gels were detected on a blue light or UV-light transilluminator. If necessary, DNA fragments were purified from gels using the QIAquick Gel Extraction Kit or the MinElute Gel Extraction Kit for small fragments (< 4 kb).

2.1.3 Southern blotting

Southern blotting was used to detect minichromosomes in DNA samples. DNA samples containing minichromosomes were separated at 65 V for 20 hrs on a 0.8% (w/v) agarose gel supplemented with 0.5 µg/ml ethidium bromide. In preparation for the Southern transfer the gel was soaked for 20 min in 0.25 M HCl and for 2 x 20 min in alkaline blotting solution to depurinate and denature the DNA respectively. In between, two short washes (2 x 4 min in water) were performed to remove the acid. The Southern blot was assembled on a plexiglas plate over a tray filled with blotting solution. Two long Whatman papers whose ends dip into the blotting solution formed the first layer, followed by two Whatman papers about the size of the gel, the gel upside-down, the Southern membrane and two further Whatman papers about the size of the gel. To ensure a good transfer all Whatman papers were soaked in blotting buffer beforehand and bubbles between the layers were removed by rolling a plastic pipet over each layer. Finally a stack of 15 cm towels, a second plexiglass plate and a weight was placed on the top. The transfer was performed for 5 h to over night. After the transfer had been completed, the blot was disassembled and the blotting membrane was washed for 3 min in 2x SSC, rinsed with 40 mM Sodium phosphate pH 7.0 to remove salts and dried on a Whatman paper. To fix the DNA to the membrane the membrane was incubated for 1 h at 65ºC. Then it was placed in a hybridization tube and incubated with prewarmed hybridization solution containing 50 µg/ml denatured fish sperm DNA at 65ºC for at least 1 hour. In the meantime the probe was prepared. 25 ng of a 2.3 kb restriction fragment of the minichromosome (3.3 kb minichromosome digested with *PvuI*, *SalI*) was labeled with α-32P dATP using the Prime it II Random Primer Labeling Kit following the instructions of the manual. The radio-labeled probe was purified from unincorporated radio-labeled nucleotides using Nick Columns and denatured for 10 min at 95ºC. The pre-hybridization solution was discarded and fresh hybridization solution, mixed with the purified labeled probe and 50 µg/ml denatured fish sperm DNA, was added to the membrane and incubated for 12-24 h at 65ºC in the hybridization oven. After the hybridization, excess probe was washed from the membrane using pre-warmed 1% (w/v) SDS/2x SSC buffer (3 x 20 min). Subsequently the membrane was rinsed in 3 mM TRIS pH 8.0, covered with Saran wrap and exposed to a phosphoimager plate for 3h or overnight. The imager plates were scanned on a FLA-7000 image analyzer and quantified with the Multi gauge software.

2.1.4 Polymerase chain reaction

To amplify specific DNA sequences from plasmids or genomic DNA polymerase chain reactions (PCRs) were performed. For preparative PCR reactions Phusion polymerase was used while in analytical PCR reactions TopTaq polymerase was

applied. PCR conditions were varied and optimized for every amplification. The reaction was generally performed in 50 µl total volume using 1.25 U polymerase, 0.2 mM dNTPs, 0.3 µM of each primer and either 50-100 ng plasmid DNA or 2 µl yeast genomic DNA. A typical programme of the thermal cycler consisted of an initial denaturation (3 min, 94ºC) followed by 35 cycles of denaturation (15 s at 94ºC), annealing (30 s at the optimal annealing temperature of the primers) and extension (1 min to 5 min at 72ºC depending on the length of the target and the extension rate of the polymerase). The PCR products were analyzed on agarose gels and if necessary purified from the gel (see Materials and Methods 2.1.2).

2.1.5 Restriction and ligation of DNA

For analytical restriction digests ~500 ng plasmid DNA was incubated with 5 U of restriction enzyme in a total volume of 10 µl in buffers according to manufacturer's instructions. The success of the digest was checked via agarose gel electrophoresis. Preparative restrictions were performed in 30-50 µl using 2-5 µg DNA or PCR product and 10 U enzyme. The digests were incubated for 1 h (analytical digests) or 2 h (for preparative digest) at 37ºC. Linearized vectors that were intended for ligation were generally dephosphorylated by addition of 1 U CIP for 30 min to prevent formation of re-ligates. Digested (and dephosphorylated) DNA fragments were separated by agarose gel electrophoresis and desired fragments were isolated as described above (Materials and Methods 2.1.2). Insert DNA was ligated into linearized dephosphorylated vectors using the Rapid DNA Ligation Kit according to the manufacturer's protocol. An insert:vector ratio of three to five was aimed and the reaction was incubated for at least 20 min at 16ºC. As a control, linearized dephosphorylated vector alone was used in a second ligation reaction. Ligation reactions were purified using the PCR Purification Kit and 10 µl of the 30 µl eluate was used for transformation of electrocompetent *E. coli* DH5α.

2.1.6 Mutagenesis

To generate single point mutations in plasmid DNA the Quick Change Site-Directed Mutagenesis Kit was used according to the manufacturer's protocol with the provided heat-shock competent *E. coli* XL10 gold cells. Quick change primers were designed using the web-based QuickChange Primer Design tool of Stratagene.

2.1.7 Oligonucleotide annealing

Complementary oligonucleotides were annealed by mixing equal amounts of oligos (100 µM stock) in 1x oligo annealing buffer. The annealing mixture was heated for 5 min at 70ºC, slowly cooled down to 37ºC and kept on ice.

2.1.8 Transformation of Bacteria

For transformation of plasmids and ligations chemical competent *E. coli* DH5α cells were used. Cell aliquots 100 µl) were thawed on ice and mixed with 5 µl purified ligation reaction or 10 ng plasmid DNA for 30 min on ice. The mixture of cells and DNA was heated for 30 sec at 42°C and put immediately after on ice for additional 2 min. Pre-warmed SOC medium was added and then cells were incubated on a rotor for 1 h at 37ºC. After the recovery phase, cells were plated on selective media (usually LB + ampicillin).

2.2 Cloning strategies

2.2.1 Generation of FRB tagging cassette

PCR primers for amplification of the FRB tagging cassette were designed as follows (Longtine et al. 1998). To the 5' end of the forward primer, whose sequence is shown in Tabel 3, were added 50 nucleotides of sequence from the sense strand at the 3' end of the *Scc2* gene immediately upstream of the stop codon (without including the stop codon). Similarly, 50 nucleotides of sequence from the antisense strand at the 3' end of the *Scc2* gene immediately downstream of the stop codon (without including the stop codon) were added to the 5' end of the reverse primer. After amplification with high fidelity thermo-stable DNA polymerase (Phusion), 5 ul of PCR reaction containing the tagging cassete were used to transform diploid yeast strains. Trasformants were then selected on hygromycin plates. To verify correct insertion of the FRB cassete at 3' end of *Scc2* gene, checking primer were designed as previously described (Knop et al., 1999; see Table 3).

2.3 Biochemistry methods

2.3.1 SDS polyacrylamide gel electrophoresis (SDS-PAGE)

Proteins were separated according to their molecular weight on SDS polyacrylamide gels. Samples were prepared by addition of SDS protein loading buffer, boiled for 5 min at 95ºC and loaded on the gel. In order to improve resolution precast NuPAGE 4-12% Bis-TRIS or 3-8% TRIS acetate mini gels were used and run at 180V for 1 h in MOPS/SDS PAGE buffer or 150V for 2.5 h in TRIS-Acetate buffer, respectively.

After electrophoresis proteins were stained with Coomassie solution for 15-30 min and destained by washing extensively with ddH2O.

2.3.2 Western blotting

To transfer proteins from SDS polyacrylamide gels to PVDF or nitrocellulose membranes a semi-dry Western blotter was used. Prior to blotting the PVDF membrane was activated by incubation in methanol for 30 s and the SDS gel was equilibrated in Towbin buffer. The blot was assembled onto the cathode in the following order: 2 Whatman papers soaked in Towbin buffer, gel, membrane and again 2 Whatman papers soaked in Towbin buffer. All layers were flattened to remove air bubbles and allow even transfer. Gels were generally blotted for 2 h with a current of 0.8 mA/cm^2. The membrane was blocked for 1h with TBST buffer containing 5% milk powder, and incubated for 1h at RT (or 16 h O/N) in a solution containing primary antibody. After extensive washing of the excess of the primary antibody with TBST buffer, the blot was incubated with a solution containing secondary antibody for 45 min at RT, and thoroughly washed in TBST again. All antibodies were dissolved in TBST containing 5 % milk powder. The secondary antibody was conjugated with horseradishperoxidase (HRP) and it was detected via chemoluminescence (Lumi-Light Western blotting substrate, Roche) on a BioMax MR film. For semi-quantitative Western Blot, alkaline phosphatase (AP) conjugated to the secondary antibody was incubated with ECF substrate. By dephosphorylating ECF, AP produces a fluorescent product. Fluorescent signals were then detected by scanning the membrane on the FLA-7000 image analyzer and quantified with the Multi gauge software.

2.3.3 ChIP-qPCR

42 ml asynchronous culture with OD600 of 0.3 were treated with nocodazole (10ug/ml) or rapamycin (100 nM) as described previously (D'Ambrosio et al., 2008; Haruki et al., 2008). At OD600 of 0.6 cell were fixed with 4.2 ml fixative at 16ºC on a rotor for 30 min. The reaction was stopped by addition of 100 mM glycine (final concentration). After 5 min incubation cells were pelleted (2,300 g), washed in 20 ml ice-cold PBS and incubated on ice in 1 ml 100 mM PIPES supplemented with 10 mM DTT. Cells were pelleted again, washed in HEMS and spheroplasted in HEMS buffer with 0.5 mg/ml zymolyase. Spheroplasts were pelleted, washed twice with ice-cold HEMS buffer, shock frozen in liquid nitrogen and either kept at -80ºC or immediately thawed again. To lyse the spheroplasts the pellet was resuspended in 2 ml lysis buffer supplemented with protease inhibitors. Chromatin was sonicated to an average length of 500 bp using the Bioruptor UCD-200 for 9 min at 'high level'

with 30 s on, 1 min off settings. Lysates were cleared by two rounds of centrifugation and incubation with 50 µl protein A dynabeads for 2 h at 4ºC. 150 µl cleared lysate was used to check sonication, 175 µl lysate was frozen at -20ºC as an input sample, and 1.4 ml was used for immunoprecipitation with 10 µl 12CA5 anti-HA antibody overnight at 4ºC, followed by a 4 h incubation with 100 µl protein A dynabeads. Beads were washed successively for 5 min at room temperature with 1 ml of four different buffers: lysis buffer, lysis buffer with 500 mM NaCl, wash buffer and TE buffer. Finally beads were eluted in TES buffer at 65ºC and 900 rpm for 8 h. Samples were treated with 100 µg/ml RNaseA for 1.5 h and with 660 µg/ml Proteinase K for 2 h. The DNA was finally purified via spin columns (Qiagen). The columns were dried for 2 min at 65ºC before the DNA was eluted in 50 µl EB buffer pre-warmed to 60°C. The qPCR reactions were performed with SYBR green PCR Master mix and contained 5 µl purified DNA, 5 µM primers (see Table 3) in a total volume of 20 µl. 1:5 and 1:25 dilutions of immunoprecipitated samples and 1:5, 1:50, 1:500, and 1:5000 dilutions of input samples were used. The reactions were run on an ABI 7500 real-time PCR system and the baseline adjustment method of the SDS software was used to determine the Ct value. A melting curve was recorded for each primer pair to verify the absence of non- specific PCR products.

2.3.4 Immunoprecipitation of condensin- or cohesin-minichromosome complexes and bBBr cross-linking

Yeast strains containing minichromosomes with TRP selection markers were grown at 25ºC in synthetic medium without tryptophan (-TRP). Pre-cultures were diluted into 200 ml (for cohesin strain) or 500 ml (for condensin) YEPD to a final OD_{600} of 0.2, and harvested at an OD_{600} of 1.0. After a rinsing in Pellet washing buffer twice, cell pellets were resuspendend in 1.2 ml (for cohesin) or 3 ml (for condensin) of Yeast lysis buffer supplemented with 2× complete EDTA-free protease inhibitor, 1 mM DTT, 1 mM PMSF and 100 µg/ml RNaseA on ice. To prepare extracts, 250 ul aliquots of the resuspended pellet were split into 1.5 ml micro-tubes with caps and filled with glass beads (0.2-0.5 microns, Sigma) to about 1 mm below liquid level. Lysis was obtained by vortexing the tube on a FastPrep machine with the following settings: 5 cycles of 15 sec, with 2 min cooling in between. Yeast extract was released from the tube by punching a hole into the bottom of the micro-tubes with a hot needle (27G). The lysate was then cleared by two time centrifugation at 12,000 g for 20 min. Cleared lysate was incubated rotating at 4ºC with 5 µg (for cohesin) or 10 µg (for condensin) of 12CA5 anti-HA antibody for 1 h, followed by addition of 50 or 100 µl protein A dynabeads (equilibrated in 100 mM NaP_i buffer pH 8.0) overnight. The day after, beads were washed 3 times for 5 min at 4ºC with complete lysis buffer. DTT was removed by 3 additional washes (of 3 min each) in Reaction buffer

(without DTT) followed by resuspension of each sample in 190 µl of the same buffer. Samples were then splitted into 2 aliquots of 95 µl and immediately incubated with 5 µl DMSO only or 5 mM bBBr in DMSO for 10 min on ice. The cross-linking reaction was quenched by washing the beads 3 times with 1 ml Reaction buffer supplemented with 1 mM DTT and by resuspending them in 27 µl of Elution buffer containing 1 mM DTT. For TEV cleavage, 26 µl of the quenched cross-linked reaction was mixed with 1 µl TEV protease (1µg/µl) or elution buffer alone and incubated at 30°C for 1 h. Protein denaturation and elution from the beads was achieved by mixing samples with 3 µl of 10% SDS followed by heat denaturation at 65°C for 10 min. After addition of 6 µl of 6× DNA loading dye, denatured sample were run on a 0.8% (w/v) agarose gel containing 0.5 µg/ml ethidium bromide and minichromosomes were visualized by Southern blotting (see Materials and Methods 2.1.3).

2.3.6 Co-immunoprecipitation assays of condensin subunits from yeast extracts followed by cross-linking on the beads or in solution

1 l yeast cultures were grown at 30ºC up to OD_{600}=1 by diluting a stationary overnight culture in YPAD media. Cells were harvested by centrifugation at room temperature for 10 min (3,500 rpm) and the pellet washed twice with 400 ml ice-cold PBS buffer and once in 40 ml lysis buffer. Cells were resuspended in 7 ml of lysis buffer complemented with 2× protease inhibitor cocktail EDTA free, 1 mM PMSF and 1 mM DTT to a total volume of 12.5 ml. Drops of cell suspension were then flash frozen by plunging them into liquid nitrogen. Cells were disrupted at -196ºC in a Freezer/Mill (Spex) with the following settings: precooling = 5 min, cycles = 5, pulse = 3, cooling time = 4 min, rate = 12 cps. Cell lysate was collected from the grinding chamber, quickly thawed at 4ºC and insoluble cell debris was removed by centrifugation at 4ºC for 15 min at 21,000 rpm. Supernatants were spun again at 21,000 rpm and 4°C for 30 min to obtain cleared lysates. These cell total extracts were incubated in a 15 ml Falcon tube at 4ºC for 5 h on a rotating wheel with 10 µg of anti-V5 tag antibody or 10 µg of 12CA5 antibody, and overnight after adding 100 µL of Dynabeads protein G or protein A, respectively. The beads were then transferred to a 2 ml Eppendorf tubes and washed 5 times with 1 ml yeast lysis buffer containing 2 mM DTT and then split in two 1.5 ml tubes. DTT was removed by 3 additional washes (as above) followed by resuspension of each sample in 95 µl Reaction buffer. Release of condensin complexes from the beads was obtained by mixing samples with 5 µl of Prescission protease (1µg/µl) and incubation on the Vibrax (1,000 rpm) for 2 h at 4°C. For cross-linking on the beads, condensin complexes still bound to dynabeads were mixed with 5 µl DMSO or 5 µl 5 mM bBBr (dissolved in DMSO) for 10 min on ice. For cross-linking in solution, 95 µl of eluted sample after Prescission protease cleavage were incubated at 4°C with

DMSO or bBBr as before. In both case, the reaction was stopped by mixing the samples with 20 µl of 6× Laemmli buffer. Proteins denaturation and/or elution was obtained by incubation for 5 min at 95ºC. Denatured sample were then run on precast minigels in Tris-Acetate buffer and processed for Western Blot analysis

2.4 Yeast methods

2.4.1 Maintenance of yeast cultures

To maintain yeast strains fresh patches of yeast strains were resuspended in 15 % (v/v) glycerol. The glycerol stocks were frozen at -80ºC and used to inoculate agar plates.

2.4.2 Genomic DNA preparation

A fresh patch was resuspended in 200 µl SCE buffer supplemented with 1.6 µl β-mercatoethanol and 60 µg zymolyase and incubated for 1 h at 37ºC with shaking. Subsequently 200 µl SDS lysis buffer was added, the mixture was incubated at 65ºC for 5 min. Cell debris was pelleted after addition of 200 µl 5 M potassium acetate. The DNA was finally precipitated from the supernatant by addition of ethanol (350 µl supernatant + 800 µl Ethanol) and resuspended in 100 µl EB buffer. For PCR reaction 2 µl of genomic DNA was used as a template.

2.4.3 Transformation of yeast strains

For transformation of circular or linearized plasmids into yeast strains the 'Lithium Acetate/SS Carrier DNA/PEG transformation method' was applied (Gietz and Woods, 2006). Exponentially grown cells were harvested, washed with 1M LiAc and resuspended in 1 M LiAc to a 50% suspension to permeabilize the cell wall. After the LiAc treatment 30 µl cells were mixed with 5 µl DNA, 100 µg denatured salmon sperm DNA, and 112,5 µl 50% PEG 3350. This mixture was incubated for 30 min at room temperature without agitation. Then, 15 µl 60% (v/v) glycerol was added, the mixture was incubated for another 30 min and heat-shocked at 42ºC for 10 min. After the heat shock, cells transformed with plasmids carrying auxothropy markers were immediately plated on selective plates. Cells transformed with plasmids carrying resistance markers (e. g. KanMX) required a recovery period in YPAD medium to express the transformed resistant gene (5 h, 30ºC, shaking). To test transformation of circular minichromosomes genomic DNA was prepared from transformed strains, RNase A treated (30 min, 37ºC), loaded on an agarose gel and

visualized by Southern blotting. The success of integration of linearized vectors (e. g. in *LEU2* or *URA3*) was tested by several PCR reactions on genomic DNA using locus- as well as vector-specific primers (see Table 3).

2.4.4 Mating sporulation and tetrad dissection

Yeast strains with combinations of genes from different already available strains were generated via mating and sporulation. Two haploid yeast strains with opposite mating types were mated by mixing equal amounts of these strains on YPAD plates. After 3-5 hours zygotes were identified by light microscopy. Either those zygotes were isolated using a dissection microscope or diploid cells were selected on double-selective medium (markers from both haploid strains). If haploid yeast strains were intended, sporulation was induced by plating diploid strains on sporulation plates. After three days usually tetrads had been formed. To separate the four spores from a tetrad the cell wall of the ascus was digested by zymolyase treatment. For this a toothpick of sporulated yeast culture was incubated with 100 µg zymolyase in 1 M sorbitol for 20 min at 30ºC. 10 µl of the digested suspension was distributed along a line across the middle of a YPAD plate and tetrads were dissected by picking up one tetrad at a time and transferring the single spores to four different positions using a dissection microscope. Depending on the number of selection markers 8 - 60 tetrads were dissected per mating. After 2 days the spores were patched on a new YPAD plate, incubated for another day and replica plated onto different selective plates (drop out plates). The mating type was determined by replica plating to mating type tester strains (K216, K217) on minimal medium. Neither the tester strains (**his1**, *HIS3)* nor the commonly used lab strains (*HIS1,* **his3**) are able to grow on minimal plates due to mutations in different histidine biosynthesis genes. When strains of opposite mating type mate, the mutations are complemented and the resulting diploid is able to grow.

2.4.5 Spot test

Growth of yeast strains under various conditions (different temperatures, media) was tested by spot assays on agar plates. Exponentially cycling cells were diluted to a final OD of 0.5, ten fold dilution series were prepared (1:10, 1:100, 1:1000, 1:10000), and 8 µl of each dilution was spotted on agar plates (i.e. rapamycin plates).

2.5 Techniques in mammalian cell biology

2.5.1 Mammalian cell line storage and maintenance

Cell were cultured in DMEM (high glucose) supplemented with 10 % fetal bovine serum, 1 % glutamine and 1% Pen-Strep and diluted (1 to 3) three times per week. Frozen stock were made by resuspending 15×10^6 cell in 4 ml of complete medium supplemented with 10 % DMSO. 1 ml Aliquot were transferred immediately to -20°C for one hour, followed by -80°C overnight before permanent storage in liquid nitrogen.

2.5.2 Generation of HEK stably expressing ectopic modified SMC2 and CAP-H subunits

HEK Flp-In™ T-REx™ were seeded (6×10^6 cells) in two 100-mm dish. After 24 hrs cells were transfected with plasmids harboring the Flp-recombinase and SMC2*-SNAP-EGFP-2A-FLAG3-4cys-CAP-H* or no DNA (negative control) by Fugene HD accordingly to the manufacturer's instructions. 48 post-transfection fresh medium supplemented with the corresponding antibiotic (i.e. Blastidicin, Hygromycin B) was added for starting the selection process. Medium was replaced two time per week until single colonies were observed only in the dish transfected with plasmids and not in the negative control dish. Colonies were then trypsinized, pull together in a 60-mm dishes and expanded before making frozen stock.

2.5.3 Co-immunoprecipitation assays of condensin subunits from Flp-In-293 HEK cells extracts

Approximately 10×10^6 cells were harvested and lysed with 1 ml of HNTG buffer supplemented with 2x EDTA-free protease inhibitor cocktail, 1mM PMSF, 1mM DTT. Insoluble cell debris was removed by centrifugation at 4 ºC for 20 min (10000 rpm) and supernatant was incubated either with 10 ul GFP beads or 10 ul FLAG agarose beads overnight at 4°C. After 3 time washing with HNTG buffer, samples were eluted from the beads by adding 5 ul of SDS sample buffer 6X. Denatured sample were run on precast minigels in MOPS buffer and then processed for Western Blot analysis.

2.5.4 Chromatin fractionation protocol for Flp-In-293 HEK

1×10^6 cells per 60-mm dish were seeded for the chromatin fractionation experiment. After 2 days, seeded cells were either treated with 100 ng/ml nocodazole or DMSO alone for 16 hrs to induce pro-metephase arrest. Cells were then treated as described in Wysocka et al., 2001. After 2 wash with PBS, cell were resuspended in solution A supplemented with 1mM DTT and protease inhibitor (as above). Triton X-100 was added to a final concentration of 0.1%, and the cells were incubated for 5 min on ice.

Cytosolic proteins were separated from nuclei by centrifugation (4 min, 1,300 × *g*). Nuclei were washed once in solution A, and then lysed in solution B containing DTT and protease inhibitor for 30 min. Insoluble chromatin was then separated from soluble nuclear proteins by centrifugation (4 min, 1,700 × *g*), washed once in solution B, and collected by centrifugation (1 min, 10,000 × *g*). Equal amount of soluble nuclear fraction and the final chromatin pellet were resuspended in SDS sample buffer and boiled at 95 °C for 5 min. Denatured sample were run on precast minigels in MES buffer (to allow resolution of histones) and then processed for Western Blot analysis.

2.5.5 Production of siRNA coated plates and SMC2 and CAP-H knockdown

Cells were transfected with siRNAs by solid-phase transfection on siRNA-coated 24-well plates. Coated plates were prepared in advance using the following protocol, adapted from Erfle et al., 2008. In brief, transfection mix was prepared by combining 0.4 M sucrose/Opti-MEM Reduced Serum Medium GlutaMAX, Lipofectamine 2000 diluted 1:2 in ddH2O and 3 μ M siRNA at 1.7:1:2.8 ratio and incubated for 20 min at room temperature. A 0.2% gelatin solution was prepared ahead of time by dissolving 0.2 g of gelatin (from bovine skin, type B) in 100 ml ddH2O at 56°C. The gelatin was allowed to cool to room temperature and filtered through a 0.45 μ m filter membrane. The transfection reagents were then gently mixed with the gelatin at 1:0.6 ratio. Next, the reaction was gently diluted at 1:50 in ddH2O and distributed into wells of a 24-well plate using 4.2 pmols of siRNA per well. The plates were immediately dried in miVac vacuum concentrator at 37°C and stored in sealed boxes with drying pearls for further use. The plates were coated with the SMC2- (ID: s20795), CAP-H -specific (ID: s23734) siRNA and scrambled siRNA. 9 x 10^4 cell were trasferred onto a siRNA coated weli. 72 hrs later cell were lysed and efficiency of knockdown was checked by Western Blot analysis.

2.5.6 *In vivo* cross-linking by BG-CrAsH

BG-CrAsH was used in a final concentration between 1 and 5 µM in the presence of 12.5 µM 1,2-ethanedithiol (EDT). To remove cell medium, cell culture dish was washed twice in Imaging buffer. The cross-linking was performed for 2 hrs at 37°C by resuspending cell in Imaging Buffer supplemented by BG-CrAsH. Free and non-specifically bound BG-CrAsH was removed by washing with Imaging buffer supplemented with 200 µM BAL (2,3-dimercapto-1-propanol). Cell were then lysed and cleared extract were used for IP followed by Western blot analysis.

3 General bioinformatic methods

3.1 Bioinformatic sequence analysis

DNA and protein sequences of condensin subunits were derived from the Saccharomyces Genome Database (www.yeastgenome.org), the *Saccharomyces cerevisiae* strains Blast Server (SGRP, Sanger Institute, Hinxton, UK) and Uniprot. Analyses of DNA sequences, including multiple DNA sequence alignments, design of primers, cloning strategies, and restriction digests were generally performed with SnapGene software.

3.2 Generation of homolgy model for the Smc2-Smc4 and Brn1-Smc4 interfaces

A structure model of the yeast Smc2–Smc4 hinge structure was generated with the SWISS-MODEL (Biozentrum) using an alignment of S. cerevisiae Smc2 amino acid residues 555–708 and Smc4 amino acid residues 679–818 with residues 475–679 of the T. maritima SMC protein and the coordinates of PDB accession code 1GXL. The same procedure was followed for modeling Brn1 C-terminal (669–749aa)-Smc4hd (head domain; residues 154–348 and 1251-1418) with the crystal structure of yeast Scc1-Smc1hd (1W1W). Structures were then visualized by using PyMol.

Abbreviations

ABC	ATP-binding cassette
AFM	Atomic force microscopy
AP	Alkaline phosphatase
ATP	Adenosine triphosphate
BSA	Bovine serum albumin
BMOE	1,2-Bismaleimidoethane
CIP	Calf intestinal phosphatase
ChIP	Chromatin immunoprecipitation
DMSO	Dimethyl sulfoxide
dNTP	Deoxyribonucleoside triphosphate
DTT	Dithiothreitol
EM	Electron microscopy
FKBP	FK506 binding protein
FRB	FKBP binding domain
kb	Kilobase pair
NBD	Nucleotide binding domain
NEBD	Nuclear envelope break down
PCR	Polymerase chain reaction
rDNA	ribosomal DNA
SAC	Spindle assembly checkpoint
SDS	Sodium dodecyl sulfate
SMC	Structural maintenance of chromosomes
SD	Standard deviation
TEV	Tobacco etch virus
topo	topoisomerase
UV	Ultraviolet
WHD	Winged helix domain

Contributions

Anna Rutkowska (Cellzome GSK, DE) cloned the SMC2*-SNAP-EGFP-2A-FLAG$_3$-4cys-CAP-H* construct.

Alberto Riera (MRC, UK) built the structure model for Smc2-Smc4 and Brn1-Smc4 interfaces and generated strain 3197.

Acknowledgements

I am grateful to Christian for having given me the opportunity to join his lab and the EMBL community as well. I also want to thank him for reading and correcting the thesis.

I'm very grateful to the rest of the Haering group, especially Markus Ilaria and Christoph, for all the discussions we have together. My gratitude goes also to Jutta, one of the best lab technician I ever met.

Bibliography

Abe S, Nagasaka K, Hirayama Y, Kozuka-Hata H, Oyama M, Aoyagi Y, Obuse C, Hirota T. The initial phase of chromosome condensation requires Cdk1-mediated phosphorylation of the CAP-D3 subunit of condensin II. Genes Dev. 2011 Apr 15;25(8):863-74

Adachi Y, Luke M, Laemmli UK. Chromosome assembly in vitro: topoisomerase II is required for condensation. Cell. 1991 Jan 11;64(1):137-48.

Alipour E, Marko JF. Self-organization of domain structures by DNA-loop-extruding enzymes. Nucleic Acids Res. 2012 Dec;40(22):11202-12

Anderson DE, Losada A, Erickson HP, Hirano T. Condensin and cohesin display different arm conformations with characteristic hinge angles. J Cell Biol. 2002 Feb 4;156(3):419-24.

Aono N, Sutani T, Tomonaga T, Mochida S, Yanagida M. Cnd2 has dual roles in mitotic condensation and interphase. Nature. 2002 May 9;417(6885):197-202.

Arumugam P, Gruber S, Tanaka K, Haering CH, Mechtler K, Nasmyth K. ATP hydrolysis is required for cohesin's association with chromosomes. Curr Biol. 2003 Nov 11;13(22):1941-53

Badrinarayanan A, Lesterlin C, Reyes-Lamothe R, Sherratt D. The Escherichia coli SMC complex, MukBEF, shapes nucleoid organization independently of DNA replication. J Bacteriol. 2012 Sep;194(17):4669-76

Bauer CR, Hartl TA, Bosco G. Condensin II promotes the formation of chromosome territories by inducing axial compaction of polyploid interphase chromosomes. PLoS Genet. 2012;8(8)

Baxter J, Aragón L. A model for chromosome condensation based on the interplay between condensin and topoisomerase II. Trends Genet. 2012 Mar;28(3)

Bazett-Jones DP, Kimura K, Hirano T. Efficient supercoiling of DNA by a single condensin complex as revealed by electron spectroscopic imaging. Mol Cell. 2002 Jun;9(6)

Bazile F, St-Pierre J, D'Amours D. Three-step model for condensin activation during mitotic chromosome condensation. Cell Cycle. 2010 Aug 15;9(16)

Beckouët F, Hu B, Roig MB, Sutani T, Komata M, Uluocak P, Katis VL, Shirahige K, Nasmyth K. An Smc3 acetylation cycle is essential for establishment of sister chromatid cohesion. Mol Cell. 2010 Sep 10;39(5):689-99.

Belshaw PJ, Ho SN, Crabtree GR, Schreiber SL. Controlling protein association and subcellular localization with a synthetic ligand that induces heterodimerization of proteins. Proc Natl Acad Sci U S A. 1996 May 14;93(10):4604-7.

Belmont AS. Mitotic chromosome structure and condensation. Curr Opin Cell Biol. 2006 Dec;18(6):632-8.

Berger JM, Gamblin SJ, Harrison SC, Wang JC. Structure and mechanism of DNA topoisomerase II. Nature. 1996 Jan 18;379(6562):225-32. Erratum in: Nature 1996 Mar 14;380(6570):179.

Bhalla N, Biggins S, Murray AW. Mutation of YCS4, a budding yeast condensin subunit, affects mitotic and nonmitotic chromosome behavior. Mol Biol Cell. 2002 Feb;13(2):632-45.

Bhat MA, Philp AV, Glover DM, Bellen HJ. Chromatid segregation at anaphase requires the barren product, a novel chromosome-associated protein that interacts with Topoisomerase II. Cell. 1996 Dec 13;87(6):1103-14.

Bilodeau S, Côté J. A chromatin switch for chromosome condensation. Dev Cell. 2012 Dec 11;23(6):1127-8

Birkenbihl RP, Subramani S. The rad21 gene product of Schizosaccharomyces pombe is a nuclear, cell cycle-regulated phosphoprotein. J Biol Chem. 1995 Mar 31;270(13)

Borges, V., Lehane, C., Lopez-Serra, L., Flynn, H., Skehel, M., Rolef Ben-Shahar, T., and Uhlmann, F. Hos1 deacetylates Smc3 to close the cohesin acetylation cycle. Mol Cell 2010. 39, 677-688.

Buheitel J, Stemmann O. Prophase pathway-dependent removal of cohesin from human chromosomes requires opening of the Smc3-Scc1 gate. EMBO J. 2013 Mar 6;32(5):666-76.

Bürmann F, Shin HC, Basquin J, Soh YM, Giménez-Oya V, Kim YG, Oh BH, Gruber S. An asymmetric SMC-kleisin bridge in prokaryotic condensin. Nat Struct Mol Biol. 2013 Mar;20(3):371-9.

Burrack LS, Applen Clancey SE, Chacón JM, Gardner MK, Berman J. Monopolin recruits condensin to organize centromere DNA and repetitive DNA sequences. Mol Biol Cell. 2013 Sep;24(18):2807-19.

Chan KL, Roig MB, Hu B, Beckouët F, Metson J, Nasmyth K. Cohesin's DNA exit gate is distinct from its entrance gate and is regulated by acetylation. Cell. 2012 Aug 31;150(5):961-74.

Chatterjee A, Zakian S, Hu XW, Singleton MR. Structural insights into the regulation of cohesion establishment by Wpl1. EMBO J. 2013 Mar 6;32(5):677-87.

Chen J, Zheng XF, Brown EJ, Schreiber SL. Identification of an 11-kDa FKBP12-rapamycin-binding domain within the 289-kDa FKBP12-rapamycin-associated protein and characterization of a critical serine residue. Proc Natl Acad Sci U S A. 1995 May 23;92(11):4947-51.

Christensen MO, Larsen MK, Barthelmes HU, Hock R, Andersen CL, Kjeldsen E, Knudsen BR, Westergaard O, Boege F, Mielke C. Dynamics of human DNA topoisomerases IIalpha and IIbeta in living cells. J Cell Biol. 2002 Apr 1;157(1):31-44.

Ciosk R, Shirayama M, Shevchenko A, Tanaka T, Toth A, Shevchenko A, Nasmyth K. Cohesin's binding to chromosomes depends on a separate complex consisting of Scc2 and Scc4 proteins. Mol Cell. 2000 Feb;5(2):243-54.

Cipak L, Spirek M, Gregan J. Sister chromatids caught in the cohesin trap. Nat Struct Mol Biol. 2008 Sep;15(9):899-900.

Cui Y, Cheng X, Zhang C, Zhang Y, Li S, Wang C, Guadagno TM. Degradation of the human mitotic checkpoint kinase Mps1 is cell cycle-regulated by APC-cCdc20 and APC-cCdh1 ubiquitin ligases. J Biol Chem. 2010 Oct 22;285(43):32988-98.

Cuvier O, Hirano T. A role of topoisomerase II in linking DNA replication to chromosome condensation. J Cell Biol. 2003 Mar 3;160(5):645-55.

Cuylen S, Metz J, Haering CH. Condensin structures chromosomal DNA through topological links. Nat Struct Mol Biol. 2011 Jul 17;18(8):894-901.

Cuylen S, Metz J, Hruby A, Haering CH. Entrapment of chromosomes by condensin rings prevents their breakage during cytokinesis. Dev Cell. 2013 Nov 25;27(4):469-78.

D'Ambrosio C, Schmidt CK, Katou Y, Kelly G, Itoh T, Shirahige K, Uhlmann F. Identification of cis-acting sites for condensin loading onto budding yeast chromosomes. Genes Dev. 2008 Aug 15;22(16):2215-27.

Davey CA, Sargent DF, Luger K, Maeder AW, Richmond TJ. Solvent mediated interactions in the structure of the nucleosome core particle at 1.9 a resolution. J Mol Biol. 2002 Jun 21;319(5):1097-113.

Dowen JM, Bilodeau S, Orlando DA, Hübner MR, Abraham BJ, Spector DL, Young RA. Multiple structural maintenance of chromosome complexes at transcriptional regulatory elements. Stem Cell Reports. 2013 Oct 24;1(5):371-8.

Dubey RN, Gartenberg MR. A tDNA establishes cohesion of a neighboring silent chromatin domain. Genes Dev. 2007 Sep 1;21(17):2150-60.

Eichinger CS, Kurze A, Oliveira RA, Nasmyth K. Disengaging the Smc3/kleisin interface releases cohesin from Drosophila chromosomes during interphase and mitosis. EMBO J. 2013 Mar 6;32(5):656-65.

Erfle H, Neumann B, Rogers P, Bulkescher J, Ellenberg J, Pepperkok R. Work flow for multiplexing siRNA assays by solid-phase reverse transfection in multiwell plates. J Biomol Screen. 2008 Aug;13(7):575-80.

Earnshaw WC, Halligan B, Cooke CA, Heck MM, Liu LF. Topoisomerase II is a structural component of mitotic chromosome scaffolds. J Cell Biol. 1985 May;100(5):1706-15.

Farcas AM, Uluocak P, Helmhart W, Nasmyth K. Cohesin's concatenation of sister DNAs maintains their intertwining. Mol Cell. 2011 Oct 7;44(1):97-107.

Freeman L, Aragon-Alcaide L, Strunnikov A. The condensin complex governs chromosome condensation and mitotic transmission of rDNA. J Cell Biol. 2000 May 15;149(4):811-24.

Gandhi R, Gillespie PJ, Hirano T. Human Wapl is a cohesin-binding protein that promotes sister-chromatid resolution in mitotic prophase. Curr Biol. 2006 Dec 19;16(24):2406-17.

Gerlich D, Hirota T, Koch B, Peters JM, Ellenberg J. Condensin I stabilizes chromosomes mechanically through a dynamic interaction in live cells. Curr Biol. 2006 Feb 21;16(4):333-44.

Gillespie PJ, Hirano T. Scc2 couples replication licensing to sister chromatid cohesion in Xenopus egg extracts. Curr Biol. 2004 Sep 7;14(17):1598-603.

Green LC, Kalitsis P, Chang TM, Cipetic M, Kim JH, Marshall O, Turnbull L, Whitchurch CB, Vagnarelli P, Samejima K, Earnshaw WC, Choo KH, Hudson DF. Contrasting roles of condensin I and condensin II in mitotic chromosome formation. J Cell Sci. 2012 Mar 15;125(Pt 6):1591-604.

Griese JJ, Witte G, Hopfner KP. Structure and DNA binding activity of the mouse condensin hinge domain highlight common and diverse features of SMC proteins. Nucleic Acids Res. 2010 Jun;38(10):3454-65.

Gruber S, Haering CH, Nasmyth K. Chromosomal cohesin forms a ring. Cell. 2003 Mar 21;112(6):765-77.

Gruber S, Arumugam P, Katou Y, Kuglitsch D, Helmhart W, Shirahige K, Nasmyth K. Evidence that loading of cohesin onto chromosomes involves opening of its SMC hinge. Cell. 2006 Nov 3;127(3):523-37.

Guacci V, Koshland D, Strunnikov A. A direct link between sister chromatid cohesion and chromosome condensation revealed through the analysis of MCD1 in S. cerevisiae. Cell. 1997 Oct 3;91(1):47-57.

Haering CH, Löwe J, Hochwagen A, Nasmyth K. Molecular architecture of SMC proteins and the yeast cohesin complex. Mol Cell. 2002 Apr;9(4):773-88.

Haering CH, Schoffnegger D, Nishino T, Helmhart W, Nasmyth K, Löwe J. Structure and stability of cohesin's Smc1-kleisin interaction. Mol Cell. 2004 Sep 24;15(6):951-64.

Haering CH, Farcas AM, Arumugam P, Metson J, Nasmyth K. The cohesin ring concatenates sister DNA molecules. Nature. 2008 Jul 17;454(7202):297-301.

Hagstrom KA, Holmes VF, Cozzarelli NR, Meyer BJ. C. elegans condensin promotes mitotic chromosome architecture, centromere organization, and sister chromatid segregation during mitosis and meiosis. Genes Dev. 2002 Mar 15;16(6):729-42

Hansen JC, Ausio J, Stanik VH, van Holde KE. Homogeneous reconstituted oligonucleosomes, evidence for salt-dependent folding in the absence of histone H1. Biochemistry. 1989 Nov 14;28(23):9129-36.

Haruki H, Nishikawa J, Laemmli UK. The anchor-away technique: rapid, conditional establishment of yeast mutant phenotypes. Mol Cell. 2008 Sep 26;31(6):925-32.

Hauf S, Roitinger E, Koch B, Dittrich CM, Mechtler K, Peters JM. Dissociation of cohesin from chromosome arms and loss of arm cohesion during early mitosis depends on phosphorylation of SA2. PLoS Biol. 2005 Mar;3(3):e69.

Hiraga S, Niki H, Imamura R, Ogura T, Yamanaka K, Feng J, Ezaki B, Jaffé A. Mutants defective in chromosome partitioning in E. coli. Res Microbiol. 1991 Feb-Apr;142(2-3):189-94.

Hirano T, Mitchison TJ. A heterodimeric coiled-coil protein required for mitotic chromosome condensation in vitro. Cell. 1994 Nov 4;79(3):449-58.

Hirano T, Kobayashi R, Hirano M. Condensins, chromosome condensation protein complexes containing XCAP-C, XCAP-E and a Xenopus homolog of the Drosophila Barren protein. Cell. 1997 May 16;89(4):511-21.

Hirano T. At the heart of the chromosome: SMC proteins in action. Nat Rev Mol Cell Biol. 2006 May;7(5):311-22. Review.

Hirano T. SMC proteins and chromosome mechanics: from bacteria to humans. Philos Trans R Soc Lond B Biol Sci. 2005a. Mar 29;360(1455):507-14. Review.

Hirano T. Condensins: organizing and segregating the genome. Curr Biol. 2005b. Apr 12;15(7):R265-75. Review.

Hirano T. Chromosome cohesion, condensation, and separation. Annu Rev Biochem. 2000;69:115-44. Review.

Hirota T, Gerlich D, Koch B, Ellenberg J, Peters JM. Distinct functions of condensin I and II in mitotic chromosome assembly. J Cell Sci. 2004 Dec 15;117(Pt 26):6435-45.

Houchmandzadeh B, Dimitrov S. Elasticity measurements show the existence of thin rigid cores inside mitotic chromosomes. J Cell Biol. 1999 Apr 19;145(2):215-23.

Hu B, Itoh T, Mishra A, Katoh Y, Chan KL, Upcher W, Godlee C, Roig MB, Shirahige K, Nasmyth K. ATP hydrolysis is required for relocating cohesin from sites occupied by its Scc2/4 loading complex. Curr Biol. 2011 Jan 11;21(1):12-24.

Hudson DF, Ohta S, Freisinger T, Macisaac F, Sennels L, Alves F, Lai F, Kerr A, Rappsilber J, Earnshaw WC. Molecular and genetic analysis of condensin function in vertebrate cells. Mol Biol Cell. 2008 Jul;19(7):3070-9.

Hudson DF, Marshall KM, Earnshaw WC. Condensin: Architect of mitotic chromosomes. Chromosome Res. 2009;17(2):131-44.

Ivanov D, Schleiffer A, Eisenhaber F, Mechtler K, Haering CH, Nasmyth K. Eco1 is a novel acetyltransferase that can acetylate proteins involved in cohesion. Curr Biol. 2002 Feb 19;12(4):323-8.

Ivanov D, Nasmyth K. A topological interaction between cohesin rings and a circular minichromosome. Cell. 2005 Sep 23;122(6):849-60.

Ivanov D, Nasmyth K. A physical assay for sister chromatid cohesion in vitro. Mol Cell. 2007 Jul 20;27(2):300-10.

Iwasaki O, Tanaka A, Tanizawa H, Grewal SI, Noma K. Centromeric localization of dispersed Pol III genes in fission yeast. Mol Biol Cell. 2010 Jan 15;21(2):254-65.

Jansen LE, Black BE, Foltz DR, Cleveland DW. Propagation of centromeric chromatin requires exit from mitosis. J Cell Biol. 2007 Mar 12;176(6):795-805.

Johzuka K, Horiuchi T. The cis element and factors required for condensin recruitment to chromosomes. Mol Cell. 2009 Apr 10;34(1):26-35.

Kagami Y, Nihira K, Wada S, Ono M, Honda M, Yoshida K. Mps1 phosphorylation of condensin II controls chromosome condensation at the onset of mitosis. J Cell Biol. 2014 Jun 23;205(6):781-90.

Keppler A, Pick H, Arrivoli C, Vogel H, Johnsson K. Labeling of fusion proteins with synthetic fluorophores in live cells. Proc Natl Acad Sci U S A. 2004 Jul 6;101(27):9955-9.

Kim JH, Zhang T, Wong NC, Davidson N, Maksimovic J, Oshlack A, Earnshaw WC, Kalitsis P, Hudson DF. Condensin I associates with structural and gene regulatory regions in vertebrate chromosomes. Nat Commun. 2013;4:2537.

Kim ST, Xu B, Kastan MB. Involvement of the cohesin protein, Smc1, in Atm-dependent and independent responses to DNA damage. Genes Dev. 2002 Mar 1;16(5):560-70.

Kimura K, Hirano T. ATP-dependent positive supercoiling of DNA by 13S condensin: a biochemical implication for chromosome condensation. Cell. 1997 Aug 22;90(4):625-34.

Kimura K, Hirano T. Dual roles of the 11S regulatory subcomplex in condensin functions. Proc Natl Acad Sci U S A. 2000 Oct 24;97(22):11972-7.

Kimura K, Rybenkov VV, Crisona NJ, Hirano T, Cozzarelli NR. 13S condensin actively reconfigures DNA by introducing global positive writhe: implications for chromosome condensation. Cell. 1999 Jul 23;98(2):239-48.

Kitajima TS, Sakuno T, Ishiguro K, Iemura S, Natsume T, Kawashima SA, Watanabe Y. Shugoshin collaborates with protein phosphatase 2A to protect cohesin. Nature. 2006 May 4;441(7089):46-52.

Knop M, Siegers K, Pereira G, Zachariae W, Winsor B, Nasmyth K, Schiebel E. Epitope tagging of yeast genes using a PCR-based strategy: more tags and improved practical routines. Yeast. 1999 Jul;15(10B):963-72.

Kong X, Stephens J, Ball AR Jr, Heale JT, Newkirk DA, Berns MW, Yokomori K. Condensin I recruitment to base damage-enriched DNA lesions is modulated by PARP1. PLoS One. 2011;6(8):e23548.

Kornberg RD. Chromatin structure: a repeating unit of histones and DNA. Science. 1974 May 24;184(4139):868-71.

Kueng S, Hegemann B, Peters BH, Lipp JJ, Schleiffer A, Mechtler K, Peters JM. Wapl controls the dynamic association of cohesin with chromatin. Cell. 2006 Dec 1;127(5):955-67.

Lam WW, Peterson EA, Yeung M, Lavoie BD. Condensin is required for chromosome arm cohesion during mitosis. Genes Dev. 2006 Nov 1;20(21):2973-84.

Lammens A, Schele A, Hopfner KP. Structural biochemistry of ATP-driven dimerization and DNA-stimulated activation of SMC ATPases. Curr Biol. 2004 Oct 5;14(19):1778-82.

Lammens K, Bemeleit DJ, Möckel C, Clausing E, Schele A, Hartung S, Schiller CB, Lucas M, Angermüller C, Söding J, Strässer K, Hopfner KP. The Mre11:Rad50 structure shows an ATP-dependent molecular clamp in DNA double-strand break repair. Cell. 2011 Apr 1;145(1):54-66.

Laugsch M, Seebach J, Schnittler H, Jessberger R. Imbalance of SMC1 and SMC3 cohesins causes specific and distinct effects. PLoS One. 2013 Jun 12;8(6).

Lavoie BD, Hogan E, Koshland D. In vivo requirements for rDNA chromosome condensation reveal two cell-cycle-regulated pathways for mitotic chromosome folding. Genes Dev. 2004 Jan 1;18(1):76-87.

Leitner A, Walzthoeni T, Kahraman A, Herzog F, Rinner O, Beck M, Aebersold R. Probing native protein structures by chemical cross-linking, mass spectrometry, and bioinformatics. Mol Cell Proteomics. 2010 Aug;9(8):1634-49.

Leitner A, Joachimiak LA, Bracher A, Mönkemeyer L, Walzthoeni T, Chen B, Pechmann S, Holmes S, Cong Y, Ma B, Ludtke S, Chiu W, Hartl FU, Aebersold R, Frydman J. The molecular architecture of the eukaryotic chaperonin TRiC/CCT. Structure. 2012 May 9;20(5):814-25.

Lindroos HB, Ström L, Itoh T, Katou Y, Shirahige K, Sjögren C. Chromosomal association of the Smc5/6 complex reveals that it functions in differently regulated pathways. Mol Cell. 2006 Jun 23;22(6):755-67.

Liu X, Winey M. The MPS1 family of protein kinases. Annu Rev Biochem. 2012;81:561-85.

Longtine MS, McKenzie A 3rd, Demarini DJ, Shah NG, Wach A, Brachat A, Philippsen P, Pringle JR. Additional modules for versatile and economical PCR-based gene deletion and modification in Saccharomyces cerevisiae. Yeast. 1998 Jul;14(10):953-61.

Losada A, Hirano M, Hirano T. Cohesin release is required for sister chromatid resolution, but not for condensin-mediated compaction, at the onset of mitosis. Genes Dev. 2002 Dec 1;16(23):3004-16.

Losada A, Yokochi T, Hirano T. Functional contribution of Pds5 to cohesin-mediated cohesion in human cells and Xenopus egg extracts. J Cell Sci. 2005 May 15;118(Pt 10):2133-41.

Luger K, Mäder AW, Richmond RK, Sargent DF, Richmond TJ. Crystal structure of the nucleosome core particle at 2.8 A resolution. Nature. 1997 Sep 18;389(6648):251-60.

Machín F, Paschos K, Jarmuz A, Torres-Rosell J, Pade C, Aragón L. Condensin regulates rDNA silencing by modulating nucleolar Sir2p. Curr Biol. 2004 Jan 20;14(2):125-30.

Maeshima K, Eltsov M. Packaging the genome: the structure of mitotic chromosomes. J Biochem. 2008 Feb;143(2):145-53.

Maeshima K, Laemmli UK. A two-step scaffolding model for mitotic chromosome assembly. Dev Cell. 2003 Apr;4(4):467-80.

Maeshima K, Hihara S, Eltsov M. Chromatin structure: does the 30-nm fibre exist in vivo? Curr Opin Cell Biol. 2010 Jun;22(3):291-7.

Mannini L, Menga S, Musio A. The expanding universe of cohesin functions: a new genome stability caretaker involved in human disease and cancer. Hum Mutat. 2010 Jun;31(6):623-30. Review.

Mascarenhas J, Volkov AV, Rinn C, Schiener J, Guckenberger R, Graumann PL. Dynamic assembly, localization and proteolysis of the Bacillus subtilis SMC complex. BMC Cell Biol. 2005 Jun 29;6:28.

Matoba K, Yamazoe M, Mayanagi K, Morikawa K, Hiraga S. Comparison of MukB homodimer versus MukBEF complex molecular architectures by electron microscopy reveals a higher-order multimerization. Biochem Biophys Res Commun. 2005 Aug 5;333(3):694-702.

Michaelis C, Ciosk R, Nasmyth K. Cohesins: chromosomal proteins that prevent premature separation of sister chromatids. Cell. 1997 Oct 3;91(1):35-45.

Möckel C, Lammens K, Schele A, Hopfner KP. ATP driven structural changes of the bacterial Mre11:Rad50 catalytic head complex. Nucleic Acids Res. 2012 Jan;40(2):914-27.

Moehle EA, Rock JM, Lee YL, Jouvenot Y, DeKelver RC, Gregory PD, Urnov FD, Holmes MC. Targeted gene addition into a specified location in the human genome using designed zinc finger nucleases. Proc Natl Acad Sci U S A. 2007 Feb 27;104(9):3055-60.

Moir RD, Yoon M, Khuon S, Goldman RD. Nuclear lamins A and B1: different pathways of assembly during nuclear envelope formation in living cells. J Cell Biol. 2000 Dec 11;151(6):1155-68.

Morgan, T. H. 1915. Localization of the Hereditary Material in the Germ Cells. Proc Natl Acad Sci U S A, 1, 420-9.

Moriya S, Tsujikawa E, Hassan AK, Asai K, Kodama T, Ogasawara N. A Bacillus subtilis gene-encoding protein homologous to eukaryotic SMC motor protein is necessary for chromosome partition. Mol Microbiol. 1998 Jul;29(1):179-87.

Murayama Y, Uhlmann F. Biochemical reconstitution of topological DNA binding by the cohesin ring. Nature. 2014 Jan 16;505(7483):367-71.

Nakazawa N, Mehrotra R, Ebe M, Yanagida M. Condensin phosphorylated by the Aurora-B-like kinase Ark1 is continuously required until telophase in a mode distinct from Top2. J Cell Sci. 2011 Jun 1;124(Pt 11):1795-807.

Nasmyth K, Haering CH. The structure and function of SMC and kleisin complexes. Annu Rev Biochem. 2005;74:595-648. Review.

Nicklas RB. Measurements of the force produced by the mitotic spindle in anaphase. J Cell Biol. 1983 Aug;97(2):542-8.

Niki H, Jaffé A, Imamura R, Ogura T, Hiraga S. The new gene mukB codes for a 177 kd protein with coiled-coil domains involved in chromosome partitioning of E. coli. EMBO J. 1991 Jan;10(1):183-93.

Nishiyama T, Ladurner R, Schmitz J, Kreidl E, Schleiffer A, Bhaskara V, Bando M, Shirahige K, Hyman AA, Mechtler K, Peters JM. Sororin mediates sister chromatid cohesion by antagonizing Wapl. Cell. 2010 Nov 24;143(5):737-49.

Nolivos S, Sherratt D. The bacterial chromosome: architecture and action of bacterial SMC and SMC-like complexes. FEMS Microbiol Rev. 2014 May;38(3):380-92.

Oliveira RA, Coelho PA, Sunkel CE. The condensin I subunit Barren/CAP-H is essential for the structural integrity of centromeric heterochromatin during mitosis. Mol Cell Biol. 2005 Oct;25(20):8971-84.

Onn I, Aono N, Hirano M, Hirano T. Reconstitution and subunit geometry of human condensin complexes. EMBO J. 2007 Feb 21;26(4):1024-34.

Ono T, Losada A, Hirano M, Myers MP, Neuwald AF, Hirano T. Differential contributions of condensin I and condensin II to mitotic chromosome architecture in vertebrate cells. Cell. 2003 Oct 3;115(1):109-21.

Ono T, Fang Y, Spector DL, Hirano T. Spatial and temporal regulation of Condensins I and II in mitotic chromosome assembly in human cells. Mol Biol Cell. 2004 Jul;15(7):3296-308.

Onn I, Aono N, Hirano M, Hirano T. Reconstitution and subunit geometry of human condensin complexes. EMBO J. 2007 Feb 21;26(4):1024-34.

Oudet P, Gross-Bellard M, Chambon P. Electron microscopic and biochemical evidence that chromatin structure is a repeating unit. Cell. 1975 Apr;4(4):281-300.

Panizza S, Tanaka T, Hochwagen A, Eisenhaber F, Nasmyth K. Pds5 cooperates with cohesin in maintaining sister chromatid cohesion. Curr Biol. 2000 Dec 14-28;10(24):1557-64.

Paulson JR, Laemmli UK. The structure of histone-depleted metaphase chromosomes. Cell. 1977 Nov;12(3):817-28.

Peters JM, Nishiyama T. Sister chromatid cohesion. Cold Spring Harb Perspect Biol. 2012 Nov 1;4(11).

Phair RD, Misteli T. High mobility of proteins in the mammalian cell nucleus. Nature. 2000 Apr 6;404(6778):604-9.

Phipps J, Nasim A, Miller DR. Recovery, repair, and mutagenesis in Schizosaccharomyces pombe. Adv Genet. 1985;23:1-72. Review.

Piazza I, Haering CH, Rutkowska A. Condensin: crafting the chromosome landscape. Chromosoma. 2013 Jun;122(3):175-90.

Piazza I, Rutkowska A, Ori A, Walczak M, Metz J, Pelechano V, Beck M, Haering CH. Association of condensin with chromosomes depends on DNA binding by its HEAT-repeat subunits. Nat Struct Mol Biol. 2014 Jun;21(6):560-8.

Poirier M, Eroglu S, Chatenay D, Marko JF. Reversible and irreversible unfolding of mitotic newt chromosomes by applied force. Mol Biol Cell. 2000 Jan;11(1):269-76.

Poirier MG, Marko JF. Micromechanical studies of mitotic chromosomes. Curr Top Dev Biol. 2003;55:75-141. Review.

Poirier MG, Marko JF. Mitotic chromosomes are chromatin networks without a mechanically contiguous protein scaffold. Proc Natl Acad Sci U S A. 2002 Nov 26;99(24):15393-7.

Pope LH, Xiong C, Marko JF. Proteolysis of mitotic chromosomes induces gradual and anisotropic decondensation correlated with a reduction of elastic modulus and structural sensitivity to rarely cutting restriction enzymes. Mol Biol Cell. 2006 Jan;17(1):104-13.

Rawlings JS, Gatzka M, Thomas PG, Ihle JN. Chromatin condensation via the condensin II complex is required for peripheral T-cell quiescence. EMBO J. 2011 Jan 19;30(2):263-76.

Richmond TJ, Finch JT, Rushton B, Rhodes D, Klug A. Structure of the nucleosome core particle at 7 A resolution. Nature. 1984 Oct 11-17;311(5986):532-7.

Riedel CG, Katis VL, Katou Y, Mori S, Itoh T, Helmhart W, Gálová M, Petronczki M, Gregan J, Cetin B, Mudrak I, Ogris E, Mechtler K, Pelletier L, Buchholz F, Shirahige K, Nasmyth K. Protein phosphatase 2A protects centromeric sister chromatid cohesion during meiosis I. Nature. 2006 May 4;441(7089):53-61.

Ris H, Kubai DF. Chromosome structure. Annu Rev Genet. 1970;4:263-94. Review.

Rivera T, Losada A. Recycling cohesin rings by deacetylation. Mol Cell. 2010 Sep 10;39(5):657-9..

Rowland BD, Roig MB, Nishino T, Kurze A, Uluocak P, Mishra A, Beckouët F, Underwood P, Metson J, Imre R, Mechtler K, Katis VL, Nasmyth K. Building sister chromatid cohesion: smc3 acetylation counteracts an antiestablishment activity. Mol Cell. 2009 Mar 27;33(6):763-74.

Rutkowska A, Haering CH, Schultz C. A FlAsH-based cross-linker to study protein interactions in living cells. Angew Chem Int Ed Engl. 2011 Dec 23;50(52):12655-8.

Saka Y, Sutani T, Yamashita Y, Saitoh S, Takeuchi M, Nakaseko Y, Yanagida M. Fission yeast cut3 and cut14, members of a ubiquitous protein family, are required for chromosome condensation and segregation in mitosis. EMBO J. 1994 Oct 17;13(20):4938-52.

Sakai A, Hizume K, Sutani T, Takeyasu K, Yanagida M. Condensin but not cohesin SMC heterodimer induces DNA reannealing through protein-protein assembly. EMBO J. 2003 Jun 2;22(11):2764-75.

Savvidou E, Cobbe N, Steffensen S, Cotterill S, Heck MM. Drosophila CAP-D2 is required for condensin complex stability and resolution of sister chromatids. J Cell Sci. 2005 Jun 1;118(Pt 11):2529-43.

Schmitz J, Watrin E, Lénárt P, Mechtler K, Peters JM. Sororin is required for stable binding of cohesin to chromatin and for sister chromatid cohesion in interphase. Curr Biol. 2007 Apr 3;17(7):630-6.

Schuster AT, Sarvepalli K, Murphy EA, Longworth MS. Condensin II subunit dCAP-D3 restricts retrotransposon mobilization in Drosophila somatic cells. PLoS Genet. 2013 Oct;9(10):e1003879.

Seitan VC, Banks P, Laval S, Majid NA, Dorsett D, Rana A, Smith J, Bateman A, Krpic S, Hostert A, Rollins RA, Erdjument-Bromage H, Tempst P, Benard CY, Hekimi S, Newbury SF, Strachan T. Metazoan Scc4 homologs link sister chromatid cohesion to cell and axon migration guidance.

Shintomi K, Hirano T. The relative ratio of condensin I to II determines chromosome shapes. Genes Dev. 2011 Jul 15;25(14):1464-9.

Smith HF, Roberts MA, Nguyen HQ, Peterson M, Hartl TA, Wang XJ, Klebba JE, Rogers GC, Bosco G. Maintenance of interphase chromosome compaction and homolog pairing in

Drosophila is regulated by the condensin cap-h2 and its partner Mrg15. Genetics. 2013 Sep;195(1):127-46.

Soppa J, Kobayashi K, Noirot-Gros MF, Oesterhelt D, Ehrlich SD, Dervyn E, Ogasawara N, Moriya S. Discovery of two novel families of proteins that are proposed to interact with prokaryotic SMC proteins, and characterization of the Bacillus subtilis family members ScpA and ScpB. Mol Microbiol. 2002 Jul;45(1):59-71.

St-Pierre J, Douziech M, Bazile F, Pascariu M, Bonneil E, Sauvé V, Ratsima H, D'Amours D. Polo kinase regulates mitotic chromosome condensation by hyperactivation of condensin DNA supercoiling activity. Mol Cell. 2009 May 14;34(4):416-26.

Steffensen S, Coelho PA, Cobbe N, Vass S, Costa M, Hassan B, Prokopenko SN, Bellen H, Heck MM, Sunkel CE. A role for Drosophila SMC4 in the resolution of sister chromatids in mitosis. Curr Biol. 2001 Mar 6;11(5):295-307.

Stray JE, Lindsley JE. Biochemical analysis of the yeast condensin Smc2/4 complex: an ATPase that promotes knotting of circular DNA. J Biol Chem. 2003 Jul 11;278(28):26238-48.

Strick TR, Kawaguchi T, Hirano T. Real-time detection of single-molecule DNA compaction by condensin I. Curr Biol. 2004 May 25;14(10):874-80.

Ström L, Lindroos HB, Shirahige K, Sjögren C. Postreplicative recruitment of cohesin to double-strand breaks is required for DNA repair. Mol Cell. 2004. Dec 22;16(6):1003-15.

Strukov YG, Belmont AS. Mitotic chromosome structure: reproducibility of folding and symmetry between sister chromatids. Biophys J. 2009 Feb 18;96(4):1617-28.

Strunnikov AV, Hogan E, Koshland D. SMC2, a Saccharomyces cerevisiae gene essential for chromosome segregation and condensation, defines a subgroup within the SMC family. Genes Dev. 1995 Mar 1;9(5):587-99.

Stubblefield E, Wray W. Architecture of the Chinese hamster metaphase chromosome. Chromosoma. 1971;32(3):262-94.

Sundin O, Varshavsky A. Arrest of segregation leads to accumulation of highly intertwined catenated dimers: dissection of the final stages of SV40 DNA replication. Cell. 1981 Sep;25(3):659-69.

Sutani T, Yuasa T, Tomonaga T, Dohmae N, Takio K, Yanagida M. Fission yeast condensin complex: essential roles of non-SMC subunits for condensation and Cdc2 phosphorylation of Cut3/SMC4. Genes Dev. 1999 Sep 1;13(17):2271-83.

Sutani T, Kawaguchi T, Kanno R, Itoh T, Shirahige K. Budding yeast Wpl1(Rad61)-Pds5 complex counteracts sister chromatid cohesion-establishing reaction. Curr Biol. 2009 Mar 24;19(6):492-7.

Szymczak-Workman AL, Vignali KM, Vignali DA. Design and construction of 2A peptide-linked multicistronic vectors. Cold Spring Harb Protoc. 2012 Feb 1;2012(2):199-204.

Tachibana-Konwalski K, Godwin J, van der Weyden L, Champion L, Kudo NR, Adams DJ, Nasmyth K. Rec8-containing cohesin maintains bivalents without turnover during the growing phase of mouse oocytes. Genes Dev. 2010 Nov 15;24(22):2505-16.

Tada K, Susumu H, Sakuno T, Watanabe Y. Condensin association with histone H2A shapes mitotic chromosomes. Nature. 2011 Jun 1;474(7352):477-83.

Takemoto A, Kimura K, Yokoyama S, Hanaoka F. Cell cycle-dependent phosphorylation, nuclear localization, and activation of human condensin. J Biol Chem. 2004 Feb 6;279(6):4551-9.

Takemoto A, Kimura K, Yanagisawa J, Yokoyama S, Hanaoka F. Negative regulation of condensin I by CK2-mediated phosphorylation. EMBO J. 2006 Nov 15;25(22):5339-48.

Takemoto A, Maeshima K, Ikehara T, Yamaguchi K, Murayama A, Imamura S, Imamoto N, Yokoyama S, Hirano T, Watanabe Y, Hanaoka F, Yanagisawa J, Kimura K. The chromosomal association of condensin II is regulated by a noncatalytic function of PP2A. Nat Struct Mol Biol. 2009 Dec;16(12):1302-8.

Tanaka A, Tanizawa H, Sriswasdi S, Iwasaki O, Chatterjee AG, Speicher DW, Levin HL, Noguchi E, Noma K. Epigenetic regulation of condensin-mediated genome organization during the cell cycle and upon DNA damage through histone H3 lysine 56 acetylation. Mol Cell. 2012 Nov 30;48(4):532-46.

Tang Z, Shu H, Qi W, Mahmood NA, Mumby MC, Yu H. PP2A is required for centromeric localization of Sgo1 and proper chromosome segregation. Dev Cell. 2006 May;10(5):575-85.

Taylor, J.H. Nucleic acid synthesis in relation to the cell division cycle. Ann. N. Y. Acad. Sci. 1960. 90:409–421.

Thadani R, Uhlmann F, Heeger S. Condensin, chromatin crossbarring and chromosome condensation. Curr Biol. 2012 Dec 4;22(23).Review

Tóth A, Ciosk R, Uhlmann F, Galova M, Schleiffer A, Nasmyth K. Yeast cohesin complex requires a conserved protein, Eco1p(Ctf7), to establish cohesion between sister chromatids during DNA replication. Genes Dev. 1999 Feb 1;13(3):320-33.

Tsang CK, Li H, Zheng XS. Nutrient starvation promotes condensin loading to maintain rDNA stability. EMBO J. 2007 Jan 24;26(2):448-58.

Uemura T, Yanagida M. Isolation of type I and II DNA topoisomerase mutants from fission yeast: single and double mutants show different phenotypes in cell growth and chromatin organization. EMBO J. 1984 Aug;3(8):1737-44.

Urnov FD, Miller JC, Lee YL, Beausejour CM, Rock JM, Augustus S, Jamieson AC, Porteus MH, Gregory PD, Holmes MC. Highly efficient endogenous human gene correction using designed zinc-finger nucleases. Nature. 2005 Jun 2;435(7042):646-51.

Vagnarelli P. Mitotic chromosome condensation in vertebrates. Exp Cell Res. 2012 Jul 15;318(12):1435-41.

Waizenegger IC, Hauf S, Meinke A, Peters JM. Two distinct pathways remove mammalian cohesin from chromosome arms in prophase and from centromeres in anaphase. Cell. 2000 Oct 27;103(3):399-410.

Wang BD, Eyre D, Basrai M, Lichten M, Strunnikov A. Condensin binding at distinct and specific chromosomal sites in the Saccharomyces cerevisiae genome. Mol Cell Biol. 2005 Aug;25(16):7216-25.

Watrin E, Peters JM. Cohesin and DNA damage repair. Exp Cell Res. 2006a. Aug 15;312(14):2687-93. Review.

Watrin E, Schleiffer A, Tanaka K, Eisenhaber F, Nasmyth K, Peters JM. Human Scc4 is required for cohesin binding to chromatin, sister-chromatid cohesion, and mitotic progression. Curr Biol. 2006b. May 9;16(9):863-74.

Weitzer S, Lehane C, Uhlmann F. A model for ATP hydrolysis-dependent binding of cohesin to DNA. Curr Biol. 2003 Nov 11;13(22):1930-40.

Woo JS, Lim JH, Shin HC, Suh MK, Ku B, Lee KH, Joo K, Robinson H, Lee J, Park SY, Ha NC, Oh BH. Structural studies of a bacterial condensin complex reveal ATP-dependent disruption of intersubunit interactions. Cell. 2009 Jan 9;136(1):85-96.

Wood AJ, Severson AF, Meyer BJ. Condensin and cohesin complexity: the expanding repertoire of functions. Nat Rev Genet. 2010 Jun;11(6):391-404. Review.

Wu N, Yu H. The Smc complexes in DNA damage response. Cell Biosci. 2012 Feb 27;2:5.

Wysocka J, Reilly PT, Herr W. Loss of HCF-1-chromatin association precedes temperature-induced growth arrest of tsBN67 cells. Mol Cell Biol. 2001 Jun;21(11):3820-9.

Yamazoe M, Onogi T, Sunako Y, Niki H, Yamanaka K, Ichimura T, Hiraga S. Complex formation of MukB, MukE and MukF proteins involved in chromosome partitioning in Escherichia coli. EMBO J. 1999 Nov 1;18(21):5873-84.

Yeong FM, Hombauer H, Wendt KS, Hirota T, Mudrak I, Mechtler K, Loregger T, Marchler-Bauer A, Tanaka K, Peters JM, Ogris E. Identification of a subunit of a novel Kleisin-beta/SMC complex as a potential substrate of protein phosphatase 2A. Curr Biol. 2003 Dec 2;13(23):2058-64.

Yoshimura SH, Hizume K, Murakami A, Sutani T, Takeyasu K, Yanagida M. Condensin architecture and interaction with DNA: regulatory non-SMC subunits bind to the head of SMC heterodimer. Curr Biol. 2002 Mar 19;12(6):508-13.

Zhang J, Shi X, Li Y, Kim BJ, Jia J, Huang Z, Yang T, Fu X, Jung SY, Wang Y, Zhang P, Kim ST, Pan X, Qin J. Acetylation of Smc3 by Eco1 is required for S phase sister chromatid cohesion in both human and yeast. Mol Cell. 2008 Jul 11;31(1):143-51.